BARYON SPECTROSCOPY

Eberhard Klempt[*]

Helmholtz-Institut für Strahlen- und Kernphysik der Rheinische Friedrich-Wilhelms Universität Nußallee 14-16, D–53115 Bonn, Germany

Jean-Marc Richard[†]

Laboratoire de Physique Subatomique et Cosmologie Université Joseph Fourier–CNRS-IN2P3–INPG, 53, avenue des Martyrs, F–38026 Grenoble Cedex, France

(Dated: January 14, 2009)

About 120 baryons and baryon resonances are known, from the abundant nucleon with u and d light-quark constituents up to the recently discovered $\Omega_b^- = bss$, and the $\Xi_b^- = bsd$ which contains one quark of each generation. In spite of this impressively large number of states, the underlying mechanisms leading to the excitation spectrum are not yet understood. Heavy-quark baryons suffer from a lack of known spin-parities. In the light-quark sector, quark-model calculations have met with considerable success in explaining the low-mass excitations spectrum but some important aspects like the mass degeneracy of positive-parity and negative-parity baryon excitations are not yet satisfactorily understood. At high masses, above $1.8\,\mathrm{GeV}$, quark models predict a very high density of resonances per mass interval which is not observed. In this review, issues are identified discriminating between different views of the resonance spectrum; prospects are discussed how open questions in baryon spectroscopy may find answers from photo- and electro-production experiments which are presently carried out in various laboratories.

Contents

[*]Electronic address: klempt@hiskp.uni-bonn.de
[†]Electronic address: jean-marc.richard@lpsc.in2p3.fr

I. INTRODUCTION

A. Why baryons?

Understanding meson resonances and the search for glueballs, hybrids and multiquark states has remained an active field of research since the time when the high-energy frontier brought into light the existence of the zoo of elementary particles. At that time, baryon spectroscopy flourished as well; but it came to a still-stand when the complexity of the three-quark system was realized.

In the recent years, interest in baryon spectroscopy has grown again. In his memorable closing speech at the workshop on Excited Nucleons and Hadronic Structure in Newport News, 2000, Nathan Isgur asked "Why N^*'s ?" (Isgur, 2000), and gave three answers: "The first is that nucleons are the stuff of which our world is made. My second reason is that they are the simplest system in which the quintessentially nonabelian character of QCD is manifest. The third reason is that history has taught us that, while relatively simple, baryons are sufficiently complex to reveal physics hidden from us in the mesons". Indeed, baryons were at the roots of the development of the quark model. For refs. to some early papers, see, e.g., (Gell-Mann and Ne'eman, 1964; Kokkedee, 1969). For an introduction to Quantum ChromoDynamics (QCD), see, e.g., (Narison, 2004; Ynduráin, 1999).

Today, we have a series of precise questions for which we would like to see answers from experiments which are presently on the floor or are being planned. While the spectroscopy of baryons with b quarks is still in its infancy, the number of known charmed baryon ground-states and resonances has increased substantially in recent years. But we do not know,

1. will baryons with triple charm reveal the genuine spectroscopy of three color charges bound by gluons, which is somewhat hidden by the chiral dynamics in light baryons?

2. Will baryons with two heavy quarks combine a charmonium-like heavy quark dynamics and a charmed-meson-like relativistic motion of a light quark bound around a static color source?

3. Will single-charm baryons, and their beauty analogs help understanding the hierarchy of light-quark excitations and provide keys to disentangle the pattern of highly-excited nucleon and Δ resonances?

Several questions should be answered by studying light baryons:

4. Can we relate the occurrence of Regge trajectories and the confinement property of QCD?

5. Can high-mass excitations be described by the dynamics of three quarks (in symmetric quark models) or do diquark effects play an important role? Quark models describe baryons as dynamics of three flavored quarks. Chiral symmetry breaking is supposed to provide constituent masses; the color-degrees of freedom are integrated out. In spite of the indisputable success of the quark model, the question needs to be raised if this type of mean-field theories can be applied.

6. Can we identify leading interactions between constituent quarks? Can we find signature of the property of flavor independence which is expected in QCD?

7. Are hyperfine splittings and other spin-dependent effects generated by an effective one-gluon exchange, even for light quarks? Or by the exchange of Goldstone bosons? Or are instanton-induced interactions at work?

8. What are missing resonances and why are they missing? Mostly, missing resonances are defined as resonances which are predicted by symmetric quark models but which have not (yet) been found. More restricted is a definition where baryons expected in symmetric but not in diquark models are considered to be missing resonances. The lowest-mass example of this type of resonances is the not-well established quartet of nucleon resonances consisting of $N_{1/2^+}(1880)$, $N_{3/2^+}(1900)$, $N_{5/2^+}(1890)$, $N_{7/2^+}(1990)$.

9. The observed spectrum of baryon resonances seems to exhibit a rather simple pattern. Is this pattern accidental or does it reflect a phase transition which may occur when baryons are highly excited?

10. Are high-mass baryons organized in the form of spin-parity doublets or chiral multiplets, of mass-degenerate states having identical spin and parity ?

11. Do we understand baryon decays, or what can be learned studying decays?

B. The structure of baryons

From deep inelastic scattering we know that the nucleon has a complicated structure. The structure functions reveal the longitudinal momentum distributions of valence and sea quarks; transversity distributions give access to their transverse momenta and their correlation with the longitudinal momenta. By integration, a few interesting global features follow. The number N_v of valence quarks (integrated over Feyman x) is $N_v = N_q - 2N_s = 3$. The nucleon has a strange quark sea with $N_s \approx 0.1 N_{u,d}$. In the infinite momentum frame, gluons carry a large (≈ 0.5) fraction of the total momentum. From the hadronization of $e^+ e^-$ pairs it is known that there are three colors, $N_c = 3$. And the width of the neutral weak interaction boson Z^0 reveals the number of generations N_G (with at least one neutrino with mass below $45\,\mathrm{GeV}$), $N_G = 3$. Time-like and spatial form-factors of protons differ by factor 2 at $Q^2 \approx 10\,\mathrm{GeV}^2$. Perturbatively, this factor should be 1. The discrepancy teaches us that even at this large momentum transfer, quark correlations play an important role.

C. Naming scheme

The Particle Data Group (PDG) (Amsler *et al.*, 2008) identifies a baryon by its name and its mass. The particle name is N or Δ for baryons having isospin $1/2$ or $3/2$, respectively, with three u, d quarks; the name is Λ or Σ for baryons having two u, d quarks and one s quark; the two light quarks couple to isospin 0 or 1, respectively. Particles with one u or d quark are called Ξ, they have isospin $1/2$. The Ω with no u or d quark has isospin 0. If no suffix is added, the remaining quarks are strange. Thus, the Ω has three s quarks. Any s quark can be replaced by a c (or b) quark which is then added as a suffix. Depending on isospin, Λ_c or Σ_c (or Λ_b or Σ_b) are formed by replacing one s quark by a heavy quark. Resonances with one charmed and one strange quark are called Ξ_c, those two or three charmed quarks Ξ_{cc} or Ω_{ccc}. The Ξ_b with one b, one s, and one u or d quark has already been mentioned.

Resonances are characterized by adding $L_{2I,2J}$ behind the particle name where L defines the lowest orbital-angular momentum required when they disintegrate into the ground state and a pseudoscalar meson, I and J are isospin and total angular momentum, respectively.

We deviate from this definition. E.g. the two particles $N(1535)S_{11}$ and $N(1520)D_{13}$ derive their name from the fact that they form an S-wave (D-wave) in πN scattering. The first "1" indicates that they have isospin $1/2$ (which is already clear for a nucleon excitation), the second "1" defines its total spin to be $J = 1/2$. The parity of the states is deduced from the positive parity of the orbital angular momentum state and the intrinsic parities of the ground state baryon (which is $+1$) and of the pseudoscalar meson (which is -1).

We call these two states $N_{1/2^-}(1535)$ and $N_{3/2^-}(1520)$. These are the observed states. They can be mixtures of quark model states. E.g. the $N_{1/2^-}(1535)$ can be written in the form

$$N(1535)S_{11} = \cos\Theta_{S_{11}} |\,^2N_{1/2^-}\,\rangle - \sin\Theta_{S_{11}} |\,^4N_{1/2^-}\,\rangle$$
$$N(1650)S_{11} = \sin\Theta_{S_{11}} |\,^2N_{1/2^-}\,\rangle + \cos\Theta_{S_{11}} |\,^4N_{1/2^-}\,\rangle \quad (1)$$

where $^2N_{1/2^-}$ has intrinsic quark spin $s = 1/2$ while $^4N_{1/2^-}$ belongs to the $s = 3/2$ quartet. As will be discussed below, baryons develop a band structure. Mixing between states belonging to different bands but having identical external quantum numbers is possible (even though calculations give small effects). Further components to the states in eq. (1) could come from the third excitation band with $\mathsf{N} = 3$. A state

$$|\,^2N_{1/2^-}, D_{56}(L=1)^{P=-1}_{\mathsf{N}=3}\,\rangle$$

is a spin-doublet quark model state belonging to the third excitation band with one unit of orbital angular momentum, having a 56-plet SU(3) flavor structure.

D. Guide to the literature

Prime sources of original information is found in three conference series' on the Structure of Baryons and on N^*. The latest conferences where hold as tri-annual International Conference on the Structure of Baryons, Baryons'07, in Seoul, Korea (2007), and as bi-annual International Conference on Meson-Nucleon Physics and the Structure of the Nucleon (MENU 2007) in Jülich, Germany, (2007). Irregularly takes place the NSTAR Workshop (Physics of Excited Nucleons) which, in 2007, was hosted in Bonn.

Experimentally indispensable is the Review of Particle Properties published by the PDG (Amsler *et al.*, 2008) which will be used throughout this review. It includes a few minireviews on baryons: (Höhler and Workman, 2008; Trilling, 2008; Wohl, 2008a,b). Still very useful is the broad review by (Hey and Kelly, 1983). The advances of the quark model to describe the baryon excitation spectrum and baryon decays are reviewed by (Capstick and Roberts, 2000). Low-energy photoproduction and implications for low-lying resonances are critically discussed by (Krusche and Schadmand, 2003). Not included here is the physics of cascade resonances: of Ξ's and Ω's where little information has been added since the review of (Hey and Kelly, 1983). There is a proposal to study Ξ resonances at Jlab, and first results demonstrated the feasibility (Guo *et al.*, 2007). The latest review on Ξ baryons can be found in (Meadows, 1980).

E. Abbreviations

For the sake of readability, we collect here abbreviations used in the text.

$\boldsymbol{\rho}$, $\boldsymbol{\lambda}$ are the Jacobi variables for the 3-body problem,
$\boldsymbol{L}$ is the orbital angular momentum, $\boldsymbol{L} = \boldsymbol{l}_\rho + \boldsymbol{l}_\lambda$,
$\boldsymbol{S} = \boldsymbol{s}_1 + \boldsymbol{s}_2 + \boldsymbol{s}_3$ is the total quark spin,
$\boldsymbol{J} = \boldsymbol{L} + \boldsymbol{S}$ is the total angular momentum,
$J, L, S, l_\rho, l_\lambda$ are the corresponding quantum numbers,
L is the sum L $= l_\rho + l_\lambda$,
$\boldsymbol{I}$ is the isospin having components I_k,
I the isospin quantum number,
S is the strangeness, Y the hypercharge,
$\Upsilon = (b\bar{b})$ stands for the bottomonium family,
P is the parity, Q the charge, $+e$ is the unit charge,
$N(xxx)$ represents a nucleon N with mass xxx,
$\mathbb{N} = \mathbb{n}_\rho + \mathbb{n}_\lambda$ is the radial number,
N gives the band number,
p, n represent proton and neutron,
$n = u, d$ are light quarks, $q = u, d, s$ include strangeness,
$Q = c, b$ are heavy quarks,
$M_{p,n}$ are proton and neutron mass,
$\kappa_{p,n}$ their anomalous magnetic moments,
α, α_s are the electromagnetic and strong couplings.

F. Outline

Exciting new results have been obtained for heavy baryons containing a charmed or a bottom quark. The results are reviewed in section II. Most information on light-quark baryons stems from πN or $K N$ elastic or charge exchange scattering but new information is now added from photo- and electro-production experiments. The progress is discussed in section III. Section IV provides a frame within which baryon excitations can be discussed and gives an outline of current theoretical ideas. The rich spectrum of light baryon resonances reveals symmetries and a mass pattern. Based on these observation, an interpretation of the baryon spectrum is offered. In the summary (V), conclusions are given to which extend the new experiments have contributed to baryon spectroscopy and suggestions for further work are made.

II. HEAVY-QUARK BARYONS

With the discovery of the J particle (Aubert *et al.*, 1974) at BNL and of the ψ (Augustin *et al.*, 1974) and ψ' (Abrams *et al.*, 1974) at Stanford, charmed baryons had of course to exist as well, and their properties were predicted early (De Rujula *et al.*, 1975). Experimental evidence for the first charmed baryon was reported at BNL in the reaction $\nu_\mu p \to \mu^- \Lambda \pi^+ \pi^+ \pi^+ \pi^-$ with Λ decaying into $p\pi^-$ (Cazzoli *et al.*, 1975). None of the π^+ could be interpreted as K^+ and no $\pi^+\pi^-$ pair formed a K^0, hence the event could signal either violation of the $\Delta S = \Delta Q$ rule, or be due to production of a baryon with charm. Now we know that a Σ_c^{++} was produced.

At present, 34 charmed baryons and 7 beauty baryons

are known. For most of them, spin and parity have not been measured; for some states the quantum numbers can be deduced from their decay modes or by comparison of measured masses with quark-model expectations.

The study of charmed baryons is mostly pursued by searching for resonances which decay into Λ_c^+ plus one (or more) pion(s). The momenta of the - comparatively slow - pions can be measured with high precision. Hence the best precision is obtained for the mass difference to the Λ_c^+. The Λ_c^+ is sometimes reconstructed from up to 15 different decay modes. In other cases, the most prominent and well measurable modes $\Lambda_c^+ \to p\bar{K}^0$ and $\Lambda_c^+ \to pK^-\pi^+$ are sufficient to obtain a significant signal. The study of charmed baryons was often a by-product: the main aim of the experiments at Cornell, SLAC or KEK was the study of CP violation in B decays from $\Upsilon(4S)$ and, perhaps, of the Υ family. Charmed baryons are then produced in the $e^+e^- \to q\bar{q}$ continuum and in B decays.

A. The life time of charmed particles

Weak interaction physics is not covered in this review. However, the finite lifetime of hadrons with heavy flavors plays an important rôle in their experimental identification. In Table I are summarized the measured lifetime of flavored mesons and baryons.

Comments are in order:

- While the lifetimes of particles carrying a b quark are very similar, this is not the case with strangeness, where more than a factor of 3 is observed from the most stable hyperon to the shortest-lived.

- The differences are even more pronounced for charmed baryons. When the difference between the charged and the neutral D-meson lifetime was discovered, this was a striking surprise, and it took

TABLE I Lifetime of flavored mesons and baryons (in s).

$K^\pm$	$(123.85 \pm 0.24) \times 10^{-10}$	K_S^0	$(0.8953 \pm 0.0005) \times 10^{-10}$
K_L^0	$(511.4 \pm 2.1) \times 10^{-10}$	$D^\pm$	$(1040 \pm 7) \times 10^{-15}$
D^0	$(410.1 \pm 1.5) \times 10^{-15}$	D_s	$(500 \pm 7) \times 10^{-15}$
$B^\pm$	$(1638 \pm 11) \times 10^{-15}$	B^0	$(1530 \pm 9) \times 10^{-15}$
B_s	$(1466 \pm 59) \times 10^{-15}$		
Λ	$(2.631 \pm 0.020) \times 10^{-10}$	$\Sigma^\pm$	$(0.8018 \pm 0.0026) \times 10^{-10}$
Ξ^0	$(2.90 \pm 0.09) \times 10^{-10}$	Ξ^-	$(1.639 \pm 0.015) \times 10^{-10}$
Ω^-	$(0.821 \pm 0.011) \times 10^{-10}$	Λ_c	$(200 \pm 6) \times 10^{-15}$
Ξ_c^+	$(442 \pm 26) \times 10^{-15}$	Ξ_c^0	$(112^{+13}_{-10}) \times 10^{-15}$
Ω_c^0	$(69 \pm 12) \times 10^{-15}$	Λ_b	$(1230 \pm 74) \times 10^{-15}$
Ξ_b^-	$(1420^{+280}_{-240}) \times 10^{-15}$	Ω_b^-	(not measured)

some time to realize that besides the simplest mechanism, where the c quark emits a virtual W boson which dissociates into a lepton pair or a quark-antiquark pair, there are diagrams in which the W is exchanged. This is, however, permitted for D^0 and D_s but forbidden for $D^\pm$. The lifetime is also influenced by interferences. If $c \to s + W^+ \to s + u + \bar{d}$, for instance, initiates some hadronic decay, this $\bar{d}$ should antisymmetrize with the $\bar{d}$ of D^0, an effect that does not exist for D^+. In principle, a fusion mechanism such as $c + \bar{s} \to u + \bar{d}$ should also contribute to the D_s decay.

- The analysis was then extended to charmed baryons, with predictions by (Guberina *et al.*, 1986); see, also (Fleck and Richard, 1990; Guberina *et al.*, 2000). Some effects are enhanced with respect to the case of meson, for instance the role of antisymmetrization. The fusion mechanism, on the other hand, is suppressed as requiring an antiquark from the sea. The trend of the predicted hierarchy is well reproduced by the experimental data, but the observed differences are even more pronounced.

- It would be particularly interesting to measure the lifetime of double-charm baryons, or heavier baryons with triple charm, or with charm and beauty. Another effect should be taken into account, that of the deep binding of the heavy quarks. This is already discussed for the B_c meson with quark content $(b\bar{c})$.

- At COMPASS, LHC, PANDA, or at a second generation of B-factories, there is the possibility to search for for weak decays of $\Xi_{cc}(3520)^+$ and Ξ_{cc}^{++} double charmed baryons into charmless final states (Liu *et al.*, 2008). Such decays would signal new physics.

- The lifetimes of charmed particles are just sufficiently long to identify them by a decay vertex separated from the interaction vertex. For $\beta\gamma \approx 1$, the lifetime of B-mesons leads to a separation of 500μm. Precise vertexing is therefore a major experimental requirement.

B. Major experiments in heavy-baryon spectroscopy

A large fraction of our knowledge of charmed baryons comes from the CLEO detector at the intersecting storage ring CESR. The CLEO detector was upgraded continuously. It consisted of a four-layer silicon-strip vertex detector, a wire drift chamber and a particle identification system based on Cherenkov ring imaging, time-of-flight counters, a 7800-element CsI electromagnetic calorimeter, a 1.5 T superconducting solenoid, iron for flux return and muon identification, and muon chambers (Kopp, 1996; Viehhauser, 2000). The integrated luminosity on the $\Upsilon(4S)$ resonance accumulated in the years 1999-2003 was 16 fb^{-1}.

Of course, the B-factories have reached a much higher luminosity; BaBar collected about 400 fb^{-1}, BELLE 700 fb^{-1} and is continuing data taking. The data shown below are mostly based on a fraction of the data. Both B-factories operated mostly at the peak cross section for formation of the $\Upsilon(4S)$, at 10.58 GeV, with energies of the colliding electron and positron beam of 9 (8) GeV and 3.1 (3.5) GeV, for BaBar and BELLE respectively, resulting in a Lorentz boost of the center of mass of $\beta = 0.55$ (0.425).

The inner part of the BaBar detector (Aubert *et al.*, 2002) includes tracking, particle identification and electromagnetic calorimetry. It is surrounded by a superconductive solenoid providing a magnetic field of 1.5 T. The tracking system is composed of a Silicon Vertex Tracker and a drift chamber. A 40-layer drift chamber is used to measure particle momenta and the ionization loss dE/dx. Particle identification is provided by the dE/dx measurement and a ring-imaging detector. The electromagnetic calorimeter is a finely segmented array of CsI(Tl) crystals with energy resolution of $\sigma_E/E \approx 2.3\% \cdot E^{-1/4} + 1.9\%$ (E in GeV). The iron return yoke is instrumented with resistive plate chambers and limited streamer tubes for detection of muons and neutral hadrons.

Tracking, identification and calorimetric systems of the BELLE detector (Iijima and Prebys, 2000) at KEKB are placed inside a 1.5 T superconducting solenoid magnet. Tracking and vertex measurements are provided by a silicon vertex detector and a central drift chamber. The central drift chamber has 50 layers of anode wires for tracking and dE/dx measurements. Particle identification is achieved using the central drift chamber, time of flight counters, and aerogel Cherenkov counters. The electromagnetic calorimeter consists of CsI(Tl) crystals of projective geometry. The flux return is instrumented with 14 layers of resistive plate chambers for muon identification and detection of neutral hadrons.

We will mention results obtained by the ARGUS and SELEX collaborations without introducing the detectors here and refer the reader interested in their performance to the two reports (Albrecht *et al.*, 1989; Engelfried *et al.*, 1998). Also some early bubble chamber results and results from the CERN ISR and SPS will be mentioned. At Fermilab, the photoproduction experiments E687, E691, E791 and Focus and SELEX using a hadron beam produced interesting results on charmed baryons.

So far, only a few baryons with beauty have been discovered. The energy of the B-factories operating at the $\Upsilon(4S)$ is obviously not sufficient to produce beauty baryons. These are however produced abundantly by Tevatron at Fermilab, in which antiprotons and protons collide at 1.96 TeV center-of-mass energy. Two major experiments - CDF and DØ, exploit the physics; the discovery of the top quark, the measurement of its mass to a precision of nearly 1%, and the study of B_s oscillations belong to the highlights of the Tevatron results. Earlier important results on beauty baryons were achieved at the

CERN ISR and at LEP.

The CDF detector (Acosta *et al.*, 2005) consists of multiple layers of silicon micro-strip detectors, providing for a precise measurement of a track's impact parameter with respect to the primary vertex, and a large open-cell drift chamber enclosed in a 1.4 T superconducting solenoid, which in turn is surrounded by calorimeters. The electromagnetic calorimeters use lead-scintillator sampling, the hadron calorimeters iron-scintillator sampling.

The inner tracking of DØ (Abazov *et al.*, 2006) is composed of a silicon microstrip tracker for vertexing and a central fiber tracker, both located within a 2 T superconducting solenoidal magnet. Calorimetry relies on liquid-argon and uranium detectors. An outer muon system consists of a layer of tracking detectors and scintillation trigger counters in front of and behind 1.8 t iron toroids.

C. Charmed baryons

1. The Λ_c states

a. Λ_c^+: The first observation of a charmed baryon, of Λ_c^+, was reported two years after the J/ψ discovery (Knapp *et al.*, 1976). Now, Λ_c^+ is the best known charmed baryon. Due to its high mass, it has a large number of decay modes. Among these, $\Lambda_c^+ \to p\bar{K}n\pi$ and $\Lambda\pi^+n\pi$ (n=1,2) have the largest decay fractions, summing up to about 20%. The most precise mass measurement was made by the BABAR collaboration (Aubert *et al.*, 2005) finding

$$M_{\Lambda_c} = 2286.46 \pm 0.14 \,\text{MeV}. \tag{1}$$

The lifetime was measured by E687, CLEO, Focus, and SELEX. The lifetimes of all stable heavy baryons are collected in Table I.

b. $\Lambda_c(2593)^+$ and $\Lambda_c(2625)^+$: The $\Lambda_c(2625)^+$ was discovered by the ARGUS collaboration at the e^+e^- storage ring DORIS II at DESY (Albrecht *et al.*, 1993). Fig. 1 shows the $\Lambda_c^+\pi^+\pi^-$ invariant mass distribution with increased statistics (Albrecht *et al.*, 1997) in which the $\Lambda_c(2593)^+$ is observed as well. The latter state was first observed by CLEO (Edwards *et al.*, 1995). Table II compares the results on both states from the ARGUS (Albrecht *et al.*, 1997), the CLEO (Edwards *et al.*, 1995), and the E687 (Frabetti *et al.*, 1994, 1996) collaborations.

The $\Lambda_c(2593)^+$ decays with a large fraction (>70%) via $\Sigma_c\pi$; the small phase space favors vanishing orbital angular momentum. The Σ_c is the lowest mass charmed isovector state and is thus expected to have $J^P = 1/2^+$. Then, $J^P = 1/2^-$ follows for the $\Lambda_c(2593)^+$. Most likely, the $\Lambda_c(2625)^+$ is its $J^P = 3/2^-$ companion and the two states correspond to $\Lambda(1405)$ and $\Lambda(1520)$. See section IV.F for further discussion.
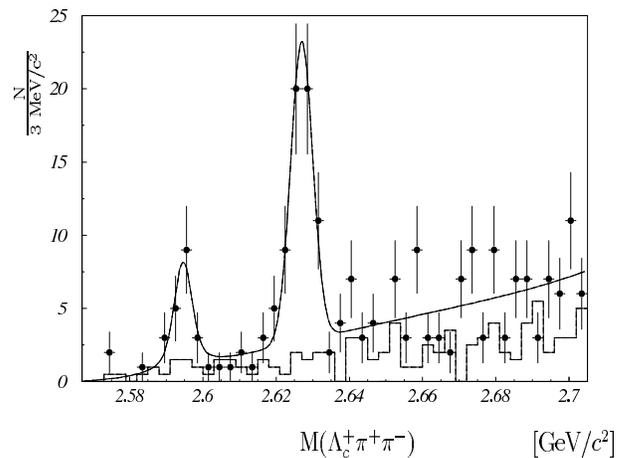
FIG. 1 The $\Lambda_c^+\pi^+\pi^-$ invariant mass distribution after a cut on the Λ_c^+ (reconstructed from five decay modes) and using side bins (dashed line) (Albrecht *et al.*, 1997).

TABLE II Mass and width of the $\Lambda_c(2593)^+$ and $\Lambda_c(2625)^+$ measured at CLEO, BABAR and BELLE.

		M, MeV/c^2	Γ, MeV/c^2
ARGUS	$\Lambda_c(2593)$	$2596.3 \pm 0.9 \pm 0.6$	$2.9^{+2.9+1.8}_{-2.1-1.4}$
CLEO	$\Lambda_c(2593)$	$2594.0 \pm 0.4 \pm 1.0$	$3.9^{+1.4+2.0}_{-1.2-1.0}$
E687	$\Lambda_c(2593)$	$2581.2 \pm 0.2 \pm 0.4$	
ARGUS	$\Lambda_c(2625)$	$2628.5 \pm 0.5 \pm 0.5$	< 3.2
CLEO	$\Lambda_c(2625)$	$2629.5 \pm 0.2 \pm 0.5$	< 1.9
E687	$\Lambda_c(2625)$	$2627.7 \pm 0.6 \pm 0.3$	

c. $\Lambda_c(2765)^+$ (or $\Sigma_c(2765)^+$), $\Lambda_c(2880)^+$ and $\Lambda_c(2940)^+$: The CLEO Collaboration reported two peaks in the $\Lambda_c^+\pi^+\pi^-$ final state (Artuso *et al.*, 2001) which could be Λ_c^+ or Σ_c^+ excitations. One of them is found 480 MeV above the Λ_c^+ baryon and is rather broad, $\Gamma \approx 50$ MeV; the other one is narrow, $\Gamma < 8$ MeV), and its mass lies $596 \pm 1 \pm 2$ MeV above the Λ_c^+.

The BABAR Collaboration observed two peaks in the $D^0 p$ invariant mass distribution (see Figure 2) (Aubert *et al.*, 2007). It is the first observation of a heavy baryon disintegration into a heavy-quark meson and a light-quark baryon. Due to the kinematics, the larger part of the released energy is carried away by the baryon. The $D^+ p$ final state shows no peaks; thus the isospin of the heavy baryon must be zero which identifies the peaks as $\Lambda_c(2880)^+$ and $\Lambda_c(2940)^+$ (and not belonging to the Σ_c^+ series). The former one coincides with the narrow state observed by (Artuso *et al.*, 2001) and is called $\Lambda_c(2880)^+$.

The BELLE Collaboration confirmed the $\Lambda_c(2940)^+$ in $\Lambda_c^+\pi^+\pi^-$. The decay proceeds via formation of $\Sigma_c(2455)^{++}$ or $\Sigma_c(2455)^0$ resonances in the intermediate state (Abe *et al.*, 2007). The $\Lambda_c(2880)^+$ and $\Lambda_c(2940)^+$
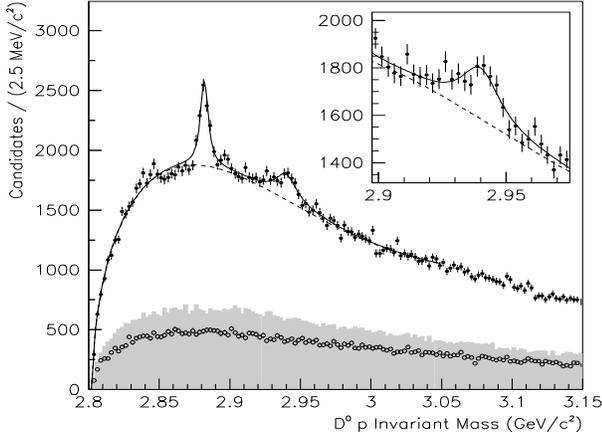
FIG. 2 Invariant mass distribution for D^0p candidates at BABAR (Aubert *et al.*, 2007). Also shown are the contributions from D^0 sidebands (grey) and wrong-sign combinations (open dots).

mass and width measured by BABAR and BELLE are consistent (see Table III).

TABLE III Mass and width of the $\Lambda_c(2880)$ and $\Lambda_c(2940)$ measured at CLEO (Artuso *et al.*, 2001), BABAR (AUBERT *et al.*, 2007) and BELLE (Abe *et al.*, 2007).

		M, MeV/c^2	Γ, MeV/c^2
CLEO	$\Lambda_c(2880)$	$2882.5 \pm 1 \pm 2$	< 8
BABAR	$\Lambda_c(2880)$	$2881.9 \pm 0.1 \pm 0.5$	$5.8 \pm 1.5 \pm 1.1$
BELLE	$\Lambda_c(2880)$	$2881.2 \pm 0.2 \pm 0.4$	$5.8 \pm 0.7 \pm 1.1$
BABAR	$\Lambda_c(2940)$	$2939.8 \pm 1.3 \pm 1.0$	$17.5 \pm 5.2 \pm 5.9$
BELLE	$\Lambda_c(2940)$	$2938.0 \pm 1.3^{+2.0}_{-4.0}$	13^{+8+27}_{-5-7}

The two sequential decay modes improve the sensitivity to study the spin of the resonance. The helicity angle of the $\Lambda_c(2880)^+ \rightarrow \Sigma_c(2455)\pi$ decay favors $J = 5/2$ over $3/2$ and $1/2$. The experimental ratio of the $\Lambda_c(2880)^+$ partial width $\Gamma[\Sigma_c(2520)\pi]/\Gamma[\Sigma_c(2455)\pi] = 0.23 \pm 0.06 \pm 0.03$ is calculated to be 1.45 for $J^P = 5/2^-$ and 0.23 $J^P = 5/2^-$. Thus the spin-parity assignment $5/2^+$ is favored over $5/2^-$.

Finally we notice that the mass of the $\Lambda_c(2940)^+$ is at the D^*p threshold, a fact which invites interpretations of this state as a D^*p molecule (He *et al.*, 2007).

2. The Σ_c states

a. $\Sigma_c(2455)$ and $\Sigma_c(2520)$: These two states have been observed in a large number of experiments; here we show only the results of the most recent publication of the CLEO collaboration. Σ_c^+ and Σ_c^{*+} were observed in their $\Lambda_c^+\pi^0$ decay (Ammar *et al.*, 2001), and Σ_c^{*++} and
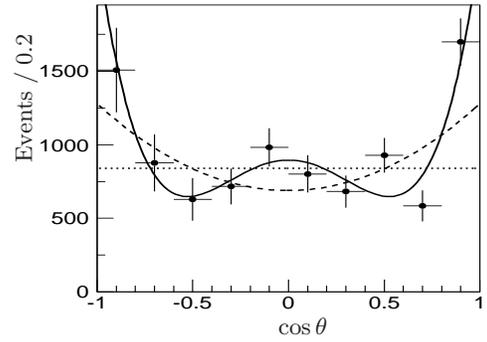
FIG. 3 The yield of $\Lambda_c(2880)^+ \rightarrow \Sigma_c(2455)^0\pi^+$ and $\Sigma_c(2455)^{++}\pi^-$ decays as a function of the helicity angle. The fits correspond to $\Lambda_c(2880)^+$ spin hypotheses $J = 1/2$ (dotted line), $3/2$ (dashed curve), $5/2$ (solid curve), respectively (Abe *et al.*, 2007).

Σ_c^{*0} in their decay into $\Lambda_c^+\pi^\pm$ (Athar *et al.*, 2005). The data of (Athar *et al.*, 2005) cover the energy range 9.4 to 11.5 GeV while (Ammar *et al.*, 2001) used data at the $\Upsilon(4S)$. But B decays were suppressed by kinematic cuts and in both cases, the Σ_c^* baryons are likely produced from the $e^+e^- \rightarrow q\bar{q}$ continuum. Fig. 4 shows the momentum of pions recoiling against the Λ_c^+ which defines the mass gap between Σ_c or Σ_c^* and Λ_c^+. Even though the quantum numbers of the two resonances have not been measured, all their properties are compatible with the assignment $J^P = 1/2^+$ and $J^P = 3/2^+$, respectively. The numerical results are reproduced in Table IV.

b. $\Sigma_c(2800)^+$: The BELLE Collaboration observed an isotriplet of charmed baryons decaying to the $\Lambda_c^+\pi$ final state at 2800 MeV (Mizuk *et al.*, 2005). An additional peak at $\Delta M \sim 0.42$ GeV/c^2, visible in the $\Lambda_c^+\pi^+$ and $\Lambda_c^+\pi^-$ invariant mass distributions, was identified as a reflection from the $\Lambda_c(2880)^+ \rightarrow \Sigma_c(2455)\pi \rightarrow$
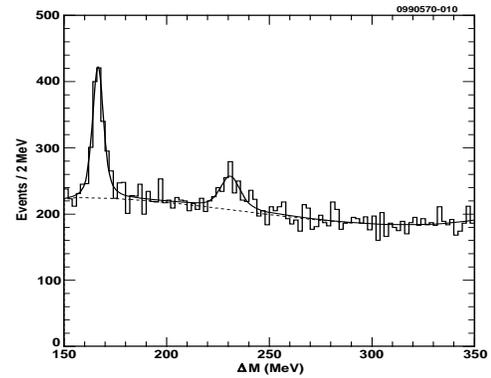
FIG. 4 Mass difference spectrum, $M(\Lambda_c^+\pi^0) - M(\Lambda_c^+)$. The solid line fit is to a third-order polynomial background shape and two P-wave Breit–Wigner functions smeared by Gaussian resolution functions for the two signal shapes. The dashed line shows the background function.

TABLE IV Mass and width of the $\Sigma_c(2455)$ and $\Sigma_c(2520)$ measured at CLEO.

		M, MeV/c^2	Γ, MeV/c^2
$\Sigma_c(2455)$	$M(\Sigma_c^{++}) - M(\Lambda_c^+)$	$167.4 \pm 0.1 \pm 0.2$	$2.3 \pm 0.2 \pm 0.3$
	$M(\Sigma_c^+) - M(\Lambda_c^+)$	$166.4 \pm 0.2 \pm 0.3$	< 4.6
	$M(\Sigma_c^0) - M(\Lambda_c^+)$	$167.2 \pm 0.1 \pm 0.2$	$2.5 \pm 0.2 \pm 0.3$
$\Sigma_c(2520)$	$M(\Sigma_c^{*++}) - M(\Lambda_c^+)$	$231.5 \pm 0.4 \pm 0.3$	$14.4^{+1.6}_{-1.5} \pm 1.4$
	$M(\Sigma_c^{*+}) - M(\Lambda_c^+)$	$231.0 \pm 1.1 \pm 2.0$	< 17
	$M(\Sigma_c^{*0}) - M(\Lambda_c^+)$	$231.4 \pm 0.5 \pm 0.3$	$16.6^{+1.9}_{-1.7} \pm 1.4$

TABLE V Mass and width of the $\Sigma_c(2800)$ measured at CLEO.

		M, MeV/c^2	Γ, MeV/c^2
$\Sigma_c(2800)$	$M(\Sigma_c(2800)^{++}) - M(\Lambda_c^+)$	$514.5^{+3.4+2.8}_{-3.1-4.9}$	75^{+18+12}_{-13-11}
	$M(\Sigma_c(2800)^+) - M(\Lambda_c^+)$	$505.4^{+5.8+12.4}_{-4.6-2.0}$	62^{+37+52}_{-23-38}
	$M(\Sigma_c(2800)^0) - M(\Lambda_c^+)$	$515.4^{+3.2+2.1}_{-3.1-6.0}$	61^{+18+22}_{-13-13}

$\Lambda_c^+ \pi^+ \pi^-$ decays. The parameters of all isospin partners are consistent (see Table V). Based on the mass and width, the $3/2^-$ assignment for these states was proposed (Mizuk *et al.*, 2005). Note that the mass of the new resonances is at the $D^0 p$ threshold.

3. The Ξ_c states

a. Ξ_c and Ξ_c': The Ξ_c^+ was discovered by (Biagi *et al.*, 1983) at the CERN SPS hyperon beam in Σ^- nucleon collisions, $\Sigma^- + \text{Be} \to (\Lambda K^- \pi^+ \pi^+) + X$, its isospin partner Ξ_c^0 by the CLEO collaboration (Avery *et al.*, 1989) through its decay to $\Xi^- \pi^+$. Both states were studied in different production and decay modes. The PDG quotes

$$\begin{aligned} \Xi_c^+ & \quad M = 2467.9 \pm 0.4\,\text{MeV} \quad \tau = 442 \pm 26\,\text{fs} \\ \Xi_c^0 & \quad M = 2471.0 \pm 0.4\,\text{MeV} \quad \tau = 112^{+13}_{-10}\,\text{fs} \end{aligned} \quad (2)$$

The $\Xi_c(2645)$: The spin wave-function of the isospin doublet Ξ_c^+, and Ξ_c^0 contains a pair of light quarks, $[su]$ and $[sd]$, mostly in a spin $S = 0$ state. There should exist a second doublet in which the light quark pair is mostly in spin triplet $S = 1$. This pair is denoted $\Xi_c^{0,+\prime}$.

These two expected states were discovered by the CLEO collaboration (Jessop *et al.*, 1999). In a first step, the two ground-state Ξ_c baryons were reconstructed using several decay modes (see Fig. 5). The ground-state Ξ_c baryons were observed jointly with a low-energetic photon. The $\Xi_c^+ \gamma$ and $\Xi_c^0 \gamma$ invariant masses show two signals which were interpreted as the missing $\Xi_c^{+,0\prime}$ partners of the ground state $\Xi_c^{+,0}$ baryons. The mass differences $M(\Xi_c^{+\prime}) - M(\Xi_c^+)$ and $M(\Xi_c^{0\prime}) - M(\Xi_c^0)$ were measured
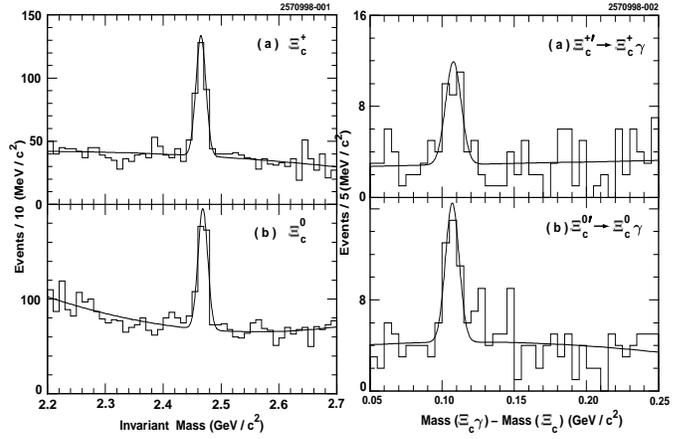
FIG. 5 Left: (a) Summed invariant mass distributions for $\Xi^- \pi^+ \pi^+$ and $\Xi^0 \pi^+ \pi^0$ combinations with $x_p > 0.5$ and 0.6, respectively, and (b) for $\Xi^- \pi^+$, $\Xi^- \pi^+ \pi^0$, $\Omega^- K^+$, and $\Xi^0 \pi^+ \pi^-$ combinations. Right: Invariant mass difference $\Delta M(\Xi_c \gamma - \Xi_c)$ distributions for $\Xi_c^+ \gamma$ and $\Xi_c^0 \gamma$, where contributions from the different Ξ_c decay modes have been summed in each case.

to be $107.8 \pm 1.7 \pm 2.5$ and $107.0 \pm 1.4 \pm 2.5 MeV/c^2$, respectively.

BaBar confirmed the existence of the Ξ_c' and found that the rate of Ξ_c' production over Ξ_c is about 18% in the e^+e^- continuum but about $1/3$ in B decays. The angular distribution of $\Xi_c' \to \Xi_c \gamma$ decays was found it to be consistent with the prediction for $J^P = 1/2^+$ even though higher spins cannot yet be ruled out (Aubert *et al.*, 2006d).

b. $\Xi_c(2790)$ and $\Xi_c(2815)$: In (Csorna *et al.*, 2001), decay of Ξ_c resonances to Ξ_c' plus a pion were observed. Mass differences for the two states to the $\Xi_c^{+,0}$ ground states are given in Table VI. This observation complements an earlier observation of the CLEO collaboration (Alexander *et al.*, 1999) in which a doublet of Ξ_c resonances was observed, one decaying into $\Xi_c^+ \pi^+ \pi^-$ via an intermediate Ξ_c^{*0}, and its isospin partner decaying into $\Xi_c^0 \pi^+ \pi^-$ via an intermediate Ξ_c^{*+}. Mass differences and widths are again collected in Table VI. These resonances are interpreted as the $J^P = 1/2^-$ and $3/2^-$ Ξ_c par-

TABLE VI Mass and width of the $\Xi_c(2790)$ and $\Xi_c(2815)$ measured at CLEO.

		M, MeV/c^2	Γ, MeV/c^2
$\Xi_c(2790)$	$M(\Xi_c^0 \gamma \pi^+) - M(\Xi_c^0)$	$318.2 \pm 1.3 \pm 2.9$	< 15
	$M(\Xi_c^+ \gamma \pi^-) - M(\Xi_c^+)$	$324.0 \pm 1.3 \pm 3.0$	< 12
$\Xi_c(2815)$	$M(\Xi_c^0 \pi^+ \pi^-) - M(\Xi_c^0)$	$347.2 \pm 0.7 \pm 2.0$	< 6.5
	$M(\Xi_c^+ \pi^+ \pi^-) - M(\Xi_c^+)$	$348.6 \pm 0.6 \pm 1.0$	< 3.5

ticles, the charmed-strange analogues of the $\Lambda_c^+(2593)$ and $\Lambda_c^+(2625)$, or of the light-quark $\Lambda(1405)$ and $\Lambda(1520)$ pair.

c. $\Xi_c(2980)$ *and* $\Xi_c(3080)$: The BELLE Collaboration observed two new Ξ_c states, the $\Xi_c(2980)$ and $\Xi_c(3080)$, decaying to the $\Lambda_c^+ K^- \pi^+$ and $\Lambda_c^+ K_S \pi^-$ (see Figure 6, left panel (Chistov *et al.*, 2006)). In contrast to decays of other Ξ_c decay modes, the c and s quark separate forming a charmed baryon and a strange meson. (Likewise, decays into ΛD^+ are allowed above $3\,\mathrm{GeV}$ and could be searched for.) The broader of the two states was measured to have a mass of $2978.5 \pm 2.1 \pm 2.0$ MeV/c^2 and a width of $43.5 \pm 7.5 \pm 7.0$ MeV/c^2. The mass and width of the narrow state are measured to be $3076.7 \pm 0.9 \pm 0.5$ MeV/c^2 and $6.2 \pm 1.2 \pm 0.8$ MeV/c^2, respectively. A search for the isospin partner states that decay into $\Lambda_c^+ K_S^0 \pi^-$ yielded evidence for a signal at the mass of $3082.8 \pm 1.8 \pm 1.5$ MeV/c^2; the broader low-mass baryon is just visible.

The BaBaR Collaboration confirmed observations of the $\Xi_c(2980)$ and $\Xi_c(3080)$ (Aubert *et al.*, 2006a) by studying the $\Lambda_c^+ K_S^0$, $\Lambda_c^+ K^-$, $\Lambda_c^+ K^- \pi^+$, $\Lambda_c^+ K_S^0 \pi^-$, $\Lambda_c^+ K_S^0 \pi^- \pi^+$, and $\Lambda_c^+ K^- \pi^+ \pi^-$ mass distributions. In addition, BaBaR studied the resonant structure of the $\Lambda_c^+ K^- \pi^+$ final state (Aubert *et al.*, 2008). The $\Xi_c(3080)$ was found to decay through the intermediate $\Sigma_c(2455)$ and $\Sigma_c(2520)$ states with roughly equal probability. The $\Xi_c(2980)$ was found to decay through the intermediate $\Sigma_c(2455)\bar{K}$; the $\Sigma_c(2455)\bar{K}$ mass distribution show an additional signal evidencing $\Xi_c(3055)^+$. The $\Sigma_c(2520)\bar{K}$ shows evidence for $\Xi_c(2980)$ as strong threshold enhancement, for $\Xi_c(3080)$ and for a third signal at $\Xi_c(3123)$. The BELLE and BaBaR parameters for the new Ξ_c states are summarized in Table VII.
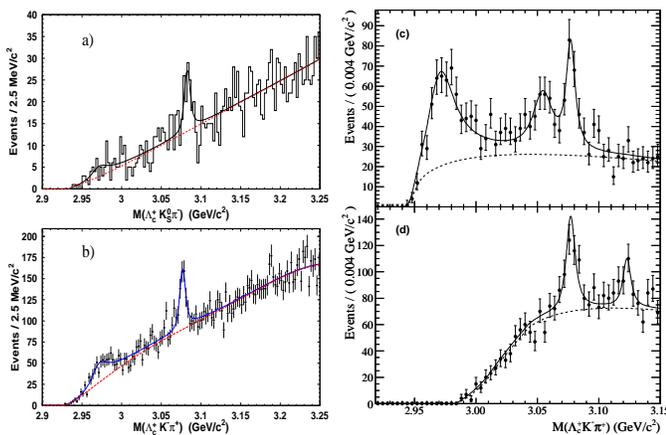
FIG. 6 (a) $M(\Lambda_c^+ K^- \pi^+)$ and (b) $M(\Lambda_c^+ K_S^0 \pi^-)$ distribution at BELLE (Chistov *et al.*, 2006). (c) The $\Lambda_c^+ K^- \pi^+$ invariant mass distribution for $M(\Lambda_c^+ \pi^+)$ consistent with the $\Sigma_c(2455)$ and (d) with the $\Sigma_c(2520)$, measured at BaBaR (Aubert *et al.*, 2006a, 2008).

TABLE VII Mass and width of the $\Xi_c(2790)$ and $\Xi_c(2815)$ measured at CLEO (Chistov *et al.*, 2006) and BaBaR (Aubert *et al.*, 2008).

	M, MeV/c^2	Γ, MeV/c^2
BELLE $\Xi_c(2980)^+$	$2978.5 \pm 2.1 \pm 2.0$	$43.5 \pm 7.5 \pm 7.0$
BaBaR $\Xi_c(2980)^+$	$2969.3 \pm 2.2 \pm 1.7$	$27 \pm 8 \pm 2$
BaBaR $\Xi_c(3055)^+$	$3054.2 \pm 1.2 \pm 0.5$	$17 \pm 6 \pm 11$
BELLE $\Xi_c(2980)^0$	$2977.1 \pm 8.8 \pm 3.5$	43.5 (fixed)
BaBaR $\Xi_c(2980)^0$	$2972.9 \pm 4.4 \pm 1.6$	$31 \pm 7 \pm 8$
BELLE $\Xi_c(3080)^+$	$3076.7 \pm 0.9 \pm 0.5$	$6.2 \pm 1.2 \pm 0.8$
BaBaR $\Xi_c(3080)^+$	$3077.0 \pm 0.4 \pm 0.2$	$5.5 \pm 1.3 \pm 0.6$
BELLE $\Xi_c(3080)^0$	$3082.8 \pm 1.8 \pm 1.5$	$5.2 \pm 3.1 \pm 1.8$
BaBaR $\Xi_c(3080)^0$	$3079.3 \pm 1.1 \pm 0.2$	$5.9 \pm 2.3 \pm 1.5$
BaBaR $\Xi_c(3123)^+$	$3122.9 \pm 1.3 \pm 0.3$	$4.4 \pm 3.4 \pm 1.7$

Based on their mass and width, the $\Xi_c(3080)$ state is proposed to be a strange partner of the spin-parity $J^P = 5/2^+$ $\Lambda_c(2880)^+$ resonance, while the $\Xi_c(2980)$ should have $J^P = 1/2^+$ or $3/2^+$ (Cheng and Chua, 2007; Ebert *et al.*, 2008; Garcilazo *et al.*, 2007; Rosner, 2007).

4. The Ω_c states

a. Ω_c: The discovery of the Ω_c ($= csd$) marked a milestone, it completed the number of stable single-charmed baryons. The first evidence for it was reported in (Biagi *et al.*, 1985) and confirmed in several experiments. We quote here its mass (Amsler *et al.*, 2008)

$$M_{\Omega_c} = 2697.5 \pm 2.6 \,\mathrm{MeV} \qquad (3)$$

The Ω_c lifetime (see Table I) was measured by the WA89 collaboration at CERN and, recently, by the FOCUS and SELEX experiments at Fermilab. The SELEX (E781) experiment used 600 GeV/c Σ^-, π^- and p beams (Iori *et al.*, 2007) while WA89 and Focus are photoproduction experiments. All three experiments reconstructed about 75 Ω_c^0 in the $\Omega^- \pi^- \pi^+ \pi^+$ and $\Omega^- \pi^+$ decay modes.

b. Ω_c^*: Recently, an excited Ω_c state has been discovered by the BaBaR collaboration. Its mass was found to be 70.8 ± 1.5 MeV above the ground state. Hence it is likely the $J^P = 3/2^+$ companion of the Ω_c ground state and was introduced as Ω_c^*. It was produced inclusively in the process $e^+ e^- \rightarrow \Omega_c^* X$, where X denotes the remainder of the event. The Ω_c^* was observed in its radiative decay to the Ω_c ground state. The latter was constructed from
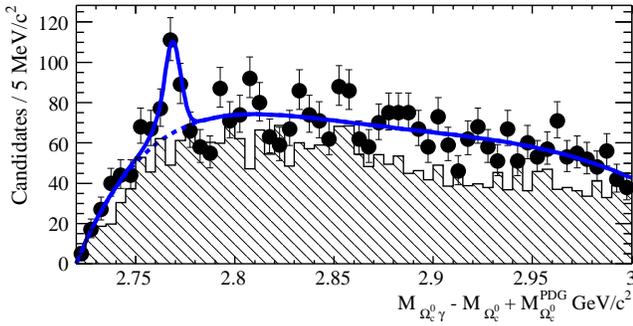
FIG. 7 The invariant mass distributions of $\Omega_c^0\gamma$ candidates, with Ω_c^0 reconstructed in various decay modes. The $M_{\Omega_c^0\gamma}$ mass is corrected for the difference between the reconstructed Ω_c^0 mass and the nominal value $M_{\Omega_c^0}^{\mathrm{PDG}}$. The shaded histograms represent the mass distribution expected from the mass sideband of Ω_c^{*0} (Aubert *et al.*, 2006b).

one of the Ω_c decay sequences

$$\Omega_c^0 \to \Omega^-\pi^+,\ \Omega^-\pi^+\pi^0,\ \Omega^-\pi^+\pi^+\pi^-,\ \Omega^- \to \Lambda K^-$$
$$\mathrm{or}\,\Omega_c^0 \to \Xi^- K^-\pi^+\pi^+,\ \Xi^- \to \Lambda\pi^-$$

Figure 7 shows the $\Omega_c^0\gamma$ invariant mass after all Ω_c decay modes were added up. A significant enhancement (with $5.2\,\sigma$) is observed above a smooth background which is identified with the $J^P = 3/2^+$ excitation of the Ω_c ground state.

5. Double-charm baryons

The SELEX Collaboration reported a statistically significant signal in the $\Lambda_c^+ K^-\pi^+$ invariant mass distribution at $3519 \pm 1\,\mathrm{MeV}$, and a lifetime of less than $33\,\mathrm{fs}$ (90% confidence level) (Mattson *et al.*, 2002), produced in a 600 GeV/c charged hyperon beam. Due to its decay mode, the signal is assigned to production of a doubly charmed baryon, Ξ_{cc}^+. The state was confirmed by SELEX in the $\Xi_{cc}^+ \to pD^+K^-$ decay mode (Ocherashvili *et al.*, 2005). In spite of intense searches, the states failed to be observed in the photoproduction experiment FOCUS (Ratti, 2003) although they observe 19,500 Λ_c^+ baryons, compared to 1.650 observed at SELEX. BaBaR reports a number of reconstructed Λ_c^+ baryons of approximately 600.000 but only upper limits for Ξ_{cc}^+ and Ξ_{cc}^{++} (Aubert *et al.*, 2006c). Of course, SELEX starts with a hyperon beam which may be better suited to produce double-charm baryons. But doubts remain concerning the evidence reported by SELEX.

The lack of double charm baryons at B-factories is surprising. In these experiments, double charm production is abundant, leading in particular to $e^+e^- \to J/\psi + X$ and the discovery of the η_c' in the missing-mass spectrum. One could thus expect double-charm production should hadronize also into two baryon-antibaryon pairs, $\Xi_{cc} + \overline{\Xi}_{cc}$.
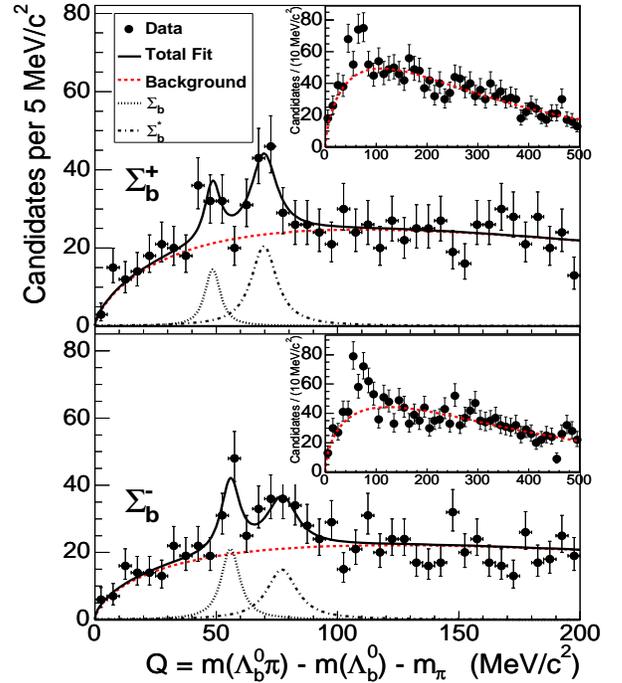
FIG. 8 The invariant mass distributions for the $\Lambda_b^0\pi^+$ (top) and $\Lambda_b^0\pi^-$ (bottom) combinations at CDF.

D. Beautiful baryons

1. The Λ_b states

The Λ_b was discovered early at the CERN ISR (Bari *et al.*, 1991a,b) and later reported by several collaborations. We give here only the PDG values for its mass (Amsler *et al.*, 2008)

$$M_{\Lambda_b} = 5620.2 \pm 1.6\,\mathrm{MeV}; \tag{4}$$

its lifetime is given in Table I.

2. The Σ_b states

a. Σ_b and Σ_b^*: The Σ_b baryon with $J^P = 1/2^+$ and a low-mass excitation identified as $J^P = 3/2^+$ Σ_b^* were discovered recently at Fermilab (Aaltonen *et al.*, 2007a) by the CDF Collaboration in the $\Lambda_b^0\pi^+$ and $\Lambda_b^0\pi^-$ final states (see Figure 8).

The signal region exhibits a clear excess of events even though the statistics is not sufficient to determine mass and widths of the expected Σ_b and Σ_b^*. Therefore the $M(\Sigma_b^{*+})-M(\Sigma_b^+)$ and $M(\Sigma_b^{*-})-M(\Sigma_b^-)$ mass differences were assumed to the same and the widths of the Breit-Wigner resonances were fixed to predictions based on the Heavy Quark Symmetry (Körner *et al.*, 1994). Both the shape and the normalization of the background were determined from Monte-Carlo simulations. The results of the fit are given in Table VIII. The significance of the
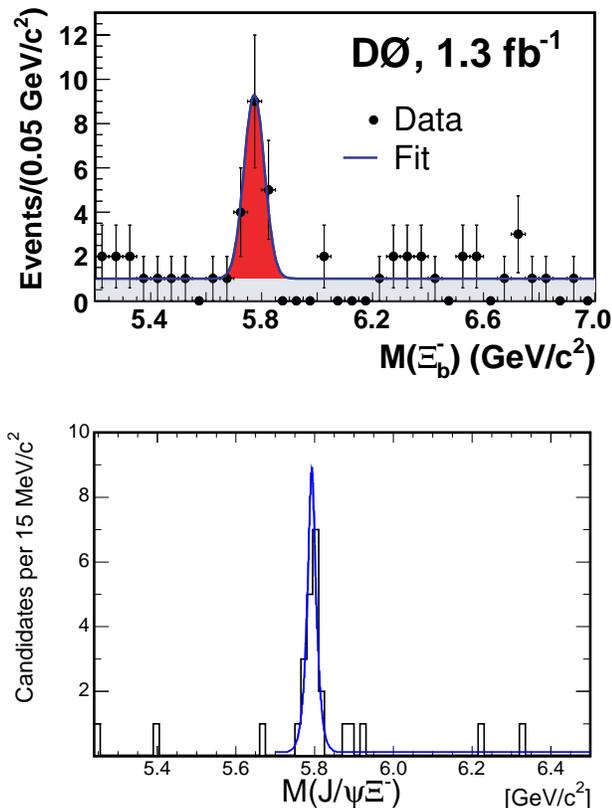
FIG. 9 The invariant mass distributions of the $J/\psi\,\Xi^-$ combinations at DØ (top) (Abazov *et al.*, 2007) and CDF (bottom) (Aaltonen *et al.*, 2007b).

four-peak structure relative to the background only hypothesis is $5.2\,\sigma$ (for 7 degrees of freedom). The significance of every individual peak is about $3\,\sigma$.

3. The Ξ_b states

a. Ξ_b: A further baryon with beauty, the Ξ_b, contains a b, s, and a d quark and thus a negatively charged quark from each family. It was discovered recently at Fermilab (Aaltonen *et al.*, 2007b; Abazov *et al.*, 2007). Its history will be outlined shortly.

Indirect evidence for the Ξ_b^- baryon based on an excess of same-sign $\Xi^-\ell^-$ events in jets was observed from experiments at the CERN LEP e^+e^- collider reported but no candidate events were reported. The first direct observation of the strange b baryon Ξ_b^- ($\overline{\Xi}_b^+$) was achieved at Fermilab (Abazov *et al.*, 2007) by the DØ collaboration by reconstruction of the decay sequence $\Xi_b^- \rightarrow J/\psi\,\Xi^-$, with $J/\psi \rightarrow \mu^+\mu^-$, and $\Xi^- \rightarrow \Lambda\pi^- \rightarrow p\pi^-\pi^-$ as outlined in Fig. 9a. The CDF collaboration reported a more precise mass value. Their $J/\psi\,\Xi^-$ invariant mass distribution exhibits a significant peak (Aaltonen *et al.*, 2007b) at a mass of

$$M_{\Xi_b} = 5792.9 \pm 2.5 \pm 1.7\,\mathrm{MeV} \tag{5}$$

which is presented in Fig. 9b. The measured parameters of the Ξ_b^- are given in Table IX.

The results of DØ and CDF are consistent.

4. The Ω_b

Figure 10 shows evidence for the Ω_b^- baryon recently reported by the DØ collaboration. It was reconstructed from the decay sequence $\Omega_b^- \rightarrow J/\psi\,\Omega^-$, with $J/\psi \rightarrow \mu^+\mu^-$, $\Omega^- \rightarrow \Lambda K^-$ and $\Lambda \rightarrow p\pi^-$. The signal has a statistical significance exceeding 5σ. Its mass was reported to be (Abazov *et al.*, 2008)

$$M_{\Omega_b} = 6.165 \pm 0.010 \pm 0.013\,\mathrm{GeV}. \tag{6}$$

Its mass is unexpectedly high, see section IV.C.

E. Summary of heavy baryons

The masses of heavy baryons are summarized in Table X. For most resonances, the quantum numbers have not been measured, except for the $\Lambda_c^+(2880)$ for which $J^P = 5/2^+$ is suggested. The quantum numbers of $J^P = 5/2^+$ the lowest-mass states can be deduced from the quark model. Determination of quantum numbers of heavy baryons is an important task for the future.

Figure 11 shows the flavor dependence of the mass difference between $J^P = 5/2^+$ and ground states. The mass gap between $\Lambda_c^+(2880)$ and Λ_c^+ is smaller than that of light-quark baryons. To test this conjecture we compare the spectrum of all observed Λ_c^+ baryons with their light-quark analogue states.

In Fig. 12, the excitation spectra of Λ, Λ_c^+, and Ξ_c are compared. In the three lowest states, the light quark pair has spin 0. In the Ξ_c spectrum, there are two additional states, the Ξ_c' with spin $1/2$ and $\Xi_c(2645)$ with spin $3/2$, in which the light quark pair has spin 1. These

TABLE IX The parameters of the Ξ_b^- measured by DØ and CDF.

	Yield	Mass, MeV/c^2	Significance
D0	$15.2 \pm 4.4^{+1.9}_{-0.4}$	$5774 \pm 11 \pm 15$	$5.5\,\sigma$
CDF	17.5 ± 4.3	$5792.9 \pm 2.5 \pm 1.7$	$7.7\,\sigma$

TABLE VIII Results of the $\Sigma_b^{(*)}$ fit.

$m(\Sigma_b^+) - m(\Lambda_b^0) = 188.1^{+2.0+0.2}_{-2.2-0.3}\,\mathrm{MeV}/c^2$
$m(\Sigma_b^-) - m(\Lambda_b^0) = 195.5 \pm 1.0 \pm 0.2\,\mathrm{MeV}/c^2$
$m(\Sigma_b^*) - m(\Sigma_b) = 21.2^{+2.0+0.4}_{-1.9-0.3}\,\mathrm{MeV}/c^2$

TABLE X Masses (in MeV) of heavy baryons quoted from (Amsler *et al.*, 2008) except for Σ_b and Ω_b (see text). The precision is truncated to 100 keV. The isospin of $\Lambda_c^+/\Sigma_c^+(2765)$ (faint) is not known.

Λ_c^+	2286.5±0.2	2595.4±0.6	2628.1±0.6	2766.6±2.4	2881.5±0.4
Σ_c^{++}	2454.0±0.2	2518.4±0.6	2801^{+4}_{-6}		$\mid \Lambda_c^+$: 2939.3±1.4
Σ_c^+	2452.9±0.4	2517.5±2.3	2792^{+14}_{-5}	2766.6±2.4	
Σ_c^+	2453.8±0.2	2518.0±0.5	2802^{+4}_{-7}		
Ξ_c^+	2467.9±0.4	2575.7±3.1	2646.6±1.4	2789.2±3.2	2816.5±1.2
		2969.3±2.8	3054.2±1.3	3077.0±0.5	3122.9±1.3
Ξ_c^0	2471.0±0.4	2578.0±2.9	2646.1±1.2	2791.9±3.3	2818.2±2.1
		2972.9±4.7		3079.3±1.1	
Ω_c^0	2697.5±2.6	2768.3±3.0		$\mid \Xi_{cc}^+$: 3518.9±0.9	
Λ_b^0	5620.2±1.6				
Σ_b^+	5807.8±2.7	5829.0±3.4		$\mid \Sigma_b^-$: 5815.2±2.0	5836.4±2.8
Ξ_b^-	5793.8±3.8			$\mid \Omega_b^-$: 6165±17	

are forbidden for the isoscalar Λ and Λ_c^+. Above these states, a doublet of negative-parity states are the lowest excitations with fully antisymmetric wave functions. In the Λ spectrum, the Roper-like $\Lambda_{1/2^+}(1600)$ follows, and then a doublet – $\Lambda_{1/2^-}(1670)$ and $\Lambda_{3/2^-}(1690)$ – and a triplet – $\Lambda_{1/2^-}(1800)$, $\Lambda_{3/2^-}(xxx)$, and $\Lambda_{5/2^-}(1830)$ – of negative parity states. The $\Lambda_{1/2^+}(1810)$ might be the analogue of $N_{1/2^+}(1710)$ and $\Delta_{1/2^+}(1750)$.

Far above, a spin doublet $\Lambda_{3/2^+}(1890)$ and $\Lambda_{5/2^+}(1820)$ is known. It is very tempting to assign $1/2^+$ quantum numbers to the isolated states in all three spectra, followed by a doublet of negative-parity states. This scenario is, however, ruled out by the $5/2^+$ assignment to $\Lambda_c^+(2880)$. We urge that the quantum number measurement should be repeated.

The CDF and $D\!\!/\!\!O$ experiments have demonstrated the potential of hadron machines for the discovery of new baryon resonances. At LHC, double charmed baryons should be produced abundantly, a total number of 10^9 is estimated by (Berezhnoi *et al.*, 1998), and one may even dream of (ccc) baryons. Baryons (and mesons) with b quarks and their excitations will also be produced; such events should not be thrown away at the trigger level.
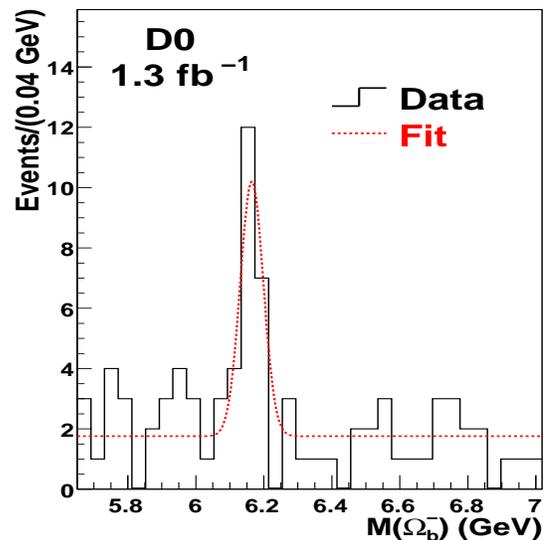
FIG. 10 The $M(\Omega_b^-)$ distribution of the Ω_b^- candidates after all selection criteria. The dotted curve is an unbinned likelihood fit to the model of a constant background plus a Gaussian signal.
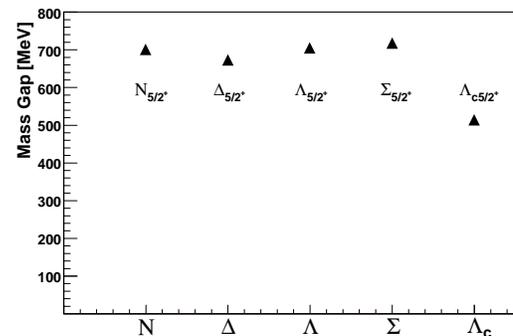
FIG. 11 Mass gap from the respective ground states to the lowest excitation with $J^P = 5/2^+$.
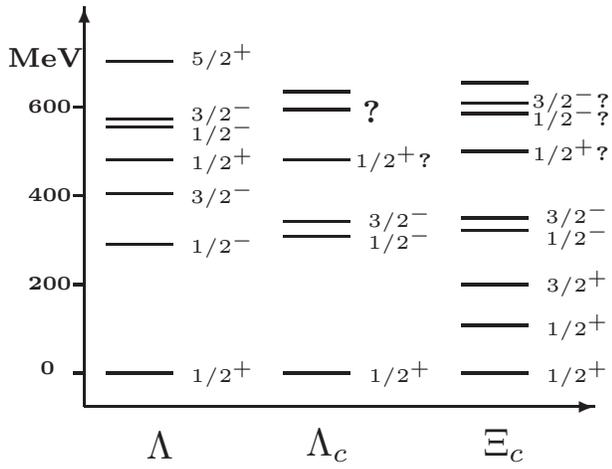
FIG. 12 Excitation spectrum of Λ, Λ_c^+, and Ξ_c. Between $\Lambda_{3/2^-}(1690)$ and $\Lambda_{5/2^+}(1690)$ there are two further states which are omitted for clarity. The quantum number assignments of Λ_c, and Ξ_c follow (Amsler *et al.*, 2008), those with question marked are our tentitive assignments. The $\Lambda_c(2880)$, marked **?** is measured to have $J^P = 5/2^-$ (Abe *et al.*, 2007).

III. LIGHT-QUARK BARYON RESONANCES

In this section we give a survey of data which have been reported in recent years and give an outline of partial wave analysis methods used to extract the physical content from the data.

A. Pion- (kaon-) nucleon elastic and charge exchange scattering

1. Cross sections

The dynamical degrees of freedom of three quarks bound in a baryon lead to a very rich excitation spectrum. It is obviously impossible to observe them all as individual resonances but a sufficiently large number of states should be known to identify the proper degrees of freedom and their effective interactions. First insight into the experimental difficulties can be gained by inspecting, in Fig. 13, the total cross section for elastic $\pi^\pm$ scattering off protons. The $\pi^+ p$ cross section is dominated by the well-known $\Delta_{3/2^+}(1232)$ resonance. A faint structure appears at $1.7\,\mathrm{GeV}$, slightly better visible in the elastic cross section, a second bump can be identified at 1.9 to $2\,\mathrm{GeV}$ in mass, and a small enhancement is seen at $2.4\,\mathrm{GeV}$. Above this mass, the spectrum becomes structureless. The total cross section for $\pi^- p$ scattering exhibits three distinctive peaks at the $\Delta_{3/2^+}(1232)$, at $1.5\,\mathrm{GeV}$ and at $1.7\,\mathrm{GeV}$; a fourth enhancement at 1.9 GeV is faint, a further peak at $2.2\,\mathrm{GeV}$ leads into the continuum. This is the *missing-resonance* problem. The gradual disappearance of the resonant structures suggest that at least part of the problem is due to the increasingly smaller elastic width of resonances when their masses increase: more and more inelastic channels open, and the resonances decouple from the elastic scattering amplitude. A second problem are overlapping resonances and their large widths. The peaks in Fig. 13 may contain several resonances. Hence a partial wave decomposition is required to determine the amplitudes which contribute to a particular energy bin. Very high statistics and polarization data are required to disentangle the different partial waves. At present, it is an open issue up to which mass baryon resonances can be identified. A second and even more exciting issue is the question whether QCD really supports the full spectrum of three-quark models. In the literature, diquark models are very popular; the experimental resonance spectrum has features which are easily understood assuming quasi-stable diquark configurations within a baryon; however, there are also resonances - albeit with one or two star classification - with require three quarks to participate in the dynamics. Less familiar in this context are two dynamical arguments: an extended object has three axes but the object rotates only around the two axes having minimal/maximal moments of inertia. And, surprisingly, a series of coupled resonators with approximately equal resonance frequencies resonate

coherently after some swinging-in period even if the oscillators start with random phases and amplitudes. Hence there may be restrictions concerning the observable spectrum of baryon resonances.

2. Angular distributions

Most of the peaks in Fig. 13 house several resonances with similar masses but different angular momenta. The differential cross sections $d\sigma/d\Omega$ in Fig. 14 allow for a first insight into the dynamics of the scattering process.

The first striking effect seen from the data is the preference for forward angles ($\theta \leq 40°$) of the scattered pion. The preference for forward pion scattering at low energies reflects the large role of background processes like t-channel exchange with a ρ meson (or a ρ Regge trajectory) transmitting four-momentum from pion to proton. Formation of resonances produces a symmetry between forward and backward scattering, at least at the amplitude level; interference between amplitudes can of course lead to forward-backward asymmetries. Here, it is useful to compare the Clebsch–Gordan coefficients for different reactions:
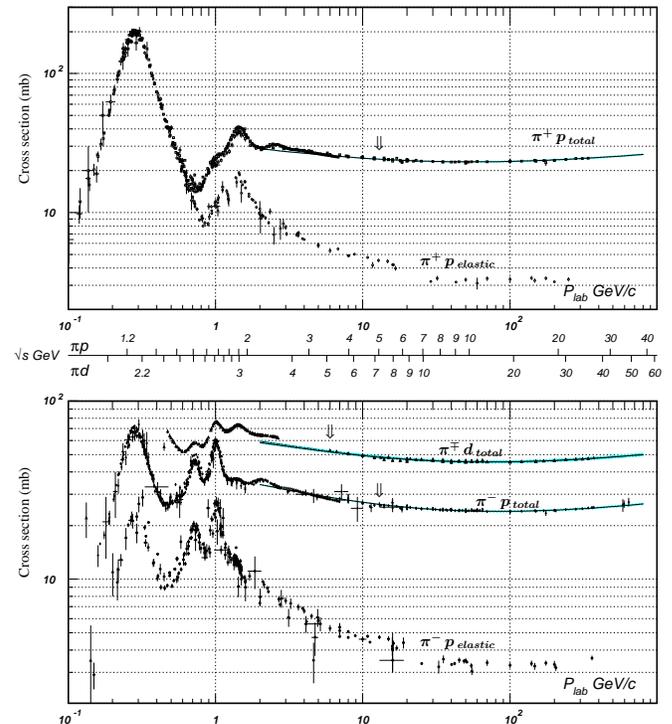
FIG. 13 The total and elastic cross sections for $\pi^\pm$ scattering off protons (Amsler *et al.*, 2008).

	$\pi^- p \to \pi^- p$	$\pi^- p \to \pi^0 n$
s, u-channel N	2/3	$1/3\sqrt{2}$
s, u-channel Δ	1/3	$1/3\sqrt{2}$
t-channel ρ	1	1

The forward cross section for elastic and charge exchange (CEX) have nearly the same size and the interpretation of the forward peak is supported. The backward peak at 1440 MeV is stronger in elastic than in charge exchange scattering suggesting strong isospin 1/2 contribution in the s-channel (via $N(1440)P_{11}$ formation) and/or u-channel nucleon exchange. At $W = 1800$ MeV, there is no CEX forward peak; a complex distribution evolves indicating contributions from high-spin s-channel resonances. The elastic cross section continues to exhibit a strong forward peak due to the exchange of isoscalar mesons, e.g. of the Pomeron. The three processes s-, t-, and u-channel exchange are visualized in Fig. 15. The data were obtained through the Scattering Analysis Interactive Dial-In (SAID) online applications http://gwdac.phys.gwu.edu/. A beautiful example illustrating the effect of t- and u-channels exchanges is shown in Fig. 16. For forward pions, the four-momentum transfer $t = -q^2$ to the proton is small; a diffractive-like decrease of the cross section as a function of t is observed. The peak is due to meson exchange in the t-channel, mostly of ρ and ω; in analyses, the exchange is reggeized to include higher mass ρ and ω excitations. The slope corresponds to the ρ/ω mass. For very large (negative) $t = -2k^2(1-\cos\theta)$, $u-2k^2(1+\cos\theta)$ becomes a small number. The slope is smaller and corresponds to the nucleon mass.

The differential cross sections σ are related to the

FIG. 15 Pion nucleon scattering: a) s-channel exchange; b) u-channel exchange; c) t-channel exchange.
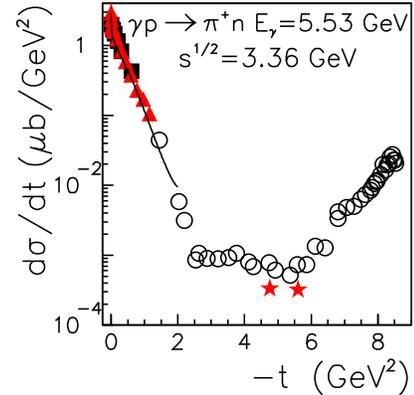
FIG. 16 The $\gamma p \to n\pi^+$ differential cross section as a function of $-t$ for $E_\gamma = 5.53$ GeV (Sibirtsev *et al.*, 2007). The data are from (Anderson *et al.*, 1969, 1976; Zhu *et al.*, 2005).

transversity scattering amplitudes

$$\sigma = |f^+|^2 + |f^-|^2 \tag{7}$$

which can be decomposed into the nucleon spin-flip amplitude g and the non-flip amplitude h, $f^+ = g + ih$, $f^- = g - ih$. The latter amplitudes can be expanded into the partial waves

$$g(k, \theta) = \frac{1}{k}\sum_l [(l+1)a_{l+} + la_{l-}] \, P_l(\cos\vartheta) \tag{8a}$$

$$h(k, \theta) = \frac{1}{k}\sum_l [a_{l+} - a_{l-}] \sin\vartheta P_l'(\cos\vartheta) \tag{8b}$$

where k is the momentum and ϑ the scattering angle in center-of-mass system. The expansion into Legendre polynomials extends over all angular momenta l, the $\pm$ sign indicates that the total angular momentum is $J = l \pm 1/2$. The dimensionless partial wave amplitudes $a_{l\pm} = [\eta_{l\pm}\exp(2i\delta_{l\pm})]/2i$ are related to the inelasticities $\eta_{l\pm}$ and the phase shifts $\delta_{l\pm}$.

It is obvious that the two amplitudes cannot be deduced from the differential cross sections alone. Polarization observables need to be measured. We discuss the polarization P and the two spin rotation parameters A and R.

FIG. 14 Differential cross section for several different center of mass energies. Solid curves correspond to our model while blue dashed lines correspond to the SP06 solution of SAID http://gwdac.phys.gwu.edu/.
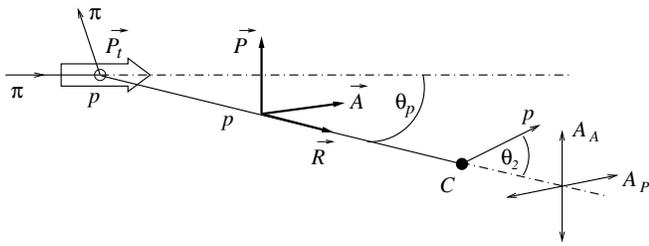
FIG. 17 Definition of polarization variables (Alekseev *et al.*, 2006).

3. Polarization variables

The polarization variable P can be measured using a polarized target. If the proton polarization vector is parallel to the decay-plane normal, there is, at any laboratory scattering angle θ, a left-right asymmetry of the number of scattered pions which defines P. The polarization of the scattered proton does not need to be known. Thus large data sets exist where P was determined, from Rutherford (Cox *et al.*, 1969), (Martin *et al.*, 1975), (Brown *et al.*, 1978) and from CERN (Albrow *et al.*, 1970, 1972), among other places. P constrains the amplitudes but does not yet yield a unique solution:

$$P\,\sigma_{\text{tot}} = |f^+|^2 - |f^-|^2 \qquad (9)$$

Further variables need to be measured. Figure 17 shows the definitions of polarization variables which can be deduced in πN elastic scattering off longitudinally polarized protons. The proton is deflected by an angle θ_{p} in the laboratory system. The proton polarization vector now has a component P which is perpendicular to the scattering plane, a component R along its direction of flight, and a component A along the third orthogonal direction. The components A and P can be measured by scattering the recoil proton off a Carbon foil as indicated in Fig. 17. The analyzing power of the π Carbon scattering process leads to a left-right asymmetry of the proton count rate A_P in the scattering plane; analogously, the A_A parameter can be determined by measuring the up-down asymmetry of proton count rate. The relation between R, A and the scattering amplitudes are given by

$$(R + iA)\,\sigma_{\text{tot}} = f^+ f^- \exp[-i(\vartheta_{cm} - \theta_p)]. \qquad (10)$$

The polarization parameters obey the relation

$$P^2 + A^2 + R^2 = 1. \qquad (11)$$

As can been seen from eqs. (7) and (9), a measurement of the differential cross-section and of the polarization P are not sufficient to reconstruct the complex amplitudes f^+ and f^- but only their absolute values. Recoil polarization data require a secondary interaction of the scattered nucleon. Such experiments have been performed at Gatchina (Alekseev *et al.*, 1991, 1995, 1997, 2000, 2006),

at Los Alamos (Mokhtari *et al.*, 1985, 1987; Seftor *et al.*, 1989) and a few other laboratories but only over a limited energy range. An unbiased energy-independent partial wave analysis is therefore not possible. Constraints from dispersion relations are necessary to extract meaningful partial wave amplitudes. For baryon masses and widths, the PDG refers mostly to five analyses which we call the reference analyses. Other results are mostly not used to calculate averages.

The analyses of the Karlsruhe-Helsinki (KH) and Carnegie-Mellon (CM) groups were published 1979 and 1980, respectively; still today, they contain the largest body of our knowledge on N^* and Δ^* as listed by the PDG. The Kent group made a systematic study of the inelastic reactions $\pi N \rightarrow N\pi\pi$. Hendry presented data taken on elastic πN scattering at 14 momenta in the range from $1.6\,\text{GeV}$ to $10\,\text{GeV}$ and extracted resonance contributions. The Virginia Tech Partial-Wave Analysis Facility (SAID) (which moved to the George Washington University ten years ago) included more and more data on πN scattering, in particular from Gatchina, Los Alamos, PSI, and TRIUMF, and publishes regularly updated solutions. In a first step, energy-independent partial wave amplitudes are constructed, and then energy dependent partial-wave fits are performed using a coupled-channel Chew–Mandelstam K-matrix. The results may not satisfy all of the requirements imposed by analyticity and crossing symmetry. These requirements are then addressed at fixed four-momentum transfer t by a complete set of fixed-t dispersion relations, which are handled iteratively with the data fitting. Fig. 18 shows the reconstructed amplitudes for some partial waves.

4. K-nucleon elastic scattering

Kaon–nucleon scattering remains at a standstill since 1980; a survey of achievements up to 1980 was presented by (Gopal, 1980). For this reason, we do not elaborate on hyperon spectroscopy in this review. We will just mention a few recent results from a low-momentum kaon beam at BNL in which differential and total cross sections and the induced hyperon polarization have been measured.

B. Inelastic π and K nucleon scattering and other reactions

Inelastic reactions like $\pi^- p \rightarrow n\pi^+\pi^-$ and $\pi^- p \rightarrow p\pi^0\pi^-$ and similar kaon induced reactions require large solid-angle coverage of the detector. The Large Aperture Superconducting Solenoid (LASS) spectrometer at SLAC was the last experiment having an intense 11 GeV/c kaon beam at its disposal. The main results are reviewed in (Aston *et al.*, 1990). The experiment had a very significant impact on the spectroscopy of mesons with open or
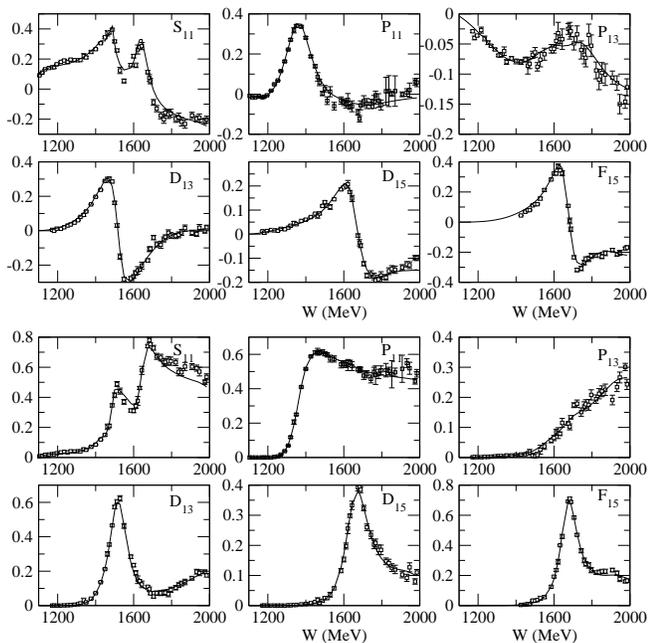
FIG. 18 Fit to the $I = \frac{1}{2}$ $Re(T_{\pi N, \pi N})$ and $Im(T_{\pi N, \pi N})$ of SAID http://gwdac.phys.gwu.edu/.

hidden strangeness. At that time the focus of the community was on glueballs and hybrids, and the LASS data were important as reference guide for quarkonium states. The data contained information on strange baryons, as well (Wright *et al.*, 1995). Lack of interest and shortage of manpower prevented an analysis of this unique data set. Only evidence for one baryon resonance was reported, an Ω^* at 2474 ± 12 MeV mass and 72 ± 33 MeV width (Aston *et al.*, 1988), in its $\Omega \pi^+ \pi^-$ decay.

The absence of appropriate beams and detectors gave a long scientific lifetime to results obtained by the use of bubble chambers in the sixties and seventieth. The most important results were reviewed by (Manley *et al.*, 1984) who fitted and data and provided amplitudes for the most important isobars. At low energies, data were recorded by the OMICRON collaboration at the CERN synchro-cyclotron (Kernel *et al.*, 1989a,b, 1990) and TRIMF and Los Alamos (Lowe *et al.*, 1991; Pocanic *et al.*, 1994; Sevior *et al.*, 1991).

1. Experiments at BNL

The Crystal Ball detector has an animated history. It started operation in 1978 at SPEAR with studies of radiative transitions between charmonium states (Gaiser *et al.*, 1986). In 1982 it was moved to DESY for spectroscopy of the Υ family and two-photon physics (Bienlein and Bloom, 1981). In the late 90'ties it was transferred to BNL where it was exposed to π^- and K^-

beams, and is presently installed at MAMI for photoproduction experiments (see section III.C). The ball consists of 672 NaI detectors covering $\approx 94\%$ of 4π.

The main results from BNL will be summarized in this section.

a. $\pi^- p \to n\pi^0$ and $n\eta$: The Crystal Ball collaboration measured the reaction $\pi^- p \to n\eta$ from threshold to 747 MeV/c pion momentum (Kozlenko *et al.*, 2003; Prakhov *et al.*, 2005) (see Fig. 19). Angular distribution with nearly full angular coverage were reported for seven π^- momenta. The total cross section $d\sigma_{tot}$ was obtained by integration of $d\sigma/d\Omega$. The rapid increase of the cross section and the rather flat angular distributions indicate that $N_{1/2^-}(1535)$ is formed as intermediate state. A small quadratic term reveals contributions from the $N\eta$ D-wave due to $N_{3/2^-}(1520)$. The effect of the η production-threshold can be seen in pion charge exchange $\pi^- p \to n\pi^0$ (Starostin *et al.*, 2005) in the form of a small cusp. For the latter reaction, the Crystal Ball collaboration measured precise differential cross section in the momentum interval $p_\pi = 649\text{-}752$ MeV/c. The cusp is rather weak and not as dramatic as in pion photoproduction. The Δ region was studied with full solid angle coverage using eight different momenta (Sadler *et al.*, 2004).

b. $K^- p \to \Lambda \pi^0$, $\Sigma^0 \pi^0$, and $\Lambda\eta$: The reaction $K^- p \to \Lambda \pi^0$ was studied in the mass range from 1565 to 1600 MeV (Olmsted *et al.*, 2004). Differential cross sections and induced Λ polarization were reported for three K^- momenta. The data were shown to be incompatible with the claimed existence of $\Sigma_{3/2^-}(1580)$, a one-star candidate with properties not fitting into expectations based on $SU(3)_f$ symmetry. A different assignment is proposed by (Melde *et al.*, 2008).

Differential distributions and hyperon recoil polarization were also reported for the reaction $K^- p \to \Sigma^0 \pi^0$
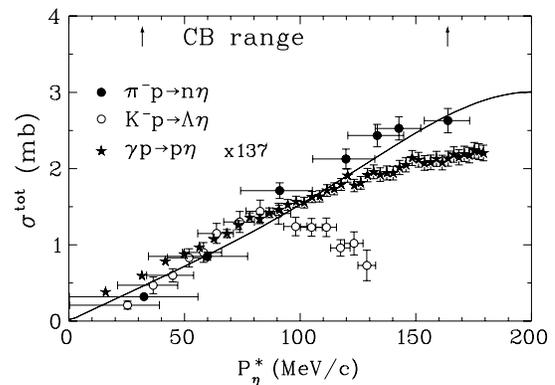
FIG. 19 Total cross section for $\pi^- p \to n\eta$, $K^- p \to \Lambda\eta$ and $\gamma p \to p\eta$ (Prakhov *et al.*, 2005). The later cross section is scaled by a factor 137.

TABLE XI Decay branching ratios to baryon plus η of spin-1/2 negative parity baryons.

Decay mode	Fraction	Decay mode	Fraction
$N_{1/2^-}(1535) \to N\eta$	45-60%	$N_{1/2^-}(1650) \to N\eta$	3-10%
$\Lambda_{1/2^-}(1670) \to \Lambda\eta$	10-25%	$\Lambda_{1/2^-}(1800) \to \Lambda\eta$	not seen
$\Sigma_{1/2^-}(1620) \to \Sigma\eta$	not seen	$\Sigma_{1/2^-}(1750) \to \Sigma\eta$	15-55%

at eight beam momenta between 514 and 750 MeV/c. The(forthcoming) partial wave analysis could have a significant impact on low-mass Λ states (Manweiler *et al.*, 2008).

Particularly interesting is the reaction $K^-p \to \Lambda\eta$ (Manley *et al.*, 2002). The cross section rises steeply from threshold and reaches a maximum of about $(1.4\,mb)$ at about $W = 1.675\,\mathrm{GeV/c}^2$. The data show a remarkable similarity to the SU(3)$_\mathrm{f}$ flavor-related $\pi^-p \to p\eta$ cross section. The latter is dominated by $N_{1/2^-}(1535)$, the former by formation of the intermediate $\Lambda_{1/2^-}(1670)$ state, for which mass and width, respectively, of $M = 1673 \pm 2\,\mathrm{MeV}$ and width $\Gamma = 23 \pm 6\,\mathrm{MeV}$, and an elasticity $x = 0.37 \pm 0.07$ were measured. The fraction with which $\Lambda_{1/2^-}(1670)$ decays to $\Lambda\eta$ is determined to $(16 \pm 6)\%$. Resonance parameters and decay modes are in striking agreement with the quark-model predictions of Koniuk and Isgur (Koniuk and Isgur, 1980) but disagree with the results of an analysis using a Bethe-Salpeter coupled-channel formalism incorporating Chiral Symmetry (Garcia-Recio *et al.*, 2003). The latter analysis finds a $\Lambda\eta$ decay fraction of $(68 \pm 1)\%$ and an inelasticity of $(24 \pm 1)\%$.

In both cases, the branching ratio of $\Lambda_{1/2^-}(1670)$ for decays into $\Lambda\eta$ is much larger than that of other resonances. In Table XI we list the branching ratios of negative-parity spin-1/2 resonances for decays into η mesons. We notice that for $N_{1/2^-}$, the lower mass state (mainly $s = 1/2$) has a strong coupling the $N\eta$ while it is smaller by about one-order-of-magnitude for the higher-mass state (mainly $s = 3/2$). The situation is similar for $\Lambda_{1/2^-}$ but opposite for $\Sigma_{1/2^-}$. We note that in $\Lambda_{1/2^-}$, the ud diquark has isospin zero while for $\Sigma_{1/2^-}$ $I = 1$. The connection is not yet understood.

c. $\pi^-p \to n2\pi^0$, $K^-p \to \Lambda2\pi^0$ *and to* $\Sigma2\pi^0$: Three reactions leading to $2\pi^0$ in the final state were studied; $\pi^-p \to n2\pi^0$ from threshold to 750 MeV/c (Craig *et al.*, 2003; Prakhov *et al.*, 2004b), $K^-p \to \pi^0\pi^0\Lambda$ and $K^-p \to \pi^0\pi^0\Sigma^0$ for p$_{K^-}$ = 514 MeV/c to 750 MeV/c (Prakhov *et al.*, 2004a,c). The cross sections for the three reactions reveals a few interesting patterns. The cross section for $K^-p \to \Lambda2\pi^0$ is smaller than that for $\pi^-p \to n2\pi^0$ by a factor 2. A reduction due to strangeness production is not unexpected. But the cross section for $K^-p \to \Sigma2\pi^0$ is much smaller than the other ones. This requires a dynamical interpretation. If the

reactions would produce σ $(=f_0(500))$ at a sizable rate, one should expect similar cross sections for all three reactions. This is not the case; at least the two reactions $\pi^-p \to n2\pi^0$ and $K^-p \to \Lambda2\pi^0$ must be dominated by production of baryon resonances. A partial wave analysis of the former data revealed a very large contribution of $N_{1/2^+}(1440)$ interfering with $N_{1/2^-}(1535)$ and $N_{3/2^-}(1520)$ (Sarantsev *et al.*, 2008) where $N_{1/2^+}(1440)$ decays via $\Delta\pi$ and via $N\sigma$. The broad shoulder in the $K^-p \to \Lambda2\pi^0$ cross section is tentatively interpreted as evidence for $\Lambda_{1/2^+}(1600)$ decaying via $\Sigma^0_{3/2^+}(1385)\pi^0$ as intermediate state (Prakhov *et al.*, 2004c). A partial wave analysis of the data has not been performed.

2. Baryon excitations from J/ψ and ψ' decays

Baryon resonances can be searched for in final states from J/ψ and ψ' decays into a baryon, an antibaryon and at least one meson. In Table XII, relevant branching fractions are given demonstrating the discovery potential of J/ψ decays for baryon spectroscopy. In particular resonances recoiling against Λ, Σ, $\Sigma(1385)$, Ξ, $\Xi(1530)$ are rewarding. In other reactions, there is no real means to decide if, e.g., $\Sigma_{1/2^-}(1750)$ belong to an SU(3)$_\mathrm{f}$ octet or decuplet, or if it a mixture. Observation of $\Sigma_{1/2^-}(1750)$ recoiling against Σ and/or $\Sigma(1385)$ in ψ' decays would identify its SU(3)$_\mathrm{f}$ nature.

As example for the use of J/psi decays in baryon spectroscopy we show in Fig. 21 the Dalitz plot $M^2_{n\pi}$ vs. $M^2_{p\pi}$ for $J/\psi \to p\pi^-\bar{n}$ decays, and the $p\pi^-$ mass projection. Four peaks can be identified. A partial wave analysis assigns the first peak to $N(1440)P_{11}$ described with Breit-Wigner mass and width of $1358 \pm 6 \pm 16\,\mathrm{MeV}$ and $179 \pm 26 \pm 50\,\mathrm{MeV}$, the N^* peaks at 1500 MeV and 1670 MeV are identified with the well known second and third resonance region, and the forth peak is interpreted as a new N^* resonance with $2068 \pm 3^{+15}_{-40}\,\mathrm{MeV}$ mass and width of $165 \pm 14 \pm 40\,\mathrm{MeV}$. The fit prefers zero angular
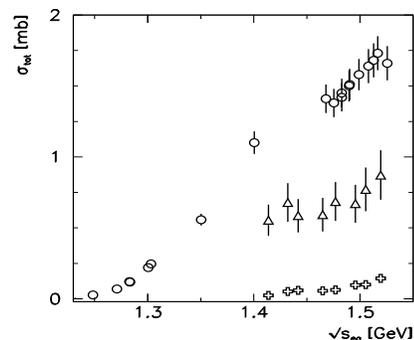
FIG. 20 The total cross sections as functions of the *equivalent total energy* $\sqrt{s_{eq}}$, defined as the standard s for pions and as $\sqrt{s_{eq}} \equiv \sqrt{s} - (m_s - m_d)$ for incident kaons. Circles: $\sigma_{tot}(\pi^-p \to \pi^0\pi^0n)$. Triangles: $\sigma_{tot}(K^-p \to \pi^0\pi^0\Lambda)$. Crosses: $\sigma_{tot}(K^-p \to \pi^0\pi^0\Sigma^0)$.

TABLE XII J/ψ and ψ' branching ratios for decays into final states containing mesons and baryons.

	J/ψ		ψ'	
$N\bar{N}\pi$	(9.7 ± 0.6)	10^{-3}	(7.6 ± 0.6)	10^{-4}
$p\bar{p}\pi^+\pi^-$	(6.0 ± 0.5)	10^{-3}	(7.6 ± 0.6)	10^{-4}
$N\bar{N}\eta$	(4.18 ± 0.36)	10^{-3}	(0.58 ± 0.13)	10^{-4}
$\Lambda\bar{\Lambda}\eta$	(0.26 ± 0.08)	10^{-3}	< 1.2	10^{-4}
$pK^-\bar{\Lambda}$	(0.9 ± 0.2)	10^{-3}		
$pK^-\bar{\Sigma}^0$	(0.29 ± 0.08)	10^{-3}		
$\Sigma\bar{\Lambda}\pi$	(0.23 ± 0.03)	10^{-3}		

momentum between the new N^* and the recoiling nucleon. Then the quantum numbers must be P_{11} or P_{13}. If $L = 1$ would be admitted, S_{11}, D_{13} and D_{15} would be possible as well.

C. Photoproduction experiments, a survey

1. Aims of photoproduction experiments

a. How many baryon resonances are known? Baryon spectroscopy defined by πN elastic scattering is at a bifurcation point. The listings of the PDG give a large number of baryon resonances which were reported by the analyses of the Karlsruhe-Helsinki group (Höhler *et al.*, 1979) and of the Carnegie-Mellon group (Cutkosky *et al.*, 1980), with star ratings from 1-star to 4-star. In the most recent analysis of the George-Washington group (Arndt *et al.*, 2006), including a large number of additional data sets from pion factories (even though mostly at low energy), practically only the 4-star resonances are confirmed. A very decisive question is therefore if Höhler is right in his critique of the GWU analysis that the method used by the GWU group suppresses weak higher-mass resonances (Höhler, 2004). The confirmation of a few resonances found by (Höhler *et al.*, 1979) and (Cutkosky *et al.*, 1980) and questioned by (Arndt *et al.*, 2006) would already help to give credit to the old analyses.
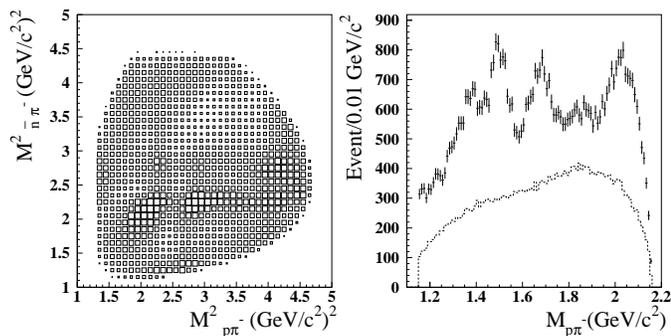
FIG. 21 Dalitz plots of $M^2_{n\pi}$ vs. $M^2_{p\pi}$ for $J/\psi \to p\pi^-\bar{n}$ and $p\pi^-$ invariant mass spectrum.

b. How many baryon resonances are expected? As will be shown below, quark models predict a very large number of baryon resonances. Experimentally, the density of states in the mass region above $1.8\,\text{GeV}$ is much smaller than expected. A reason might be that these *missing resonances* decouple from the πN channel. Then they escape detection in πN elastic scattering. These resonances are expected to have no anomalously low helicity amplitudes; then they must show up in photoproduction of multiparticle final states.

c. What is the structure of baryon resonances? Electroproduction of baryon resonances provides additional information, inaccessible to πN scattering. Helicity amplitudes, form factors, (generalized) polarizabilities can be extracted. Intense experimental and theoretical efforts have, e.g., been devoted to determinations of the E_2/M_1 (electric quadrupole versus magnetic dipole) and C_2/M_1 (longitudinal electric quadrupole versus magnetic dipole) ratio for the $N \to \Delta(1232)$ transition amplitude. For a review of the hadron structure at low-Q^2, see (Drechsel and Walcher, 2008).

2. Experimental facilities

a. Bubble chambers: Very early, in the late 60ties of last century, photoproduction was studied in bubble chamber experiments. Results at DESY were summarized by (Erbe *et al.*, 1968), those from SLAC by (Ballam *et al.*, 1972, 1973).

a. NINA: The electron synchrotron NINA at Daresbury was used to study photoproduction reactions. We quote here only two of their late publications (Barber *et al.*, 1982, 1984) where ref erences to earlier work can be found.

a. Jlab: The continuous electron beam accelerator facility at the Department of Energy's Thomas Jefferson National Accelerator Facility (Jlab) delivers a 6 GeV primary electron into three different experimental areas, Halls A, B, and C, for simultaneous experiments. Halls A and C both have two spectrometers; in Hall A, two identical high-resolution with a maximum momentum of 4 GeV/c are installed while in Hall C one is dedicated to analyze high-momentum particles, the other has a short path length for the detection of decaying particles. Hall B houses the Jlab Large Acceptance Spectrometer (CLAS), the detector most relevant for baryon spectroscopy. The CLAS detector is based on a six-coil toroidal magnet which provides a largely azimuthal field distribution. Particle trajectories are reconstructed, using drift chambers, with a momentum resolution of

0.5% at forward angles. Cherenkov counters, time-of-flight scintillators, and electromagnetic calorimeters provide good particle identification (Mecking *et al.*, 2003).

b. ELSA: The electron stretcher ring ELSA, in operation since 1987, serves either as post-accelerator and pulse stretcher delivering a continuous electron beam (1nA, duty factor ≈ 70%) with up to 3.5 GeV energy. ELSA is fed by a 20 MeV linear accelerator and a 2.3 GeV synchroton. Two detectors were installed at ELSA, SAPHIR and CBELSA in different configurations. SAPHIR was a magnetic detector with a central drift chamber, with a magnetic field perpendicular to the beam axis and the target placed in the centre of the CDC. Forward hodoscopes in coincidence with the tagging system gave a fast trigger and provided particle identification by measuring the time of flight (Schwille *et al.*, 1994). It was dismantled in 1999. The CBELSA experiment is based on the 4π photon detector Crystal Barrel (Aker *et al.*, 1992) which had been moved in 1997 from LEAR/CERN to Bonn. An inner scintillating fiber detector is used for charged particle detection and trigger purposes (van Pee *et al.*, 2007). Later, the forward direction was covered by the TAPS (Elsner *et al.*, 2007) or a MiniTaps detector.

c. ESFR: The GRAAL experiment was installed at the European Synchrotron Radiation Facility (ESRF) in Grenoble (France). The tagged and polarized γ-ray beam is produced by Compton scattering of laser photons off the 6 GeV electrons circulating in the storage ring. The tagging system uses 128 silicon microstrips with a pitch of 300 μm. The shortest UV wave length used so far was 351 nm yielding a maximal γ-ray energy of 1.5 GeV. Photons coming from neutral decay channels of π^0 and η are detected in 480 21-radiation-lengths BGO crystals supplemented by a lead-scintillator sandwich ToF wall in forward direction. The proton track is measured by two cylindrical Multi-Wire Proportional Chambers with striped cathodes and two forward planar chambers. Charged particle are identified by dE/dx and Time-of-Flight measurement (Bartalini *et al.*, 2005).

d. SPring-8: The LEPS (laser electron photons at SPRING-8) detector uses backscattered photons from the 8 GeV stored electron beam producing a tagged γ-ray beam of up to 2.4 GeV. The LEPS spectrometer consists of a wide-gap dipole magnet with charged-particle tracking detectors. An array of scintillator bars 4 meters downstream of the target and scintillator just behind the target provided a time-of-flight information. Electron-positron pairs were vetoed by an aerogel Cherenkov detector.

e. MAMI: The electron accelerator MAMI consists of three cascaded racetrack microtrons and a harmonic double-sided microtron for final acceleration. A linear accelerator provides a 4 MeV beam, the racetrack microtrons 15, 180 and 855 MeV. The maximum energy at the end of the fifth stage is 1.5 GeV, with a beam current

of up to 100 μA. Photons can be provided with linear or circular polarization. The development of a polarized target is finalized.

A major installation for baryon spectroscopy is the Crystal Ball detector (see: *Experiments at BNL* in section III.B). The detector capabilities are strengthened by a forward wall TAPS consisting of 510 hexagonally shaped BaF$_2$ detectors.

3. Total cross sections for photo-induced reactions

The total photo-absorption cross section shown in Fig. 22 exhibits a large peak ($\approx 500 \, \mu$b) due to $\Delta(1232)$ production, shows some structures in the second and third resonance region and levels off at about 150 μb a a few GeV. At very high energies, the photon splits into a $q\bar{q}$ pair with vector-meson quantum numbers and the interaction between proton and photon is dominated by Pomeron exchange exhibiting the typical relativistic rise in the multi-GeV energy range. The structure of the photon and its interaction with protons, a central issue at H1 and ZEUS, is beyond the scope of this article; we refer the reader to a review by (Butterworth and Wing, 2005).

4. The GDH sum rule

The photoproduction cross section depends on the helicity of proton and photon. The total helicity may be 3/2 or 1/2; the fractional difference

$$E = \frac{\sigma_{3/2} - \sigma_{3/2}}{\sigma_{3/2} + \sigma_{3/2}}$$

is an important quantity. Such measurements require circularly polarized photons and a target of polarized protons.

The development of techniques to produce polarized targets and photons has a long history. The most recent driving force for this development was the chance to test the Gerasimov-Drell-Hearn sum rule (Drell and Hearn, 1966; Gerasimov, 1966)

$$\int_0^\infty \frac{dE_\gamma}{E_\gamma} \left[\sigma_{3/2}(E_\gamma) - \sigma_{1/2}(E_\gamma) \right] = \frac{2\pi^2 \alpha}{M_p^2} \kappa_p^2 \qquad (12)$$

which relates the integrated cross-section helicity difference to the anomalous magnetic moment κ_p.

Fig. 23 shows the separate helicity contributions to the total cross section, measured at ELSA (Dutz *et al.*, 2003) and MAMI (Ahrens *et al.*, 2000, 2001, 2003). Obviously, most of the resonance strength of the first three resonances originates from the 3/2 helicity channel. The integrated difference, weighted with $1/E_\gamma$, needs to be corrected for the unmeasured regions. The low-energy part can be estimated using MAID (Mainz Analysis Interactive Dial-In) predictions, the integral from 2.9 GeV
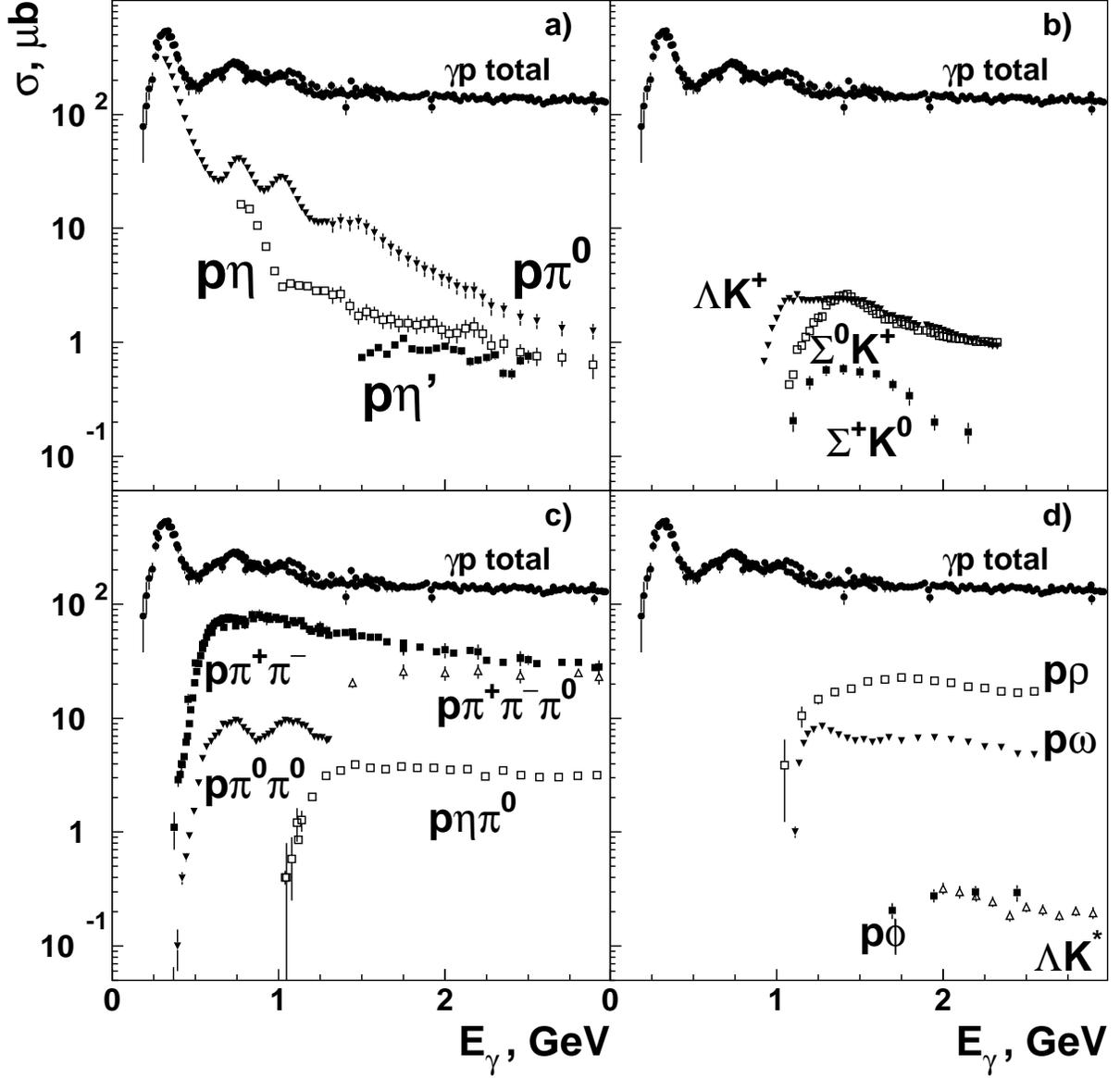
FIG. 22 Total photo-absorption cross section shown and exclusive cross sections for single- and multi-meson production. a: total, $p\pi^0$, $p\eta$, $p\eta'$; b: total, ΛK^+, $\Sigma^0 K^+$, $\Sigma^+ K^0$; c: $p\rho$, $p\omega$, $p\phi$, ΛK^{*+}, $\Sigma^+ K^{*0}$, $\Sigma^0 K^{*+}$; d: $p\pi^+\pi^-$, $p\pi^0\pi^0$, $p\pi^0\eta$, $p\pi^+\pi^-\pi^0$, pK^+K^-.

up to ∞ using deep inelastic scattering data. The comparison of calculated $205\,\mu b$ and measured $212\pm6\pm16\,\mu b$ value shows remarkable agreement (Helbing, 2006).

First measurements of the helicity difference on exclusive final states have been published recently (Ahrens *et al.*, 2006, 2007); these measurements provide an important input to partial wave analyses.

D. Photo-production of pseudoscalar mesons

1. Polarization observables

The differential cross section for electro-production of pseudoscalar mesons off nucleons is given by the product of the flux of the virtual photon field - with longitudinal (L) and transverse (T) polarization - and the virtual differential cross section which depends on 6 response functions ($R_i = R_T, R_L, R_{TL}, R_{TT}, R_{TL'}, R_{TT'}$). The response functions depend on two additional indices characterizing the target polarization and the recoil polariza-
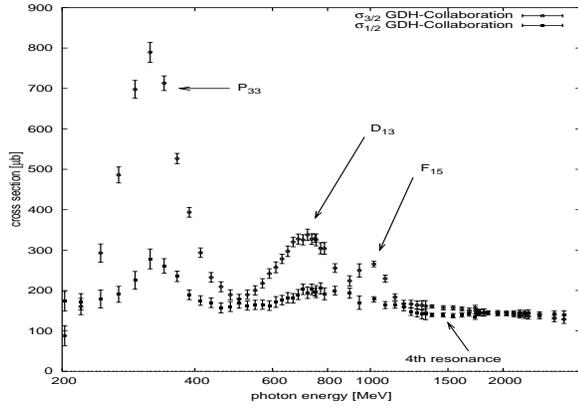
FIG. 23 Separate helicity state total cross sections $\sigma_{3/2}$ and $\sigma_{1/2}$ of the proton.

tion of the final-state baryon. The response functions can be written as CGNL (Chew, Goldberger, Low, Nambu, 1957) or helicity amplitudes. The formalism is tedious; a very useful derivation of formula and a compendium of the relations between the different schemes can be found in (Knöchlein *et al.*, 1995). In photoproduction, the longitudinal component of the photon polarization vector vanishes, and the problem is easier to handle. From the four CGNL amplitudes, *sixteen* bilinear products different can be formed which define the measurable quantities. The differential cross sections can be divided into three classes, for experiments with polarized photons and polarized target (BT, 13a) and experiments using polarized photons and measuring either the baryon recoil polarization (BR, 13b) or using a polarized target (TR, 13c).

$$\sigma = \sigma_0 \big\{ 1 - p_\perp \Sigma \cos 2\varphi + t_x \left(-p_\perp H \sin 2\varphi + p_\odot F \right)$$
$$- t_y \left(-T + p_\perp P \cos 2\varphi \right) \qquad (13a)$$
$$- t_z \left(-p_\perp G \sin 2\varphi + p_\odot E \right) \big\},$$

$$\sigma = \sigma_0 \big\{ 1 - p_\perp \Sigma \cos 2\varphi + \sigma_{x'} \left(-p_\perp O_{x'} \sin 2\varphi - p_\odot C_{x'} \right)$$
$$- \sigma_{y'} \left(-P + p_\perp T \cos 2\varphi \right) \qquad (13b)$$
$$- \sigma_{z'} \left(p_\perp O_{z'} \sin 2\varphi + P_\odot C_{z'} \right) \big\},$$

$$\sigma = \sigma_0 \big\{ 1 + \sigma_{y'} P + t_x \left(\sigma_{x'} T_{x'} + \sigma_{z'} T_{z'} \right)$$
$$+ t_y \left(T + \sigma_{y'} \Sigma \right) \qquad (13c)$$
$$- t_z \left(\sigma_{x'} L_{x'} - \sigma_{z'} L_{z'} \right) \big\} \, .$$

We use $\sigma = 2\rho_f d\sigma/d\Omega$ where ρ_f denotes the density matrix for the final state baryon, σ_0 the unpolarized differential cross section, $p_\perp$ the degree of linear photon polarization, and φ the angle between photon polarization vector and reaction plane, $p_\odot$ the circular photon polarization. The target polarization vector is represented by (t_x, t_y, t_z) with z chosen as photon beam direction and y as normal of the reaction plane. The Pauli matrices $(\sigma'_x, \sigma'_y, \sigma'_z)$ refering to the recoiling baryon are defined in a frame with the momentum vector of the outgoing meson as z'-axis and where the y'-axis is the same as the y-axis. The x and x' axes are defined by orthogonality.

The quantities defined by capital letters (and, of course, the differential cross section σ_0) are those to be determined. Some have traditional names; we mention the beam and target asymmetries Σ and T, the recoil polarization P and the helicity difference of the cross section $E\,\sigma = \sigma_{1/2} - \sigma_{3/2}$. The spin correlation coefficient $C_{x'}, C_{z'}$ ($L_{x'}, L_{z'}$) defines to the transfer of circular (oblique) polarization to a recoiling baryon.

Not all 16 observables need to be measured to arrive at a unique solution (up to an overall phase); relations between the observables reduce the number of required experiments. Seven appropriately chosen experiments can be sufficient but may lead to discrete ambiguities of the solution. Hence a minimum of up to 8 functions need to be measured (Barker *et al.*, 1975; Chiang and Tabakin, 1997). The minimum contains experiments with polarization of photons, target and recoiling baryon. This number may be smaller due to inequalities among observables (Artru *et al.*, 2008). If, e.g., $|A|^2 + |B|^2 \leq 1$, and if a first measurement gives $A \approx -1$, then a measurement of B is not anymore needed.

A set of data which allows for an energy-independent full reconstruction of the amplitude is commonly referred to as a "complete" experiment. Of course, a complete experiment requires the measurement of isospin related channels, and it remains open if the goal can be reached in practice (Workman, 1999).

2. Photoproduction of pions

The structures observed in the total photo-absorption cross section are much more pronounced in single-π^0 photo-production (Fig. 22a); the cross section reaches $400\,\mu$b at the $\Delta(1232)$ position, $40\,\mu$b at the second and $26\,\mu$b at the third resonance peak. There are indications for the forth resonance region; then, the cross section decreases rapidly. The cross section for π^0 production has been derived by integration over differential cross section $d\sigma/d\cos\theta$ where θ is the angle of the π^0 meson with respect to the direction of the photon in the γp rest frame. Most recent data from Jlab (Dugger *et al.*, 2007) and ELSA (Bartholomy *et al.*, 2005; van Pee *et al.*, 2007) cover a large energy and angular range. References to earlier data are listed in (van Pee *et al.*, 2007). The agreement between the data is remarkable; at high energy, small discrepancies in forward direction show up between the ELSA data (which are shown in Fig. 24) and the Jlab data. The Crystal Barrel collaboration has new data in the extreme forward angle which will resolve this discrepancy.

The beam asymmetry is available from MAMI in the low-energy region (Beck, 2006) (shown in Fig. 25) and from GRAAL (Bartalini *et al.*, 2005). Some data on target and proton recoil polarization and a few data on double polarization can be found at the GWU Data Analysis Center http://gwdac.phys.gwu.edu/. Data on the related reaction $\gamma p \rightarrow n\pi^+$ for the low energy region are

dσ/dΩ [μb/sr]
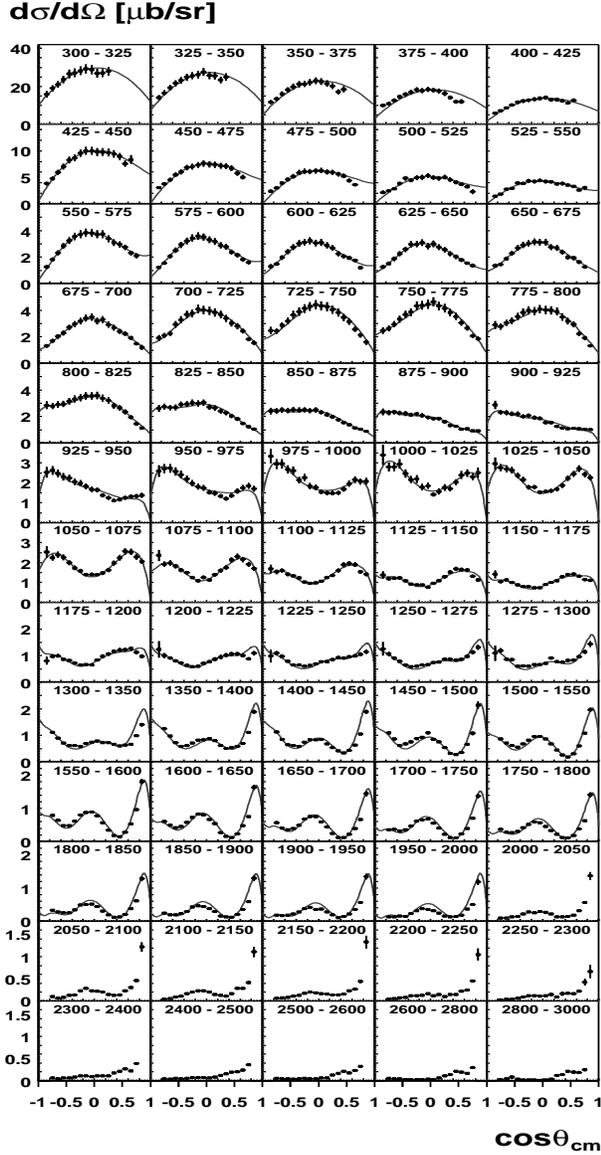
FIG. 24 Differential cross sections for $\gamma p \to p\pi^0$. The solid line represents BnGa, the dashed line the SAID (SM05), and the dotted line the MAID model.

given in (MacCormick *et al.*, 1996), angular distributions and beam asymmetry in (Bartalini *et al.*, 2002). For the photon energies ranged from 1.1 to 5.5 GeV, cross sections for $\gamma n \to p\pi^-$ and $\gamma p \to n\pi^+$ were measured at Jlab (for selected scattering angles) with the aim to test ideas in perturbative QCD (Zhu *et al.*, 2003). Further details and references to earlier data can be found in (Zhu *et al.*, 2005).

Electro-production of pions is sensitive to the Q^2 dependence of electromagnetic transition operators and provides the possibility to determine additional amplitudes; in particular the interference between real and imaginary amplitudes can be determined. The longitudinal amplitude $L_{l\pm}$ and the scalar amplitude
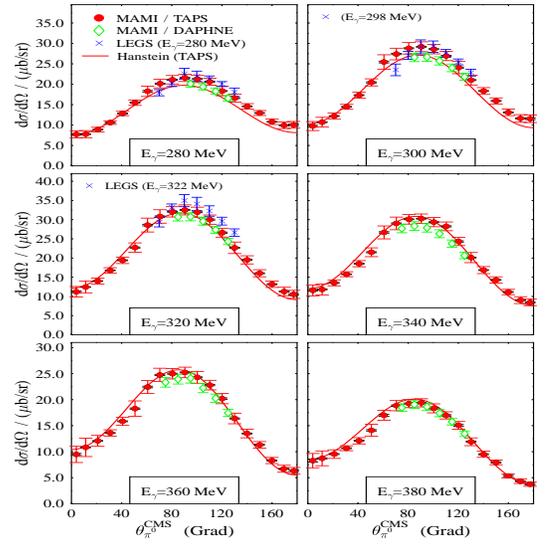
FIG. 25 Photon asymmetry Σ in the Δ resonance region for $\gamma p \to p\pi^0$ (Beck, 2006). The solid line the MAID model.

$S_{l\pm}$ are related due to gauge invariance and only $S_{l\pm}$ needs to be determined. The reaction $e^- p \to e^- p\pi^0$ was studied in the Δ region at four-momentum transfers $Q^2 = 0.2$ (Elsner *et al.*, 2006), 2.8 and 4.0 GeV^2 (Frolov *et al.*, 1999), and ratios of multipoles S_{0+}/M_{1+}, S_{1+}/M_{1+}, and E_1+/M_{1+} were extracted from decay angular distributions. The related $e^- p \to e^- n\pi^+$ reaction was investigated in the first and second nucleon resonance regions in the $0.25 < Q^2 < 0.65$ GeV^2 range (Egiyan *et al.*, 2006; Joo *et al.*, 2005). At higher invariant masses, electro-production of single pions can be discussed within the frame of generalized parton distributions or by extending the Regge formalism to high photon virtualities (Avakian *et al.*, 2004; De Masi *et al.*, 2008; Ungaro *et al.*, 2006). Recently, electro-production of pions was studied using a polarized (^{15}NH$_3$) target. The data, recorded in the first and second nucleon resonance regions in a Q^2 range from 0.187 to 0.770 GeV^2 (Biselli *et al.*, 2008), is expected to place strong constraints on the electro-coupling amplitudes $A_{1/2}$ and $S_{1/2}$ for the $N_{1/2+}(1440)$, $N_{1/2-}(1535)$, and $N_{3/2-}(1520)$ resonances. Electro-production of π^0 mesons in the threshold region, including the π^+ production threshold, was studied at very low Q^2 at MAMI (Weis *et al.*, 2007).

3. Photoproduction of η- and η'-mesons

The cross section for photo-induced production of η-mesons is sizable reaching 16 μb just above its threshold, see Fig. 22a. The most recent data can be found in (Bartalini *et al.*, 2007; Bartholomy *et al.*, 2007; Crede *et al.*, 2005; Dugger *et al.*, 2002). (Bartholomy *et al.*, 2007) contains a survey of older data. At 1 GeV photon energy, a small dip is observed

but otherwise, the cross section does not show any significant structures. (The anomaly in the GRAAL data at $1\,\mathrm{GeV}$ does not show up when the angular distributions are fitted with the BnGa amplitudes; hence the anomaly is likely due to the polynomial extrapolation of the angular distribution into a uncovered region.) At $E_\gamma = 2\,\mathrm{GeV}$, the η cross section is smaller than the π^0 cross section by a factor 3. The GRAAL beam asymmetry (Bartalini *et al.*, 2007) is confirmed and extended in range by (Elsner *et al.*, 2007). Indications for a narrow resonance (at $\approx 1680\,\mathrm{MeV}$, see below) have been reported by (Kuznetsov *et al.*, 2008).

Photoproduction of η-mesons off neutrons gives access to the helicity amplitudes $A_{1/2}^n$, $A_{3/2}^n$ of $N_{1/2^-}(1535)$ coupling to $N\eta$. The reaction has recently attracted considerable additional interest due to the possibility that a narrow $J^P = 1/2^+$ nucleon resonance at $\approx 1680\,\mathrm{MeV}$ may have been found (Kuznetsov *et al.*, 2007). Very recently, precise angular distributions (Jaegle *et al.*, 2008) and beam asymmetries (Fantini *et al.*, 2008) have been reported.

Electro-production of η-mesons was reported in (Denizli *et al.*, 2007) for total center of mass energy $W = 1.5 - 2.3\,\mathrm{GeV}$ and invariant squared momentum transfer $Q^2 = 0.13 - 3.3\,\mathrm{GeV}^2$ and photo-couplings and ηN coupling strengths of baryon resonances were deduced. A structure was seen at $W \sim 1.7\,\mathrm{GeV}$. The shape of the differential cross section is indicative of the presence of a P-wave resonance that persists to high Q^2. The data are extended by (Dalton *et al.*, 2008) to $Q^2 \sim 5.7$ and $7.0\,\mathrm{GeV}^2$ for centre-of-mass energies from threshold to $1.8\,\mathrm{GeV}$. A first double polarization experiment on η electro-production was reported by (Merkel *et al.*, 2007).

The photoproduction cross section for η'-mesons, reported by (Dugger *et al.*, 2006), rises slowly from threshold, reaches a maximum of about one μb at $E_\gamma = 1.9\,\mathrm{MeV}$; at large energies, its cross section falls below the η cross section by a factor ≈ 2. This may indicate the dominance of t-channel vector-meson (V) exchange via the $V \to \eta(\eta')\gamma$ coupling.

4. The reactions $\gamma p \to K^+\Lambda$, $K^+\Sigma^0$, and $K^0\Sigma^+$

Figure 22b show cross sections for photo-production of final states with strangeness. For ΛK^+ and $\Sigma^0 K^+$ the cross sections reach about $2.5\,\mu$b; for $\Sigma^+ K^0$, it is a factor 4 smaller. The ratio $\Sigma^+ K^0$ to $\Sigma^0 K^+$ decays of nucleon resonances is $1/2$, for Δ resonances it is 2. The $\Sigma^0 K^+$ cross section is larger than that for $\Sigma^+ K^0$; the former reaction receives contributions from kaon exchange which is forbidden for the latter reaction. In partial wave analyses (Castelijns *et al.*, 2007), the $N_{1/2^+}(1880)$ resonance is seen to make a significant contribution to final states with open strangeness.

Differential distributions for $\gamma p \to K^+\Lambda$, $K^+\Sigma^0$ and $K^0\Sigma^+$ have been measured at ELSA with SAPHIR (Glander *et al.*, 2004; Lawall *et al.*, 2005) and CBELSA/TAPS (Castelijns *et al.*, 2007), GRAAL (Lleres *et al.*, 2007), at Jlab with the CLAS detector (Bradford *et al.*, 2006), and by LEPS at SPRING-8 (Sumihama *et al.*, 2006; Zegers *et al.*, 2003). The data of (Bradford *et al.*, 2006) are shown in Fig. 27. The reconstruction of the hyperon decay defines its polarization

FIG. 26 (Color online) Differential cross sections for the reaction $\gamma p \to p\eta$ from CBELSA (Bartholomy *et al.*, 2007) and CLAS (Dugger *et al.*, 2002) and fit results (Nakayama *et al.*, 2008). The dashed line represents the S_{11}, the dash-dot-dot line the D_{13}, the dashed-dotted line the meson-exchange contribution; their sum is given as solid line.
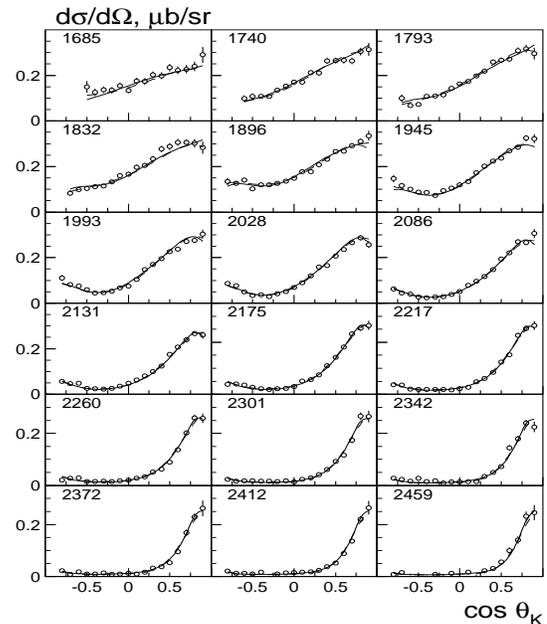
FIG. 27 Differential cross sections for $\gamma p \to K^+\Lambda$ (Bradford *et al.*, 2006). The solid curves represent a Bonn-Gatchina fit.
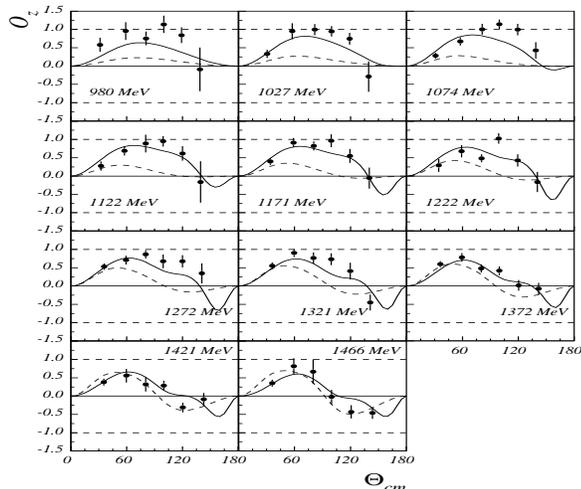
FIG. 28 Angular distributions of the beam recoil observable O_z. Data are compared with the predictions of the Bonn-Gatchina (solid line) and the Regge-plus-resonance model of (Corthals *et al.*, 2007b) (The predictions are pr. comm. to the GRAAL collaboration).

status. At GRAAL and SPRING-8 , the γ-ray beam is created by rescattering of optical photons which are easily polarized; in these measurements, the beam asymmetry is determined as well.

Recently, spin transfer from linearly and circularly polarized photons to final-state hyperons has been measured at GRAAL (Lleres *et al.*, 2008) and Jlab (Bradford *et al.*, 2007). The data exhibit a striking transfer of the photon polarization to the Λ (Schumacher, 2006); the data mark an important step towards a complete experiment.

Electro-production of $K^+\Lambda$ and $K^+\Sigma^0$ final states from a proton target was at Jlab studied using the CLAS detector. The separated structure functions σ_T, σ_L, σ_{TT}, and σ_{LT} were extracted for momentum transfers from $0.5 \leq Q^2 \leq 2.8$ GeV^2 and invariant energy from $1.6 \leq W \leq 2.4$ GeV, while spanning nearly the full center-of-mass angular range of the kaon (Ambrozewicz *et al.*, 2007). The polarized structure function $\sigma_{LT'}$ was measured for the reaction $p(e, e'K^+)\Lambda$ in the nucleon resonance region from threshold up to W=2.05 GeV for central values of Q^2 of 0.65 and 1.00 GeV^2 (Nasseripour *et al.*, 2008). The separated structure functions reveal clear differences between the production dynamics for the Λ and Σ^0 hyperons.

E. Photo-production of multi-mesonic final states

1. Vector mesons

Photons and unflavored vector mesons share the same quantum numbers. In soft vector-meson production by real photons, natural-parity (Pomeron) exchange provides the leading term to the cross section. The cross
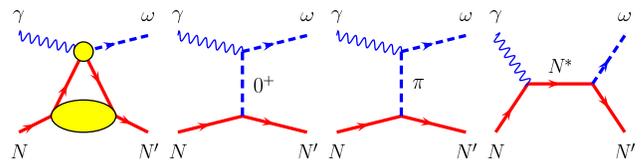
FIG. 29 Contributions to ω photoproduction: a: The hand-bag diagram for hard photo- and electro-production. The large blob represents the generalized parton distribution of the nucleon. At lower energies, processes b,c,d are more appropriate to describe the reaction. b: Natural parity t-channel exchange and c: t-channel exchange via the pion trajectory, d: s-channel intermediate resonance excitation. The same diagrams contribute to ρ production while ϕ are produced dominantly via (b). For K^* production, a kaon trajectory is exchanged, the outgoing N' is replaced by a hyperon.
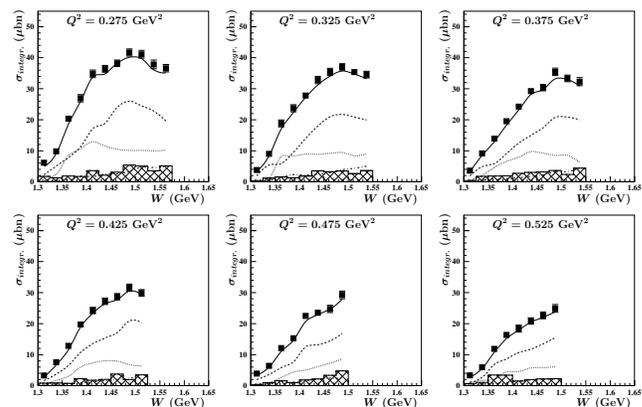
FIG. 30 Electro-production of $p\pi^+\pi^-$ after integration over the full dynamics. The cross sections are decomposed into the dominant isobar channels. The recent CLAS data are shown by full symbols. Shadowed areas represent the systematical uncertainties. The solid lines correspond to an EBAC fit (JM06). The contributions from $\pi^-\Delta^{++}$, $\pi^+\Delta^0$ channels are shown by dashed and dot-dashed lines, the contributions from direct 2π production by dotted lines, respectively.

section falls off exponentially with the squared recoil momentum t characteristic for "diffractive" production. At low energies, a significant pion (kaon) exchange contribution is expected because of the large $(\rho, \omega) \rightarrow \pi^0\gamma$ $(K^* \rightarrow K\gamma)$ coupling. Most interesting in the context of this review are contributions from N^* production since quark models predict for some N^* resonances large couplings to $N\omega$ and to $N\rho$. Fig. 29 depicts the different reaction mechanisms.

In the GeV range, electro-production is sensitive to the transition between the low energy hadronic and high energy partonic domains; at sufficiently large energies, generalized parton distributions can be determined (see, e.g., (Goloskokov, 2007)). However, there is so far no attempt to use the data for baryon spectroscopy. Here, we give reference to recent CLAS papers on electro-production of ρ- (Morrow *et al.*, 2008), ω- (Morand *et al.*, 2005), and ϕ-mesons (Santoro *et al.*, 2008).

2. $\gamma N \to N\pi\pi$ and $N\pi\eta$

Multi-meson production collects an increasing fraction of the cross section, see Fig. 22d. The most important channels are $\gamma p \to p\pi^+\pi^-$ (Wu *et al.*, 2005); above 2 GeV, $\gamma p \to p\pi^+\pi^-\pi^0$ reaches a similar strength (Barth *et al.*, 2003a). In the resonance region, photoproduction of two charged pions is dominated by diffractive ρ production and the direct production $\gamma p \to \pi^-\Delta(1232)^{++}$; $\gamma p \to \pi^+\Delta(1232)^0$ plays a less important role. Intermediate baryon resonances are much stronger in photoproduction of two neutral pions (Ahrens *et al.*, 2005; Assafiri *et al.*, 2003; Thoma *et al.*, 2008). The helicity dependence of the $\gamma p \to p\pi^+\pi^-$ total cross-section was measured at MAMI for photon energies from 400 to 800 MeV (Ahrens *et al.*, 2007). At higher energies, beam-helicity asymmetries were studied at Jlab (Strauch *et al.*, 2005). Two-pion electro-production from Jlab was reported by (Ripani *et al.*, 2003) and (Hadjidakis *et al.*, 2005), and with very high statistics, by (Fedotov *et al.*, 2008). The pion pair was produced at photon virtualities ranging in Q^2 from 0.2 to 0.6 GeV^2 and invariant mass W from 1.3 to 1.57 GeV. A phenomenological analysis found non-resonant mechanisms to provide the most significant part of cross-sections. Within the EBAC model, electrocouplings of the $N(1440)P_{11}$ and $N(1520)D_{13}$ states can be extracted. The present state-of-art of the fits is described in (Mokeev *et al.*, 2008). Data and the most significant isobar contributions are shown in Fig. 30.

Photoproduction of ρ mesons was studied by the CLAS (Ripani *et al.*, 2003) and SAPHIR (Wu *et al.*, 2005) collaborations, ω mesons by CLAS (Battaglieri *et al.*, 2003), SAPHIR – these data are shown in Fig. 31 – (Barth *et al.*, 2003a), GRAAL (Ajaka *et al.*, 2006) and CBELSA/TAPS (Klein *et al.*, 2008), ϕ photoproduction was reported by SAPHIR (Barth *et al.*, 2003b) and LEPS (Mibe *et al.*, 2005); the reactions $\gamma p \to K^{*0}\Lambda$ and $\gamma p \to K^{*0}\Sigma$ were reported by CLAS (Hleiqawi *et al.*, 2007), $\gamma p \to K^{*0}\Sigma^+$ by CBELSA/TAPS (Nanova *et al.*, 2008). The size of the cross section is about 24 μb for ρ, 8 μb for ω, 0.2 μb for ϕ production (see Fig. 22c) while ratios 9:1:2 would be expected from the direct photon-vector-meson couplings. For pion exchange, the ρ and ω cross sections should have similar magnitudes.
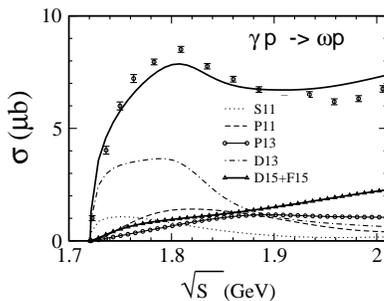
FIG. 31 The total cross section for ω photoproduction (Barth *et al.*, 2003a) and decomposition into partial waves by (Shklyar *et al.*, 2005b).
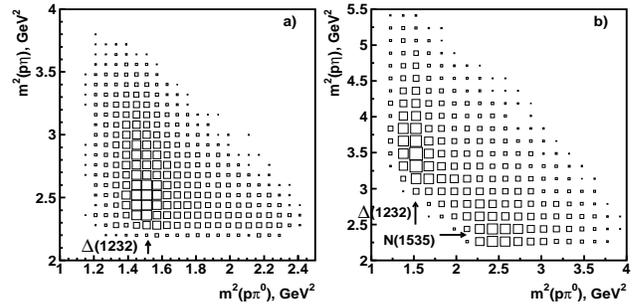
FIG. 32 Dalitz plot for the reaction $\gamma p \to p\pi^0\eta$ for $E_\gamma < 1.9$ GeV (a) and $E_\gamma > 1.9$ GeV (b). $\Delta(1232)$ is seen in both Dalitz plots; $N(1535)$ is visible only for high photon energies even though the $N(1535)\pi$ production threshold (~ 1.0 GeV) is lower than the $\Delta(1232)\eta$ production threshold (~ 1.2 GeV).

The reaction $\gamma p \to p\pi^0\eta$ gives access to resonances in the $\Delta\eta$ system. The reaction was studied at SPRING-8 (Nakabayashi *et al.*, 2006), at GRAAL (Ajaka *et al.*, 2008) and at ELSA (Gutz *et al.*, 2008; Horn *et al.*, 2007, 2008). The $p\pi^0\eta$ Dalitz plot for two different photon energy ranges are shown in Fig. 32, with $\Delta(1232)$ and $N(1535)$ as intermediate resonances in $\gamma p \to (\Delta(1232)\eta; N(1535)\pi) \to p\pi^0\eta$ cascade decays. Likewise, $\gamma p \to p\pi^0\omega$ can be used to study the $\Delta\omega$ system. However, so far data is scarce (Junkersfeld *et al.*, 2007).

3. Hyperon resonances and the $\Theta(1540)^+$

In 2003, evidence for a narrow baryon resonance with positive strangeness $\Theta(1540)^+$, i.e. with a constituent $\bar{s}$-quark, was reported by four different laboratories (Barmin *et al.*, 2003; Barth *et al.*, 2003c; Nakano *et al.*, 2003; Stepanyan *et al.*, 2003) with properties as predicted in a chiral soliton model (Diakonov *et al.*, 1997). A broad search was initiated to confirm or disprove these findings, including the search for related phenomena like $\Phi(1860)$ ($=ssdd\bar{u}$) (Alt *et al.*, 2004) and $\Theta_c(3100)$ ($=uudd\bar{c}$) (Chekanov *et al.*, 2004). The evidence for pentaquarks has now faded away (Danilov and Mizuk, 2008); memorable remarks on the coherence of experimental findings and results from lattice QCD and QCD sum rules can be found in (Tariq, 2007).

Our knowledge of excited strange baryons rests nearly entirely on KN scattering data which are not reviewed here. The $\Lambda(1520)$ hyperon was studied by CLAS in electro-production at electron beam energies of 4.05, 4.25, and 4.46 GeV. The decay angular distributions suggest that t-channel diagrams dominate the production process with either K^+ exchange or longitudinal coupling to an exchanged K^*. The Q^2 dependence of the $\Lambda(1520)$ production cross section is very similar to the one observed for $\Lambda(1116)$ photo- and electro-production (Barrow *et al.*, 2001). The reaction $\gamma p \to K^{*0}\Sigma^+$ provides hints for a significant role of $K_0(900)$ exchange (Hleiqawi *et al.*, 2007).

Differential cross sections for $\gamma p \to K^+\Lambda(1405)$ and $\gamma p \to K^+\Sigma^0(1385)$ for forward K^+ scattering angles have been reported for photon energies ranging from 1.5 to 2.4 GeV. The $\Lambda(1405)$ to $\Sigma^0(1385)$ production ratio of decreased with increasing photon energy possibly suggesting different internal structures (Niiyama *et al.*, 2008).

F. Partial wave analyses

A discussion of problems, principles and achievements of partial wave goes beyond the scope of this paper which rather concentrates on a review of the data which have been gathered and the physical significance of the results. Partial wave analyses are performed at a number of places, using different methods. Even though small groups or individuals have made significant contributions to the field, most partial wave analyses are performed at a few places only.

a. SAID and MAID: The longest continuous tradition is held by the SAID group. The group maintains and updates analyses of the elastic πN, (including πd), KN, NN databases and on photo- and electro-production of pseudoscalar mesons. The web page http://gwdac.phys.gwu.edu/ provides access to the data, to partial wave amplitudes, and to current energy-dependent predictions for observable quantities. A similar page is found at Mainz http://www.kph.uni-mainz.de/MAID/. The most recent solutions for πN elastic scattering were obtained by (Arndt *et al.*, 2006), for KN elastic scattering by (Hyslop *et al.*, 1992), for photoproduction of pions, jointly with the most recent CLAS data by (Dugger *et al.*, 2007). Amplitudes for photoproduction of η and η' were determined by (Chiang *et al.*, 2003) and (Briscoe *et al.*, 2005), those for Kaon photoproduction by (Mart and Sulaksono, 2006). Principles of multichannel analyses are discussed by (Vrana *et al.*, 2000). Electro-production amplitudes (MAID-07) were reported by (Drechsel *et al.*, 2007). The MAID and SAID data bases provide indispensable tools for physicists working in the field. Both groups determine masses, widths and quantum numbers mostly from πN scattering; photoproduction data complement the information by providing helicity amplitudes.

b. EBAC: The Excited Baryon Analysis Center (EBAC) has developed a model to study nucleon resonances pion- and photon-induced reactions (Matsuyama *et al.*, 2007). The model is based on an energy-independent Hamiltonian derived from an interaction Lagrangian. Main results on $\pi N \to N\pi$ were communicated by (Julia-Diaz *et al.*, 2007), on $\pi N \to N\eta$ (Durand *et al.*, 2008), and on $\pi N \to N\pi\pi$ by (Kamano *et al.*, 2008). Photoproduction of pions was studied by (Julia-Diaz *et al.*, 2008) and (Sibirtsev *et al.*, 2007). A review of recent achievement was presented by (Lee, 2007).

c. The Giessen model: The Giessen group analyses simultaneously pion- and photon-induced data on γN and πN to πN, $2\pi N$, ηN, $K\Lambda$, $K\Sigma$, and ωN for energies from the nucleon mass up to $\sqrt{s} = 2$ GeV. The method is based on a unitary coupled-channel effective Lagrangian model. The results of the partial wave analyses were reported by (Penner and Mosel, 2002a,b) and (Shklyar *et al.*, 2005a, 2007, 2005b).

d. The Bonn-Gatchina model: The Bonn-Gatchina group analyses large data sets, including the most recent results from photoproduction of Kaons and multiparticle final states like $p\pi^0\pi^0$ and $p\pi^0\eta$. The latter data are included in event-based likelihood fits which exploit fully the information contained in the correlations between the different variables. Methods are described by (Anisovich *et al.*, 2005, 2007a; Klempt *et al.*, 2006) and results by (Anisovich *et al.*, 2007b, 2005, 2007, 2008), and (Nikonov *et al.*, 2008; Sarantsev *et al.*, 2005, 2008; Thoma *et al.*, 2008).

e. Other approaches: We further mention the analysis of the Gent group which describes photo- and electro-production of hyperons in a Regge-plus-resonance approach (Corthals *et al.*, 2007a, 2006, 2007b) (see also (Sibirtsev *et al.*, 2007)).

A few words should be added as general remarks. Partial wave amplitudes are constrained by a number of theoretical considerations. First, amplitudes have to preserve unitarity; the number of incoming particles in a given partial wave, e.g. πN in the $J^P = 3/2^+$ wave, has to be preserved. This requirement can be met using a K-matrix in which background amplitudes and resonances can be added in a unitarity-preserving way. Amplitudes need to be analytic function in the complex s plane; the treatment of left-hand cuts due to threshold singularities can - in principle - be overcome by using the N/D formalism. Amplitudes should obey crossing symmetry; in general, amplitudes should be defined as functions of s, t, and u. In elastic πN scattering, this requirement is met approximately by forcing amplitudes to satisfy fixed-t dispersion relations. And amplitudes should respect chiral symmetry. This requirement can be enforced by including the πN scattering amplitudes in the fits.

Even when the scattering amplitudes are known, the extraction of resonance parameters from meson-nucleon and photoinduced reactions is not easy. The physical quantity which should not depend on the reaction mechanism is (supposedly) the pole position. Masses and widths can be determined, e.g. in the πN elastic scattering, by the speed-plot or the time-delay method

(Suzuki *et al.*, 2008) which may be more stable than parameters deduced from Breit-Wigner parameterizations. An alternative method (Thoma *et al.*, 2008) is to define a Breit-Wigner amplitude as a function of s which reproduces the pole position of the scattering amplitude. (Ceci *et al.*, 2008) suggest to derive resonance parameter from the trace of K- and T-matrices.

Coupling constants for decays of a resonance into $A+b$ can be determined as residues of pole of the $A+b \to A+b$ scattering amplitude in the complex s-plane. The partial decay width is usually defined as $\Gamma_{Ab} = \rho_{Ab} g_{Ab}^2$ where ρ_{Ab} is the phase space (including centrifugal barrier and Blatt-Weisskopf corrections (Anisovich *et al.*, 2005)), calculated at the nominal mass and g_{Ab}^2 the squared coupling constant, again at the nominal mass. The definition has the non-intuitive consequence that the partial decay width of a subthreshold resonance vanishes identically even though the decay is possible via the tails of the mother (and/or daughter) resonance. More intuitive, but in practice less well defined, is a definition where the ratio of partial to total width is given by the ratio of the intensity in one channel to the intensity in all channels. One particular case are the $N\gamma$ decays or the $A_{1/2}$ and $A_{3/2}$ helicity amplitudes, describing the nucleon-photon coupling for a total spin $1/2$ and $3/2$, respectively. A thorough discussion of these amplitudes, including the longitudinal helicity amplitude $S_{1/2}$ is given in (Aznauryan *et al.*, 2008). With the definition of a partial decay width as residue of a pole in the $\gamma N \to N\gamma$ amplitude, helicity amplitudes become complex quantities.

The coupling of a resonance to a decay channel has an impact on its mass. Quark model calculations usually give masses of "stable" baryons, of baryons before they are "dressed with a meson cloud". The EBAC group makes the attempt to determine bare baryon masses, masses a resonance might have before it dresses itself with a meson cloud. In meson spectroscopy, the Gatchina group (Anisovich *et al.*, 2008) identified the undressed states with the K-matrix poles. In a dedicated study (Workman and Arndt, 2008) did not find a simple association between K-matrix and T-matrix poles. We believe bare masses to be highly model-dependent quantities; the determination of the T-matrix poles is easy once the amplitudes are known, and they should be given. Finally, it is the T-matrix pole positions which are given by the PDG and which can can be compared to other analyses.

G. Summary of N^* and Δ^* resonances

The Review of Particle Properties of the PDG (Amsler *et al.*, 2008) is indispensable for any physicist working in nuclear and particle physics, and also in this review frequent use has been made of it. In baryon spectroscopy, listings of main properties of resonances are given and a selection is made which data are used to define the properties, which data are listed but used for

averaging and which results to not warrant to be mentioned. Based on these results, a status is defined, with 4 stars given to a resonance with certain existence and fairly well defined properties, 3-star resonances are almost certain but some parameters are less well defined. A resonance is given 2 stars if the evidence for its existence is fair and 1 star, if it is poor. The judgement is dominantly based on analyses from (Höhler *et al.*, 1979), (Cutkosky *et al.*, 1979) – updated in (Cutkosky *et al.*, 1980) –, (Manley and Saleski, 1992), and (Arndt *et al.*, 2006).

We suggest here "our own" version of the PDG Listings by including the results of the Bonn-Gatchina analysis (Anisovich *et al.*, 2009). So far, results from photoproduction were not yet used to estimate the status of a resonance or to determine mass or width. The reason for this decision is the following one: unlike πN elastic scattering, it is – at least so far – not possible to derive energy-independent partial wave amplitudes. For an independent observer, it is very difficult to judge how reliable a fit to data is, and if alternative solutions exists in which a particular resonance is not needed. However, in the most recent analysis of the Bonn-Gatchina group, the same amplitudes are used as in (Höhler *et al.*, 1979) and (Arndt *et al.*, 2006). The BnGa differs by constraining the amplitudes of the KH84 or SM06 solution by data on photoproduction. In previous analyses, the inelasticity of baryon resonances are mostly unknown and are fitted as free unconstrained parameters of the fit.

In Table XIII we list the N^* and Δ^* resonances, give our estimate for mass and width and our rating. Results from five analyses are given.

Four new resonances are suggested which are underlined.

1. The $N_{3/2^-}(1860)$ is found in the PDG listings under the entry $N(2080)D_{13}$ ($N_{3/2^-}(2080)$). It is observed at this mass in the KH analysis; CM suggest two states, here we list both under the two headings. Kent confirmed the lower-mass state at 1804 MeV. In the BnGa analysis it assumes a mass of 1875 MeV. $N_{3/2^-}(1860)$ is not seen by KH nor by GWU and we give it a 2-star status.

2. A second newly introduced resonance is $N_{1/2^+}(1880)$. Evidence comes from the Kent and BnGa analyses.

3. $N_{5/2^+}(1890)$ replaces the PDG entry $N(2000)F_{15}$ ($N_{5/2^+}(2000)$)

4. $N_{1/2^-}(1905)$ was reported by KH and Kent. In PDG, the two results are combined with the CM result (2180 MeV) to give $N(2090)S_{11}$.

The five analyses listed in Table XIII are used to determine our rating. Resonances get 4 stars if seen in four experiments, including the GWU analysis. One star is subtracted, if it is not seen in the GWU analysis; two stars are assigned if seen in three, one star if seen by two analyses. Resonances included in the PDG which

TABLE XIII Breit-Wigner masses W_R and widths Γ (in MeV) of N and Δ resonances.

Resonance	Our estimate	Our rating	KH	CM	Kent	GWU	BnGa
$N_{1/2+}(1440)$	1440±30; 300±100	****	1410±12; 135±10	1440±30; 340±70	1462±10; 391±34	1485± 1; 284±18	1436±15; 335±40
$N_{3/2-}(1520)$	1520± 5; 115±10	****	1519± 4; 114± 7	1525±10; 120±15	1524± 4; 124± 8	1516± 1; 99± 3	1524± 5; 112±10
$N_{1/2-}(1535)$	1535±10; 150±25	****	1526± 7; 120±20	1550±40; 240±80	1534± 7; 151±27	1547± 1; 188± 4	1530±30; 210±30
$N_{1/2-}(1650)$	1655±15; 165±30	****	1670± 8; 180±20	1650±30; 150±40	1659± 9; 170±12	1635± 1; 115± 3	1705±30; 220±30
$N_{5/2-}(1675)$	1675± 5; 150±20	****	1679± 8; 120±15	1675±10; 160±20	1676± 2; 159± 7	1674± 1; 147± 1	1670±20; 140±40
$N_{5/2+}(1680)$	1685± 5; 130±10	****	1684± 3; 128± 8	1680±10; 120±10	1684± 4; 139± 8	1680± 1; 128± 1	1667± 6; 102±15
$N_{3/2-}(1700)$	1700±50; 100±50	***	1731±15; 110±30	1675±25; 90±40	1737±44; 250±230	-	1740±20; 180±30
$N_{1/2+}(1710)$	1710±30; 150±60	**	1723± 9; 120±15	1700±50; 90±30	1717±28; 480±330	-	-
$N_{3/2+}(1720)$	1720±30; 200±80	****	1710±20; 190±30	1700±50; 125±70	1717±31; 380±180	1750± 5; 256±22	1720±30; 330±60
$N_{3/2-}(1860)$	1860±40; 200±100	**	-	1880±100;180±60	1804±55; 450±185	-	1875±25;105±25
$N_{1/2+}(1880)$	1880±40; 200±100	*	-	-	1885±30; 113±44	-	1880±40; 220±60
$N_{5/2+}(1890)$	1890±50; 300±150	**	1882±10; 95±20	-	1903±87; 490±310	-	1880±30; 250±50
$N_{3/2+}(1900)$	1900±70; 350±150	*	-	-	1879±17; 498±78	-	1915±50; 220±65
$N_{1/2-}(1905)$	1905±60; 250±150	*	1880±20; 95±30	-	1928±59; 414±157	-	-
$N_{7/2+}(1990)$	1990±80; 380±160	**	2005±150; 350±100	1970±50; 350±120	2086±28; 535±120	-	-
$N_{3/2-}(2080)$	2090±50; 300±100	**	2080±20; 265±40	2060±80; 300±100		-	2160±40; 340±65
$N_{1/2-}(2090)$	2180±80; 350±100			2180±80; 350±100	-	-	-
$N_{1/2+}(2100)$	2100±100; 300±200	*	2050±20; 200±30	2125±75; 260±100	-	-	-
$N_{5/2-}(2200)$	2150±80; 340±160	*	2228±30; 310±50	2180±80; 400±100	-	-	2060±30; 340±50
			KH	CM	Kent	GWU	Hendry
$N_{7/2-}(2190)$	2170±50; 390±120	****	2140±12; 390±30	2200±70; 500±150	2127± 9; 550±50	2152±2; 484±13	2140±40; 270±50
$N_{9/2+}(2220)$	2260±60; 500±150	****	2205±10; 365±30	2230±80; 500±150	-	2316±3; 633±17	2300±100; 450±150
$N_{9/2-}(2250)$	2250±50; 400±120	****	2268±15; 300±40	2250±80; 400±120	-	2302±6; 628±28	2200±100; 350±100
$N_{11/2-}(2600)$	2630±150; 650±300	***	2577±50; 400±100	-	-	-	2700±100; 900±100
$N_{13/2+}(2700)$	2800±160; 600±300	**	2612±45; 350±50	-	-	-	3000±100; 900±150
			KH	CM	Kent	GWU	BnGa
$\Delta_{3/2+}(1232)$	1232± 1; 118± 2	****	1232± 3; 116± 5	1232± 2; 120± 5	1231± 1; 118± 4	1233± 1; 119± 1	1231± 4; 114± 5
$\Delta_{3/2+}(1600)$	1625±75; 350±100	****	1522±15; 220±40	1600±50; 300±100	1706±10; 430±73	-	1620±80; 350±100
$\Delta_{1/2-}(1620)$	1630±30; 140±10	****	1610± 7; 139±18	1620±20; 140±20	1672± 7; 154±37	1614±1; 71±3	1650±25; 250±60
$\Delta_{3/2-}(1700)$	1710±40; 300±100	****	1680±70; 230±80	1710±30; 280±80	1762±44; 600±250	1688±3; 182±8	1640±40; 270±60
$\Delta_{1/2+}(1750)$			-	-	1744±36; 300±120	-	-
$\Delta_{1/2-}(1900)$	1900±50; 190±50	**	1908±30; 140±40	1890±50; 170±50	1920±24; 263±39	-	-
$\Delta_{5/2+}(1905)$	1890±25; 330±70	****	1905±20; 260±20	1910±30; 400±100	1881±18; 327±51	1856± 2; 321± 9	1800±50; 370±110
$\Delta_{1/2+}(1910)$	1895±25; 280±50	****	1888±20; 280±50	1910±40; 225±50	1882±10; 229±25	2068±2; 543±10	-
$\Delta_{3/2+}(1920)$	1940±60; 240±80	***	1868±10; 220±80	1920±80; 300±100	2014±16; 152±55	-	1990±35; 330±60
$\Delta_{5/2-}(1930)$	1960±60; 360±140	**	1901±15; 195±60	1940±30; 320±60	1956±22; 530±140	-	-
$\Delta_{3/2-}(1940)$	1990±60; 300±100	**	-	1940±100; 200±100	2057±110; 460±320	-	1990±40; 410±70
$\Delta_{7/2+}(1950)$	1920±25; 285±50	****	1913± 8;224±10	1950±15; 340±50	1945± 2; 300± 7	1921± 1; 271± 1	1895±20; 260±40
$\Delta_{5/2+}(2000)$			2200±125; 400±125	-	1752±32; 251±93	-	-
$\Delta_{1/2-}(2150)$			-	2200±100; 200±100	-	-	-
			KH	CM	Kent	GWU	Hendry
$\Delta_{7/2-}(2200)$	2240±60; 400±100	**	2215±10; 400±100	2200±80; 450±100	-	-	2280±80; 400±150
$\Delta_{9/2+}(2300)$	2350±80; 400±100	**	2217±80; 300±100	2400±125; 425±150	-	-	2450±100; 500±200
$\Delta_{3/2-}(2350)$	2350±50; 300±70	***	2305±26; 300±70	2400±125; 400±150	-	2233±53; 773±187	-
$\Delta_{7/2+}(2390)$	2390±100; 300±100	*	2425±60; 300±80	2350±100; 300±100	-	-	-
$\Delta_{9/2+}(2400)$	2400±100; 400±200	**	2468±50;480±100	2300±100; 330±100	-	2643±141; 895±432	2200±100; 450±200
$\Delta_{11/2+}(2420)$	2400±50; 400±100	***	2416±17; 340±28	2400±125; 450±150	-	2633±29; 692±47	2400±60; 460±100
$\Delta_{13/2-}(2750)$	2750±100; 420±200	**	2794±80; 350±100	-	-	-	2650±100; 500±100
$\Delta_{15/2+}(2950)$	2920±100; 500±200	**	2990±100; 330±100	-	-	-	2850±100; 700±200

are seen only by one of the five analyses, are kept in Table XIII but with no star. No mass or width estimate is given, and these resonances are not considered in section IV. In some cases, the ratings differ from PDG; in case of up- (down-) graded resonances, the star rating is over- (under-) lined. The mass region above 2.5 GeV was studied in the KH and Hendry analysis only; we keep their PDG rating.

With mass and width estimates we try to remain as close as possible to the PDG listings but give, for practical reasons, symmetric errors. The errors span the range given in PDG. For one- and two-star resonances, PDG gives no mass or width range; in this case we estimate errors from the spread of results. As a rule, we do not give extra weight to analyses quoting smaller errors. Mostly, small errors indicate that correlations with other variables are not sufficiently explored. For two-star resonances we give a minimum error of $\pm 3\%$ on the mass, for one-star resonances of $\pm 5\%$. The width error we assign is minimally twice larger than the error in mass.

IV. MODELS AND PHENOMENOLOGY

A. Historical perspectives

1. SU(3) symmetry

The main concern of baryon spectroscopy in the late sixties was to analyze the meson–baryon interaction and to understand the pattern of the many nucleon and Δ resonances, and the relation between these baryons and the strange baryons, Λ, Σ, Ξ, and their excitations. The dynamical mechanism proposed to generate these resonances was the meson–nucleon interaction: it accounted, e.g., for the Δ resonance in the $\pi - N$ system, but failed to predict most of the other states.

Then came flavor symmetry, based on the group SU(3), from now on called $SU(3)_f$, and its "eightfold way" version. The lowest mass baryons, with spin $S = 1/2$, form an octet (N, Λ, Σ, Ξ). The baryons with $S = 3/2$ are in a decuplet which, in 1962, included $\Delta(1232)$, $\Sigma(1385)$ and $\Xi(1530)$. One state was missing. The regular mass spacing between $\Delta(1232), \Sigma(1385)$ and $\Xi(1530)$ was used to predict the existence and the mass of the $\Omega(1672)$ baryon (Gell-Mann, 1962), with strangeness S $= -3$. Its experimental discovery (Barnes *et al.*, 1964) was a triumph for $SU(3)_f$.

It was then realized that, if $SU(3)_f$ is taken seriously, there are three states in the fundamental representation, 3, named quarks, and the actual baryons correspond to the flavor representations found in the $3 \times 3 \times 3$ product. This was the beginning of the quark model, first a tool for building the $SU(3)_f$ representations, and then becoming a dynamical model.

Today, $SU(3)_f$ is understood from the universal character of the quark interaction (flavor independence) and the approximate equality of the masses of light and strange quarks. $SU(3)_f$ remains a valuable tool to correlate data in different flavor sectors and organize the hadron multiplets.

2. SU(6) symmetry

The group SU(6) combines $SU(3)_f$ with the spin group SU(2). For instance the octet baryons with $S = 1/2$ and the decuplet baryons with $S = 3/2$ or $1/2$ built a 56 representation of SU(6). This SU(6) symmetry emerges for instance automatically in potential models with flavor independent forces, in the limit where the strange quark mass m_s is equal to that or ordinary quarks, and the spin-dependent forces are neglected.

3. Early models

The harmonic oscillator model, to be discussed shortly as well as some of its many refinements, enables to account explicitly for $SU(3)_f$ and SU(6) symmetry and their violation, and was crucial to assess the quark model not only as a mathematical tool to generate the actual representation out of the fundamental ones, but to understand the pattern of radial and orbital excitations. More refined constituent models were proposed later.

More recently, attempts were made to derive the baryon masses and properties directly from QCD, by sum rules or lattice simulations: the results are very encouraging, but often restricted to the lowest levels.

4. Heavier flavors

The discovery of charm and beauty enriched significantly the spectrum of hadrons. The quark model gained in credibility by the success of potentials fitting the J/ψ and Υ excitations. The problem was to combine these new states in the existing schemes.

The extension of $SU(3)_f$ to $SU(4)_f$ or beyond is straightforward but not very useful, as the symmetry is largely broken. However, with the advent of QCD, the ideas have evolved. The basic coupling, that of gluons to quarks, is linked to the color, not to the flavor. Hence, at least in the static limit, the quark–quark interaction should be *flavor independent* in the same way as in the physics of exotic atoms, the very same Coulomb potential binds electrons, muons, kaons and antiprotons.

Flavor independence is probed in various ways: the same "funnel" potential (Coulomb + linear) simultaneously fits the charmonium and bottomonium spectrum in the meson sectors. For baryons, regularities are also observed, which supports a picture with a flavor independent confinement and flavor symmetry broken through the quark masses entering the kinetic energy and the spin-dependent corrections. For instance, there is a very smooth evolution of hyperfine splittings from $\Delta - N$ to $\Sigma_b^* - \Sigma_b$.

It would of course be very appealing to describe all baryons within in a universal model, the light quark requiring only relativistic corrections due to their light mass. This is for instance the spirit of the work by (Capstick and Roberts, 2000). The success of this model is almost embarrassing, as QCD guides our intuition toward drastic differences between heavy and light quarks. Heavy quarks interact by exchanging gluons. On the other hand, the dynamics of light quarks is dominated by chiral symmetry, which seems hardly reducible to a local potential.

5. The role of color

One of the main motivations for introducing color was to account for the antisymmetrization of the quarks in baryons (Greenberg, 1964). In the harmonic oscillator and its various developments, the quarks in N, Δ, Ω^-, etc., are in a symmetric overall S-wave, and the spin–siopsin part is alos symmetric. An antisymmetric $3 \times 3 \times 3 \rightarrow 1$ coupling of color ensures Fermi statistics.

Then, in this color scheme, a quark in a baryon sees a color $\bar{3}$ set of two quarks, which is analogous to the antiquark seen by a quark in an ordinary meson. This is the beginning of the diquark idea which will be discussed below.

QCD gives a picture where the quarks interact moderately at short distances, according to "asymptotic freedom", and more strongly at large distances, where a linear confinement is suggested by many studies, though not yet rigorously proved. The question is whether a "funnel" potential (Coulomb plus linear) mimics QCD well enough so that reliable predictions can be done. A related question is whether the interaction among quarks in baryons is of pairwise nature.

Another problem, raised in the late 70s in papers dealing with "color chemistry" (Chan *et al.*, 1978), is whether the color representations used by hadrons are 3 (quarks, antidiquarks), $\bar{3}$ (antiquarks, diquarks) and 1 (hadrons). Namely is the octet, which corresponds to gluons, restricted to the crossed channel, i.e., used only to mediate the interaction, or does it play a constituent role (glueballs, hybrid mesons and baryons)? Are there multiquark states containing color-sextet or color-octet clusters? Experimental evidence for the existence of hadrons with "hidden color" in the pre-LEAR area was overruled in high-statistics experiments in the early phase of LEAR (Walcher, 1988).

B. Models of ground-state baryons

1. Potential models

The simplest model consists of

$$H = \sum_{i=1}^{3} \frac{\boldsymbol{p}_i^2}{2m_i} + V(\boldsymbol{r}_1, \boldsymbol{r}_2, \boldsymbol{r}_3) - \frac{(\sum_i \boldsymbol{p}_i)^2}{2 \sum_i m_i} , \qquad (1)$$

where V is a suitable translation-invariant interaction, the best known choice being the harmonic oscillator

$$V(\boldsymbol{r}_1, \boldsymbol{r}_2, \boldsymbol{r}_3) = \frac{2K}{3} \sum_{i<j} r_{ij}^2 , \qquad (2)$$

where $r_{ij} = |\boldsymbol{r}_j - \boldsymbol{r}_i|$. The ground state is the minimum of H, which can be reached for instance by variational methods. For equal masses $m_i = m$, one can introduce the Jacobi coordinates

$$\boldsymbol{\rho} = \boldsymbol{r}_2 - \boldsymbol{r}_1 , \quad \boldsymbol{\lambda} = \frac{2\boldsymbol{r}_3 - \boldsymbol{r}_1 - \boldsymbol{r}_2}{\sqrt{3}} , \qquad (3)$$

and minimize approximately (1) with the Gaussian trial wave function

$$\Psi_0(\boldsymbol{\rho}, \boldsymbol{\lambda}) = \left(\frac{\alpha^2}{\pi^2} \right)^{3/4} \exp\left[-\frac{\alpha}{2} \left(\boldsymbol{\rho}^2 + \boldsymbol{\lambda}^2 \right) \right] , \qquad (4)$$

which is the exact solution for (2) provided $\alpha = \sqrt{Km}$.

For the spin $S = 3/2$ baryons, this symmetric orbital wave function is associated with a symmetric isospin wave function and a symmetric spin state such as $| \uparrow\uparrow\uparrow \rangle$.

For the nucleon, a mixed-symmetric spin doublet (here for $S_z = +1/2$,

$$S_{\rho,\lambda} = \left\{ \frac{| \uparrow\downarrow\uparrow \rangle - | \downarrow\uparrow\uparrow \rangle}{\sqrt{2}}, \frac{2 \uparrow\uparrow\downarrow \rangle - | \downarrow\uparrow\uparrow \rangle - | \uparrow\downarrow\uparrow \rangle}{\sqrt{6}} \right\}, \quad (5)$$

is combined to an isospin doublet (here for proton)

$$I_{\rho,\lambda} = \left\{ \frac{(udu) - (duu)}{\sqrt{2}}, \frac{2(uud) - (duu) - (udu)}{\sqrt{6}} \right\}, \quad (6)$$

in a spin–isospin wave function

$$(S_\lambda I_\lambda + S_\rho I_\rho)/\sqrt{2} \qquad (7)$$

which is symmetric under permutations. The extension to unequal masses is straightforward.

It is amazing that simple potential models provide with a good survey of ground-state baryons with various flavor content. If the potential V is taken as being *flavor independent*, as suggested by QCD, then the Schrödinger equation exhibits regularity and convexity properties (Nussinov and Lampert, 2002; Richard, 1992). For instance,

$$M(QQq) + M(qqq) < 2M(Qqq) \quad \text{if} \quad Q \neq q . \qquad (8)$$

2. From mesons to baryons

In most papers dealing with potential models of baryons, a pairwise interaction is assumed,

$$V(\boldsymbol{r}_1, \boldsymbol{r}_2, \boldsymbol{r}_3) = \frac{1}{2} \sum_{i<j} v(r_{ij}) , \qquad (9)$$

for instance $v(r) = \sigma r - a/r + b$. It is then argued (Greenberg and Lipkin, 1981; Richard, 1981; Stanley and Robson, 1980) that the potential between two quarks in a baryon is half the quark–antiquark potential in a meson. This result is exact for the one-gluon-exchange potential, or more generally, any color-octet exchange, which contains an explicit $\tilde{\lambda}_i.\tilde{\lambda}_j$ color operator, with expectations values $-16/3$ for $3 \times \bar{3} \to 1$ and $-8/3$ for $3 \times 3 \to \bar{3}$. This "1/2" rule also holds if two quarks are close together and seen by the third one as a localized $\bar{3}$ source which is equivalent to an antiquark. More generally, the t-channel color structure of v contains a singlet and an octet. The singlet cannot contribute to confinement, otherwise all quarks of the universe would be tightly bound. The simplest ansatz is to assumed a pure color octet exchange, and this is why a factor $1/2$ is introduced in Eq. (9).

With this "1/2" rule, amazing Hall–Post type of inequalities can be derived between meson and baryon ground states masses (Richard, 1992). The simplest is for spin-average values

$$(Q\overline{Q})/2 \leq (QQQ)/3, \tag{10}$$

satisfied by, e.g., $\phi(1020)$ and $\Omega^-(1672)$.

However, QCD suggests that the linear potential $v(r) = \sigma r$ acting on the quark–antiquark pair of mesons is not generalized as $\sigma \sum r_{ij}/2$ in baryons, but by the so-called Y-shape potential

$$V(\boldsymbol{r}_1, \boldsymbol{r}_2, \boldsymbol{r}_3) = \sigma \min(d_1 + d_2 + d_3), \tag{11}$$

where d_i is the distance of a junction to the ith quark. Adjusting the location of the junction corresponds to the problem of Fermat and Torricelli, whose generalization to more than three terminals is called the minimal Steiner tree problem. If an angle of triangle is larger than 120°, then the junction coincides with this vertex, otherwise it views each side under 120°, as shown in Fig. 33. Unfortunately, V given by the Y-shape (11)
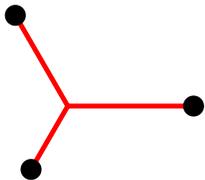
FIG. 33 Three-quark confinement in the string limit.

differs little from the result of the "1/2" rule, and one cannot probe this three-body dynamics from the baryon spectrum. The difference between the additive model $V \propto \sum \tilde{\lambda}_i.\tilde{\lambda}_j v(r_{ij})$ and the minimal-path ansatz (Steiner tree) becomes more dramatic in the multiquark sector (Vijande *et al.*, 2007).

3. Hyperfine forces

To explain why the Δ with spin $3/2$ is above the nucleon of spin $1/2$, and similarly $\Sigma^* > \Sigma$, $\Xi^* > \Xi$, etc., the spin-independent potential V has to be supplemented by a spin–spin term, which is usually treated at first order, but sometimes non-pertubatively, after suitable regularization.

a. Chromomagnetism The most popular model is the one-gluon-exchange (De Rujula *et al.*, 1975), inspired by the Breit–Fermi term of QED. A slightly more general formulation involves a *chromomagnetic* interaction of the form

$$V_{\text{CM}} = \sum_{i<j} \frac{\tilde{\lambda}_i^{(c)}.\lambda_j^{(c)} \, \boldsymbol{\sigma}_i.\boldsymbol{\sigma}_j}{m_i \, m_j} v_{ss}(r_{ij}) , \tag{12}$$

where v_{ss} is very short–ranged. One of the most striking success of chromomagnetism is the explanation of the $\Sigma - \Lambda$ splitting. For both states, $\sum_{i<j} \boldsymbol{\sigma}_i.\boldsymbol{\sigma}_j = -3$ since we have an overall spin $S = 1/2$. However, for the Λ, this strength is concentrated into the light-quark pair, and thus the downward shift is more important, due to the $m_i^{-1} m_j^{-1}$ dependence of the operator (12).

Another success is the prediction of the hyperfine splittings when the strange quark is replaced by a quark with charm or beauty. While the $\Sigma - \Lambda$ mass difference remain large, the $\Sigma^* - \Sigma$ gap is much reduced. This is exactly the pattern observed for charm and beauty baryons. See, e.g., (Richard and Taxil, 1983) for a study on how this effect depends on the assumed shape of the confining potential $v(r)$.

b. Instantons, good diquarks However, it has been stressed that chromomagnetism is not the unique solution. In particular, an *instanton-induced* interaction ('t Hooft, 1976) also accounts very well for the hyperfine splittings. See, e.g., (Löring *et al.*, 2001b; Semay *et al.*, 2001; Shuryak and Rosner, 1989). It can be written as

$$V_{SS} = -4 \sum_{i<j} g_{ij} \, \mathcal{P}^{[i,j]} \mathcal{P}^{S=0} \delta^{(3)}(\boldsymbol{r}_j - \boldsymbol{r}_j) , \tag{13}$$

with the projection on the spin $S = 0$ state and on the antisymmetric flavor state for each pair. The dimensionless coupling g_{ij} is stronger for light quarks than for $[ns]$. This explains the $\Sigma - \Lambda$ mass difference, and other splittings within the ground states. Of course, the instanton-induced interaction differs more strickingly from chromomagnetism in the case of mesons, in particular for pseudoscalar and scalar mesons (Klempt *et al.*, 1995).

An interesting concept has been introduced (Jaffe, 2005; Wilczek, 2004), that of *good diquarks* with spin $S = 0$, which is lower in mass than its vector counterpart with $S = 1$. For light quark, the favored pair is in

an antisymemtric isospin state $I = 0$. Then the spectrum can be analyzed without referring to a specific dynamical model for the hyperfine interaction. However, this concept has been often associated to an extreme quark-diquark picture of baryon excitations, with much less levels than in the usual three-quark picture. We shall come back to this discussion on the quark–diquark model later in this review. Also the concept of good diquark became rather sulfurous when associated to speculations about multiquark states which were neither supported by genuine few-body calculations nor confined by the data. We shall use here the concept of good diquark without endorsing its more extreme developments.

c. Goldstone boson exchange   In conventional potential models, one starts with a degenerate ground state near 1100 MeV, and then a splitting between the N and the Δ is introduced. More recently, models have been developed where one starts from a unique state near 2 GeV, and then introduce a Gosdstone-boson exchange (GBE) that reads, (Glozman and Riska, 1996)

$$V_{\text{OGE}} = \sum_{i<j} \frac{g^2}{4\pi} \frac{1}{4m_i m_j} \tilde{\lambda}_i^F . \tilde{\lambda}_j^F \, \boldsymbol{\sigma}_i . \boldsymbol{\sigma}_j \times$$
$$\left[\frac{\mu^2 \, \exp(-\mu r_{ij})}{r_{ij}} - 4\pi \, \delta^{(3)}(\boldsymbol{r}_{ij}) \right] . \quad (14)$$

which pushes down both N and Δ but the former with larger strength.

This interaction is inspired by the one-pion-exchange potential in nuclear physics. However, in describing the nucleon–nucleon interaction, the contact term is usually neglected, as hidden by all uncertainties about the origin of the hard-core interaction at short distances. Here this is the reverse: the Yukawa term plays a minor role, and the splitting of baryons is due to the contact term, which is regularized in explicit models exploiting this dynamics.

We note in this approach an important flavor-dependence, as the pion does not couple to heavy quarks. It is not obvious how this interaction has to be adapted to the meson sector.

The GBE model has been studied by several groups, in particular (Dziembowski *et al.*, 1996; Melde *et al.*, 2008; Valcarce *et al.*, 1996).

4. Improved pictures of ground-state baryons

The naive quark model, with its non-relativistic kinematics, frozen number of constituents, instantaneous interaction, etc., is far from being fully satisfactory. Several improved pictured have been proposed. We briefly review some of them. However, in a review devoted to baryon spectroscopy, we cannot set on the same footing constituent models giving predictions for the whole spectrum of excited states and sophisticated QCD-inspired studies which are restricted to the ground state or at most to the first excitations.

a. Quark models with relativistic kinematics   This is now rather customary to replace the non-relativistic contribution of constituent mass and kinetic energy, $m + \boldsymbol{p}^2/2$, by the relativistic operator $(m^2 + \boldsymbol{p}^2)^{1/2}$. Examples are (Basdevant and Boukraa, 1986; Capstick and Isgur, 1986; Capstick and Roberts, 2000). This is more satisfactory, but does not solve the problems inherent to the choice of the dynamics. For instance, with a standard Coulomb-plus-linear interaction, the lowest nucleon excitation has negative parity.

b. Relativistic quark models   This is a more ambitious approach, aiming at a covariant formalism, even though some approximations are eventually unavoidable in the calculations. A recent example is (Melde *et al.*, 2008) and a benchmark is the work by the Bonn group (Metsch *et al.*, 2003; Migura *et al.*, 2006; Löring *et al.*, 2001a,b,c), whose starting point is the Bethe–Salpeter equation. Here, not only the masses and the static properties can be estimated, but also the form factors and quark distributions.

c. The MIT bag model   The MIT bag model stages massless or very light quarks moving freely inside of cavity of rarius R which is adjusted to minimize the bag energy. A good fit to the ground states of light baryons was achieved (DeGrand *et al.*, 1975), and this model motivated a variety of developments. However, the model deos not permit an easy estimate of the excitation spectrum. In particular, the center-of-mass motion cannot be removed explicitly.

d. The bag model for heavy quarks   The MIT bag model is not suited for heavy quarks. For heavy $(Q\overline{Q})$ or (QQQ), (Hasenfratz and Kuti, 1978) built a bag to confine the gluon field for any given quark configuration. The gluon energy is interpreted as the quark potential. Note that in the case of baryons (Hasenfratz *et al.*, 1980), this model leads to a Y-shape interaction, as discussed above. The case of hadrons with both heavy and light quarks is less easy. See, e.g., (Bernotas and Simonis, 2008), for a recent update.

e. The cloudy bag   A problem with the MIT bag model is the discontinuity of the axial-vector current across the bag surface. Or in a more empirical point of view, the two nucleons do not interact once their separation exceeds twice the bag radius. Introducing a pion field around the nucleon (Brown and Rho, 1979) or even inside (Thomas *et al.*, 1981) restore a more physical picture.

Starting from a bag of large radius $R \sim 1$ fm, one ends with a smaller radius $R < 1$ fm for the three-quark domain, and a pion field extending beyond 1 fm. In fact R is not sharply determined, and the Stony-Brook group got even variants with rather small radius[1]. In this limit, the details of the quark part become invisible: the quark core just serves a source of the pion field, and carries the baryon number, and one recovers the Skyrmion model and other soliton models.

f. Skymions and other soliton models   In this approach, the main emphasis is the coupling of meson to baryons. Hence the aim is less to perfectly reproduce the spectrum of high excitations than to account for the low-energy interactions. There are many variants, in particular in the way of treating strangeness and heavier flavors. For instance, in (Rho *et al.*, 1992), the hyperons are considered as bound states of a topological soliton and K, D or B mesons.

g. Chiral perturbation theory   There is an old idea by Weinberg and others, QCD is replaced at low energy by effective Lagrangians which share the same symmetries. The coupling are treated as free parameters which, one tuned on a few physical quantities, can be used (consistently, i.e., at the same order in the expansion in powers of the momentum and quark masses) for calculating other properties. After fruitful developments in the physics of mesons (Donoghue *et al.*, 1989; Ecker *et al.*, 1989), this approach was also applied to nucleons (Bernard *et al.*, 1995) and became widely used. A noticeable improvement is the implementation of unitarity (Oller *et al.*, 2000).

h. QCD sum rules   This beautiful approach to non-perturbative QCD was initiated by (Shifman *et al.*, 1979), and then developed by several groups. For a summary of early applications, see (Reinders *et al.*, 1985). The extension to baryons is non trivial, since several operators can be chosen to describe a given state. After a pioneering paper (Ioffe, 1981), the situation was clarified in (Chung *et al.*, 1982), and subsequent papers devoted to various flavor combinations (Bagan *et al.*, 1993, 1994; Dosch *et al.*, 1989).

The idea is to link, via the analytic properties, the perturbative domain of QCD, where calculations can be done exactly, and the non-perturbative domain, which can be described in terms of a few basic constants, which once adjusted form a few physical quantities, can be used for others.

---

[1] In an ideal scenario, there is a perfect duality between the three-quark and the pion field picture, named the "Cheshire-cat principle" (Nadkarni and Nielsen, 1986).

i. Lattice QCD   Here, QCD is reformulated as a field theory in a discretized phase-space and solved using very astute and powerful techniques which require, however, expensive computing means. In the domain of hadron spectroscopy, the best-known applications of lattice QCD are these dealing with glueballs and hybrid mesons, and also scalar mesons, but recently the physics of baryons has also been studied.

The excitations of the nucleons have received much attention (Melnitchouk *et al.*, 2003). The question is whether, when the light quark mass vanishes, one observes a change in the hierarchy of excitation, with the positive-parity excitation becoming lower than the negative-parity one. This is still controversial.

Lattice techniques have also been applied to single-charm baryons (Lewis *et al.*, 2001) and even to double-charm baryons (Brambilla *et al.*, 2004; Flynn *et al.*, 2003).

C. Phenomenology of ground-state baryons

1. Missing states

Almost all ground-state baryons containing light or strange quarks and at most one heavy quarks are now identified. Still missing are the isospin partners Σ_b^0 and Ξ_b^0 and the spin excitations ($S = 3/2$) of the recently discovered Ξ_b and Ω_b.

The existence of $\Xi_{cc}^+(3519)$ is uncertain. Its predicted mass (Fleck and Richard, 1989; Körner *et al.*, 1994) is about 100 MeV larger and recent calculations give even larger mass values. As compared to a naive equal-spacing for $p(940)$, $\Lambda_c^+(2286)$ and Ξ_{cc}, the first correction is that Ξ_{cc} is shifted down by the heavy–heavy interaction in the chromoelectric sector, see Eq. (8). However, both p and Λ_c are shifted down by the favorable chromomagnetic interaction among light quarks.

As the $(b\bar{c})$ meson has been observed, one should be able to detect (bcq) baryons with charm and beauty, with two $S = 1/2$ states in the ground state, and one $S = 3/2$ state. Next will come the double-beauty sector, and ultimately, baryons with three heavy quarks.

2. Regularities

The masses exhibit a smooth behavior in flavor space, which is compatible with the expectation based on models incorporating flavor independence. In particular, a type of "heavy quark" symmetry is expected when comparing single-charm and single-beauty baryons, as done in Fig. 34. Clearly seen is this picture is that the cost of single-strangeness excitation $\Xi_Q - \Lambda_Q$ is very similar for $Q = c$ and $Q = b$.

However, for the double-strangeness excitations, the $\Omega_b(6165)^0$ is problematic. Any reasonable model predict Ω_b with mass of about 6050 MeV, 110–120 MeV lower than the observed mass.
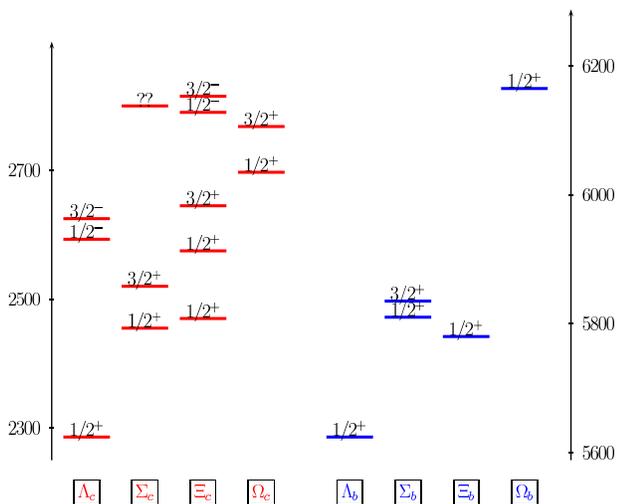
FIG. 34 Comparison of single-charm and single-beauty baryons.

TABLE XIV Masses (in MeV) of Λ and Σ and Σ^* baryons quoted from (Amsler *et al.*, 2008), and mass gaps δM between $J^P = 1/2$ baryons containing 'good' diquarks and $J^P=3/2$ baryons with all pairs in spin triplet. The quantum numbers of the heavy baryons are quark model predictions.

1/2	Mass	1/2	Mass	3/2	Mass
Λ^0	1115.68 ± 0.01	Σ^0	1192.64 ± 0.04	Σ^{*0}	1383.7 ± 1.0
δM	$[ud] = -271$		$[us] = -191$		0 MeV
Λ_c^0	2286.46 ± 0.14	Σ_c^0	2457.76 ± 0.18	Σ_c^{*0}	2518.0 ± 0.5
δM	$[ud] = -231$		$[uc] = -60$		0 MeV
Λ_b^0	5619.7 ± 1.7	Σ_b^0	5811.5 ± 1.7	Σ_b^{*0}	5832.7 ± 1.9
δM	$[ud] = -213$		$[ub] = -21$		0 MeV
Ξ_c^0	2471.0 ± 0.4	$\Xi_c'^0$	2578.0 ± 2.9	Ξ_c^{*0}	2646.1 ± 1.2
δM	$[ds] = -174$		$[dc] = -70$		0 MeV

a M_Q^{-1} in the limit where the change of the wave function is neglected. In this limit, the combination $2\Sigma_Q^* + \Sigma_Q - 3\Lambda_Q$ is expected to be constant, and this is rather well confirmed by the date, with about 613, 634 and 618 MeV for $Q = s$, c and b, respectively.

To a good approximation, the hyperfine effect in the pair $q_1 q_2$ is found independent of the third quark, this leading to a variety of sum rules if taken seriously. See, e.g., (Franklin, 2008; Lichtenberg *et al.*, 1996). Within the point of view of good diquarks, one can, indeed, measure the downward shift due to quark pairs in spin-singlet, starting from the $S = 3/2$ baryon where all pairs are in a spin triplet. As seen in Table XIV, one obtains $[ud] \approx 250$ MeV, for $[us] \approx 170$ MeV, $[uc] \approx 65$ MeV, and $[ub] \approx 20$ MeV.

FIG. 35 Mass difference between spin-3/2 baryons (Δ, Σ^*, Σ_c^*, Σ_b^*) and spin-1/2 baryons. In spin-1/2 baryons, the light-light or a heavy-light quark pair can have spin zero. The spin-0 diquark is indicated by $[q_1 q_2]$. The masses are drawn as a function of the inverse (constituent) quark mass.

3. Hyperfine splittings

The hyperfine splitting is also varying smoothly from one configuration to another. Again, this is compatible with the mass dependence introduced in the chromomagnetic model: an explicit $m_i^{-1} m_j^{-1}$ in the operator, which is partially canceled out by the reinforcement of the short-range correlations when the masses increase. However, a similar pattern could be reached in other approaches to hyperfine splitting. Figure 35 illustrates the regularities of the hyperfine effects in hyperons when the heavy quark is varied.

The $\Sigma_Q^* - \Sigma_Q$ is expected to vanish as $M_Q \to \infty$, with

4. Isospin splittings

This was a subject of many investigations. Before the quark model, the neutron to proton mass difference has been related by (Cottingham, 1963) to electron–nucleon scattering. In the quark model, as underlined in (Isgur, 1980), there are many contributions to mass differences within an isospin multiplets, and the various tems often tend to cancel. There are: the quark-mass difference $m_d - m_u$; the induced change of chromolectrci energy; the change in the strength of the chromomagnetic forces; the Coulomb repulsion; the magnetic interaction; etc. The effects have been estimated by several groups (Isgur, 1980; Varga *et al.*, 1999) and extended to heavy quarks (Franklin, 1999; Lichtenberg, 1977). There is also a contribution to isospin spittings from meson loops, with pions and baryons in the loops having different masses and couplings. This effect was emphasized recently for heavy baryons (Guo *et al.*, 2008).

D. Models of baryon excitations

While for the ground-state baryons, there are a variety of pictures, some of them being directly guided by QCD, for the excitation spectrum, one should still rely on explicit constituent models, and among them the harmonic oscillator.

1. Harmonic oscillator

a. HO: equal masses This is the simplest model, corresponding to (1) with all $m_i = m$ and (2). Then the relative motion is described by

$$\frac{\boldsymbol{p}_\rho^2}{m} + K\boldsymbol{\rho}^2 + \frac{\boldsymbol{p}_\lambda^2}{m} + K\boldsymbol{\lambda}^2 \ , \qquad (15)$$

leading the energy spectrum

$$\sqrt{\frac{K}{m}}\left(6 + 2l_\rho + 4\mathtt{n}_\rho + 2l_\lambda + 4\mathtt{n}_\lambda\right) = \sqrt{\frac{K}{m}}\left(6 + 2N\right),$$
$$(16)$$

in an obvious notation for the orbital momenta $l_{\rho,\lambda} = 0, 1, \ldots$ and radial numbers $\mathtt{n}_{\rho,\lambda} = 0, 1, \ldots$ attached to each degree of freedom. The wave functions are also explicitly known. For the ground state, it is the Gaussian (4). For excitations, it also contains a polynomial which reflects the rotation and permutation properties and ensure the orthogonality.

Note the first radial excitation of the nucleon and Δ, a symmetric combination of the states with $l_\rho = l_\lambda = 0$ and either $\mathtt{n}_{\rho,\lambda} = (0,1)$ or $(1,0)$ which is *below* the first negative-parity excitation. This will be further discussed in connection with alternative models and with the data.

b. HO: unequal masses For baryons with one heay quark, (qqQ), the masses are (m, m, M). The case of double-charm baryons is deduced by $m \leftrightarrow M$. The second term in (15) has now a reduced mass μ with $\mu^{-1} = (2M^{-1} + m^{-1})/3$ replacing m. Then the energy levels are modified as

$$\sqrt{\frac{K}{m}}\left(3 + 2l_\rho + 4\mathtt{n}_\rho\right) + \sqrt{\frac{K}{\mu}}\left(3 + 2l_\lambda + 4\mathtt{n}_\lambda\right) \qquad (17)$$

Hence the λ excitation are lower than their ρ analogs for single-flavor baryons. For baryon with double flavor, the first excitation are within the heavy-quark sector. The wave function is a slight generalization of (4), with $\sqrt{Km}\boldsymbol{\rho}^2 + \sqrt{K\mu}\boldsymbol{\lambda}^2$ in the Gaussian and the corresponding changes in the normalization.

If the three constituents masses are different, then the Hamiltonian describing the relative motion is still of the type

$$\frac{\boldsymbol{p}_x^2}{m_x} + K\boldsymbol{x}^2 + \frac{\boldsymbol{p}_y^2}{m_y} + K\boldsymbol{y}^2 \ , \qquad (18)$$

with $\boldsymbol{x}$ and $\boldsymbol{y}$ are combinations of the Jacobi variables $\boldsymbol{\rho}$ and $\boldsymbol{\lambda}$ which are obtained, together with the reduced masses m_x and m_y by the diagonalization of a 2×2 matrix.

2. Potential models

If the potential V is not harmonic, the non-relativistic Hamiltonian (1) can be solved numerically using powerful techniques developed in nuclear physics, such as Faddeev equations, hyperspherical expansion, or correlated Gaussians. While convergence is easily reached for the energy levels, some additional effort is usually required to measure the short-range correlations within the wave-function.

Some approximations can be envisaged, as an alternative to the full three-body calculation. Some of them are purely technical, for instance truncating the hyperspherical expansion to the lowest partial wave. Some others shed some light on the baryon structure. For instance, doubly-flavored baryons (QQq) have clear diquark–quark structure, but the internal diquark dynamics is influenced by the third quark, an effect which is unfortunately often forgotten[2]. (QQq) can also be treated $H_2{}^+$ in atomic physics, with QQ moving in a Born–Oppenheimer potential generated by the light degrees of freedom (Fleck and Richard, 1989).

It should be stressed that different models used for the interquark potential give similar ordering for the first levels. In the HO, the radial excitation energy is twice the orbital one. With a linear confinement, the ratio is smaller, but still the radial excitation remains above the orbital one, if the potential is local and flavor-independent (Hogaasen and Richard, 1983). Pushing the radial excitation below the orbital one require drastic changes of the dynamics, like these of the OBE model.

3. Relativistic models

For relativistic models, the solution can be found by variational methods, i.e., by expanding the wave function on a basis, usually chosen as containing Gaussians of different range parameters. The level order of the first levels is similar the pattern found in non-relativistic models.

For high orbital excitations, an interesting result was obtained (Martin, 1986). The levels are well described in the semi-classical approximation. For low L, the lowest state is symmetric, all quarks sharing equally the orbital momentum. For higher L, there is a spontaneous breaking of symmetry, and in the ground-state, two quarks have a relative $l_\rho = 0$ while the third quark takes $l_\lambda = L$.

---

[2] In the case of the harmonic oscillator, exactly 1/3 of the strength binding QQ is due to the third quark

Hence diquarks are generated *dynamically* at high L, even for a purely linear interaction. There is no need for short-range forces to form the diquark. With relativistic kinematics and linear confinement, both in the naive 1/2 rule version (9) or in the more elaborate Y-shape version (11) a linear Regge trajectory is obtained, with the same slope as for mesons.

4. Regge phenomenolgy

The Regge theory, first developed in (Regge, 1959, 1960) connects the high energy behavior of the scattering amplitude with singularities in the complex angular momentum plane of the partial wave amplitudes in the crossed (t) channel. It is based on rather general properties of the S-matrix, on unitarity, analyticity and crossing symmetry. The simplest singularities are poles (Regge poles). According to the Chew-Frautschi conjecture (Chew and Frautschi, 1961, 1962)), the poles fall onto linear trajectories in M^2, J planes. In the Regge theory, the t-channel exchange of a particle with spin J is replaced by the exchange of a trajectory. Regge-trajectory exchange is thus a natural generalization of a usual exchange of a particle with spin J to complex values of J. The method established an important connection between high energy scattering and the spectrum of hadrons. There is a discussion if Regge trajectories are linear, parallel, or not (Inopin and Sharov, 2001; Tang and Norbury, 2000). No systematic errors were, however, included in these discussions. We will assume linearity and do not see any significant deviation from linear trajectories.

5. Solving QCD

a. QCD sum rules, Lattice QCD In QCD sum rules or in lattice QCD, one can reach the ground-state configuration of any given set of quantum numbers, in particular the leading Regge trajectory. The difficulty is only to built the corresponding operators.

However, this is more delicate for radial excitations, for which one should first remove the leading contribution of the ground state. The theoretical uncertainty is this larger. The latest results are, however, encouraging: (Mathur *et al.*, 2005) compared the radial and orbital excitations of the nucleon as a function of the assumed light-quark mass m_n, and found that the former is usually above the latter except for very small m_n, where a crossing is observed, and thus the same ordering as the experimental one. This result indicates that the anomalous ordering is particular to the light quark dynamics. It remains to be checked by other groups, with attention in particular to finite size effects (Sasaki and Sasaki, 2005).

b. AdS/QCD A new approach to quantum field theory is presently pursued, the so-called AdS/CFT correspondence (Anti de Sitter/Conformal Field Theory), which establishes a duality between string theories defined on the 5-dimensional AdS space-time and conformal field theories in physical space-time, see e.g. (Brodsky, 2007). It is assumed that the effective strong coupling is approximately constant in an appropriate range of momentum transfer, and that the quark masses can be neglected. Then QCD becomes a nearly conformal field theory and the AdS/CFT correspondence can be applied to QCD. The hadron spectrum and strong interaction dynamics can then be calculated from a holographic dual string theory defined on five-dimensional AdS space. For an appropriate choice of the metrics, a semi-classical approximation to QCD follows which incorporates both color confinement and conformal short-distance behavior. Confinement is parameterized by a cut-off in AdS space in the infrared region ("hard wall") (Polchinski and Strassler, 2002). Applied to baryon spectroscopy, AdS/QCD yields a mass relation $M \propto L + N$ (Brodsky and de Teramond, 2008; de Teramond and Brodsky, 2005). Spin 1/2 and spin 3/2 baryons require different AdS boundary conditions and lead to different offset masses. The predictions
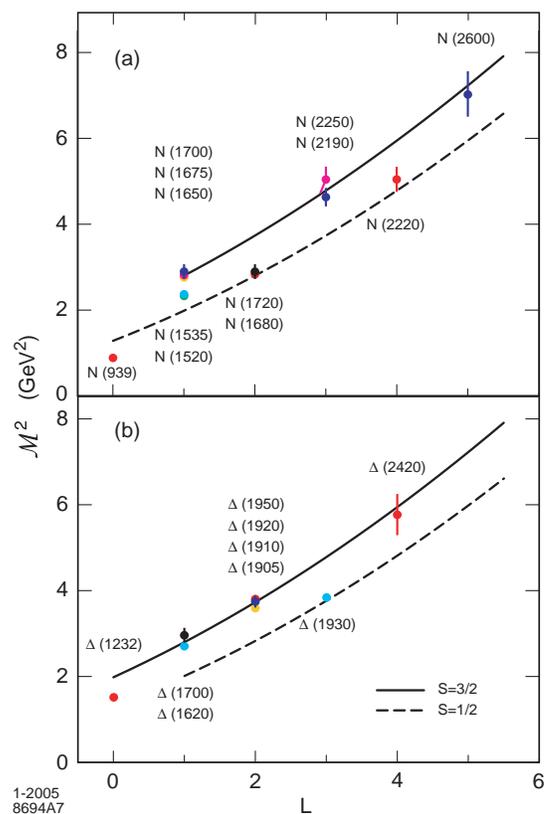
FIG. 36 Light baryon orbital spectrum for N^* (a) and Δ^* (b). The lower dashed curves correspond to baryon states dual to spin-1/2 modes in the bulk and the upper continuous curve to states dual to spin-3/2 modes (de Teramond and Brodsky, 2005).
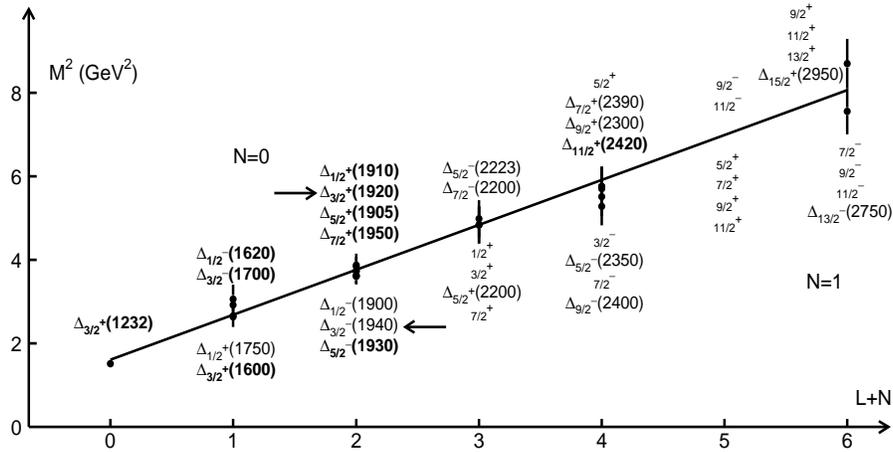
FIG. 37 Regge trajectory for Δ^* resonances as a function of the leading intrinsic orbital angular momentum L and the radial excitation quantum number N (corresponding to $n_1 + n_2$ in quark models) (Klempt, 2008). The line represents a prediction based on AdS/QCD correspondence (soft wall) (Forkel *et al.*, 2007a,b). Resonances with $N = 0$ and $N = 1$ are listed above or below the trajectory. The mass predictions are 1.27, 1.64, 1.92, 2.20, 2.43, 2.64, 2.84 GeV for $L + N = 0, 1, \cdots 6$, respectively.

are shown in Fig. 36. The lower mass of nucleon resonances with $S = 1/2$ can be related to the effect of "good" diquarks (Jaffe and Wilczek, 2003; Wilczek, 2004): diquarks with vanishing spin and isospin are energetically favored compared to "bad" diquarks. Of course, Δ resonances have isospin 3/2 and contain no "good" diquarks. Problems occur for $\Delta(1232)$ which is too low in mass and for $\Delta_{1/2^-}(1620)$ and $\Delta_{3/2^-}(1700)$ which are on the "wrong" trajectory. $\Delta_{5/2^-}(1930)$ is treated as spin 1/2 state with $L = 3$; in *the third excitation band* in section IV.F, this state is combined with $\Delta_{1/2^-}(1900)$ and $\Delta_{3/2^-}(1940)$ to form a triplet with $L = 1, S = 3/2, N = 1$ quantum numbers. (de Teramond and Brodsky, 2005) require the existence of a further to-be-discovered state with $J^P = 7/2^-$.

A general point of concern is the use of orbital angular momentum in the calculation. The dynamics of light quarks is highly relativistic, and the notion of a defined orbital angular momentum seems to make no sense. However, in section IV.F it is shown that baryon resonances are organized in spin multiplets and that orbital and spin angular momenta can be deduced from the multiplet structure. Hence in practice, the orbital-angular-momentum state can be defined.

In (Forkel *et al.*, 2007a,b), the mass spectrum of light mesons and baryons was predicted using AdS/QCD in the soft-wall approximation. The approach relies on deformations of the AdS metric, governed by one free mass scale proportional to Λ_{QCD} and leads to the same boundary conditions for $S = 1/2$ and $S = 3/2$ baryons. Relations between ground state masses and trajectory slopes

$$M^2 = 4\lambda^2(L + N + 1/2) \qquad \text{for mesons}$$
$$M^2 = 4\lambda^2(L + N + 3/2) \qquad \text{for baryons}$$
(19)

were derived. Using the slope of the Δ trajectory, baryon masses were calculated. For nucleons it is argued

(Forkel *et al.*, 2007b) that hyperfine interactions are not included in AdS/QCD and that the parameter λ in (19) should be re-tuned. This changes offset (the predicted nucleon mass) and the Regge slope, and the resulting compromise shows problems for small and large angular momenta.

The predicted masses for Δ baryons are plotted as a function of $L + N$ in Fig. 37 which includes all resonances (except the one-star $\Delta_{1/2^-}(2150)$ which would fit well with quantum numbers $L = 1, N = 2$ and 2.2 GeV predicted mass). The agreement is excellent and the remaining problems seen in Fig. 36b disappear.

For nucleons, we need to keep track of the fraction of spin-zero diquarks in a resonance, of the fraction α_D of "good diquarks". In (Forkel and Klempt, 2008), the dependence of nucleon correlators on interpolators with different diquark content was exploited to calculate the reduction in size and energy of nucleons with a "good diquark" fraction. In Table XV the masses of nucleon resonances are compared to AdS/QCD calculations. The Table specifies the quark spin and orbital angular momentum, the radial quantum number N, the "good" diquark fraction α_D, the resonances and the predicted mass. The prediction uses the eq. (19) and accounts for "good" diquarks by subtracting from the squared mass - calculated for specified $L+N$ value - the $\Delta(1232)$–$N(940)$ mass square difference, $2 \cdot (1.27^2 - 0.94^2)\,\alpha_D$.

$$M^2 = 1.04 \cdot (L + N + 3/2) - 1.46\,\alpha_D \; [GeV^2] \quad (20)$$

For spin or isospin 3/2, $\alpha_D = 0$, for baryons with $S = 1/2$ and $I = 1/2$, $\alpha_{56} = 1$ and $\alpha_{70} = 1/2$. The result is absolutely amazing: the masses of all 48 N and Δ resonances are very well reproduced using just two parameters. One parameter is related to confinement and was already used to describe the Δ mass spectrum, the second one describes "good" diquarks effects. The precision of the mass calculation is by far better than quark model predictions

even though the latter have a significant larger number of parameters.

Finally, one note on the good diquark fraction. For the ground states a those in the first excitation shell, these are determined using HO wave functions. At large excitation energies, the HO wave functions become increasingly complicated and the good diquark fraction decreases. Yet, two remote quarks does not require anti-symmetrization. Hence we assign the good diquark fraction of the ground state and first excited negative-parity states to all excitation levels.

TABLE XV Masses and suggested quantum numbers of nucleon and Δ resonances. The masses are calculated using eq. (20).

L	N	S	gdf	Resonance	Pred.
0	0	1/2	1/2	$N_{1/2+}(940)$	input: **0.94**
0	1	1/2	1/2	$N_{1/2+}(1440)$	1.40
0	2	1/2	1/2	$N_{1/2+}(1710)$	1.72
0	3	1/2	1/2	$N_{1/2+}(2090)$	2.03
2	0	1/2	1/2	$N_{3/2+}(1725)$, $N_{5/2+}(1685)$	1.72
4	0	1/2	1/2	$N_{9/2+}(2250)$	2.27
6	0	1/2	1/2	$N_{13/2+}(2800)$	2.71
1	0	1/2	1/4	$N_{1/2-}(1535)$, $N_{3/2-}(1520)$	1.53
1	1	1/2	1/4	$N_{1/2-}(1905)$, $N_{3/2-}(1860)$	1.82
1	2	1/2	1/4	$N_{1/2-}(2180)$, $N_{3/2-}(2090)$	2.12
3	0	1/2	1/4	$N_{5/2-}(2200)$, $N_{7/2-}(2190)$	2.12
5	0	1/2	1/4	$N_{11/2-}(2630)$	2.57
0	0	3/2	0	$\Delta_{3/2+}(1232)$	1.27
0	1	3/2	0	$\Delta_{3/2+}(1600)$	1.64
1	0	3/2	0	$N_{1/2-}(1655)$, $N_{3/2-}(1700)$, $N_{5/2-}(1675)$	1.64
1	0	1/2	0	$\Delta_{1/2-}(1620)$, $\Delta_{3/2-}(1700)$	1.64
1	1	3/2	0	$\Delta_{1/2-}(1900)$, $\Delta_{3/2-}(1940)$, $\Delta_{5/2-}(1930)$	1.92
1	2	1/2	0	$\Delta_{1/2-}(2150)$	2.20
2	0	3/2	0	$N_{1/2+}(1880)$, $N_{3/2+}(1900)$, $N_{5/2+}(1890)$	1.92
2	0	3/2	0	$N_{7/2+}(2020)$, $\Delta_{1/2+}(1910)$, $\Delta_{3/2+}(1920)$	1.92
2	0	3/2	0	$\Delta_{5/2+}(1905)$, $\Delta_{7/2+}(1950)$	1.92
3	0	3/2	0	$N_{9/2-}(2250)$	2.20
3	1	3/2	0	$\Delta_{5/2-}(2350)$, $\Delta_{9/2-}(2400)$	2.43
4	0	3/2	0	$\Delta_{5/2+}(2390)$, $\Delta_{7/2+}(2300)$, $\Delta_{9/2+}(2420)$	2.43
5	1	3/2	0	$\Delta_{13/2-}(2750)$	2.84
6	0	3/2	0	$\Delta_{15/2+}(2950)$	2.84

6. Hyperon resonances

Little experimental information is added since the review of (Hey and Kelly, 1983). We just notice that the mass spectrum of strange baryons is well reproduced by adding a term

$$M^2_{\Sigma^*(1385)} - M^2_{\Delta(1232)} = 0.40 \left[\mathrm{G}eV^2\right] \qquad (21)$$

to eq. (20). The $SU(3)_f$ singlet states $\Lambda_{1/2^-}(1405)$, $\Lambda_{3/2^-}(1520)$, and probably $\Lambda_{7/2^-}(2100)$ have good diquark fractions $\alpha_D = 3/2$.

E. Baryon decays

Hadron decays are a decisive element of any theory of strong interactions. The fact that so many resonances – expected in symmetric quark models – are missing in the data could find a natural explanation if the missing states have weak coupling only to $N\pi$. Indeed, this is what most models predict.

1. Hadron decays on the lattice

A intuitive understanding of hadron decays can be achieved by inspection of the potential energy between two static quarks. The energy can be described by the superposition of a Coulomb-like potential and a linearly rising (confinement) potential. At sufficiently large separations, for $R \approx 0.12\,\mathrm{fm}$, the total energy suffices to produce two (color-neutral) objects: spring breaking occurs. Spring breaking in mesons can be simulated on
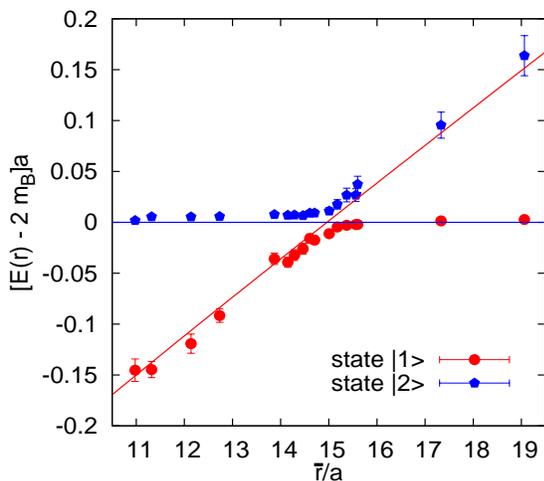
FIG. 38 Pair creation on a lattice, calculated for mesons. A sea quark-antiquark pair is created in the vacuum. At large distances, two-meson states are energetically preferred. For static quarks, the levels cross at some distance R (with $a \approx 0.083\,\mathrm{fm}$), the string breaking introduces mixing of the energy levels defined by the potential $V(R)$ and the threshold $2m(B)$ (Michael, 2006).

a lattice (Michael, 2006). Fig. 38 displays the energy levels due to a $q\bar{q}$ and a two-meson system in an adiabatic approximation. In a hadronic reaction, the sudden approximation − where the system follows the straight line − is more realistic, and mesons can be excited to large energies. Similar calculations for baryons have not yet been made but the physics picture should remain the same.

2. Models of hadron decays

The operators responsible for strong decays of baryon resonances are unknown. Models need to be constructed with some mechanism in mind; this can be either elementary meson emission from a baryon, quark pair creation, string breaking, or flux-tube breaking. In the latter three cases, a quark pair is created a process which is often modeled by assuming $^3P_0$ quantum numbers for the quark pair. A survey of models, theoretical results and a comparison with data is given by (Capstick and Roberts, 2000). They conclude that none of the models does "what can be termed an excellent job of describing what is known about baryon strong decays. The main features seem to be well described, but many of the details are simply incorrect". More recent widths calculations (Melde *et al.*, 2005; Sengl *et al.*, 2007) confirm this statement.

F. The band structure of baryon excitations

The harmonic oscillator provides a frame to classify baryons resonances. Non-harmonic corrections, relativistic effects, and in particular spin-dependent forces induce splitting of degenerate states and mixing of states with the same total spin and parity J^P but, of course, the number of expected states remains the same. In this section, the observed baryon resonances are mapped onto HO quark model states, in an attempt to identify classes of resonances which are missing. The systematic of observed and missing resonances may provide hints at the dynamics which leads to the observed spectrum of baryon resonances.

We focus the discussion on excited states of nucleon and Δ, and include low-mass Λ and Σ. There is not much known on the quantum numbers of Ξ and Ω baryons. An exception is the recent determination of the $\Xi_{1/2^+}(1690)$ quantum numbers from $\Lambda_c \to (\Lambda K^0_S)K^+$ decays (Petersen, 2006). A similar classification of baryon resonances was suggested by (Melde *et al.*, 2008). For low-lying states, most assignments agree; discrepancies show that present data do not suffice to identify all states in a unique way.

1. First excitation band

The first excitation band $(D, L_N^P) = (70, 1_1^-)$ contains negative-parity resonances. The known states are listed in Table XVI. With the $SU(3)_f$ decomposition

$$70 = {}^2 10 \ \oplus \ {}^4 8 \ \oplus \ {}^2 8 \ \oplus \ {}^2 1, \qquad (22)$$

we expect as non-strange baryons a $SU(3)_f$-octet spin doublet, a $SU(3)_f$-octet spin triplet (a degenerate quartet), and a $SU(3)_f$-decuplet spin doublet. In Table XVI, the low-mass negative parity states are collected. The multiplet structure is easily recognized in the data. Configuration mixing is of course possible for states with same J^P.

In the hyperon sector, a few expected states have not yet been observed. A missing state is indicated in Table XVI by an x. Based on eqs. (19-21), we expect all missing Λ and Σ states in the 1750 to 1850 MeV mass range. We have omitted the one-star $\Sigma_{3/2-}(1580)$. The Crystal Ball Collaboration studied the reaction $K^- p \to \Lambda \pi^0$ in the c.m. energy range 1565 to 1600 MeV (Olmsted *et al.*, 2004). Their results disagreed strikingly with older fits which included the $\Sigma_{3/2-}(1580)$ resonance. Instead, they proved the absence of any reasonably narrow resonance in this mass range.

In the Λ sector, the $\Lambda_{1/2-}(1405)$ and $\Lambda_{3/2-}(1520)$ are considerably lower in mass than $\Lambda_{1/2-}(1670)$ and $\Lambda_{3/2-}(1690)$. In quark models, this might be due to favorable hyperfine effects acting on a pair of light quarks with $l_\rho = 0$ and spin 0. There is also a copious literature on the effect of coupling to decay channels, or multiquark components in these states (Choe, 1998; Oset and Ramos, 1998).

A similar effect can be observed in heavy-flavor baryons. The mass difference between the Λ_c^+ ground state and the first excited states (a doublet) is 325 MeV, rather low for an orbital excitation. Like the $\Lambda_{1/2-}(1405)$, the two negative-parity states $\Lambda_c^+(2595)$

TABLE XVI The negative parity states of the first excitation band $(D, L_N^P) = (70, 1_1^-)$.

D; s	$J = 1/2$	$J = 3/2$	$J = 5/2$
70, 8; 1/2	$N_{1/2-}(1535)$	$N_{3/2-}(1520)$	
70, 8; 3/2	$N_{1/2-}(1650)$	$N_{3/2-}(1700)$	$N_{5/2-}(1675)$
70, 10; 1/2	$\Delta_{1/2-}(1620)$	$\Delta_{3/2-}(1700)$	
1, 1; 1/2	$\Lambda_{1/2-}(1405)$	$\Lambda_{3/2-}(1520)$	
70, 8; 1/2	$\Lambda_{1/2-}(1670)$	$\Lambda_{3/2-}(1690)$	
70, 8; 3/2	$\Lambda_{1/2-}(1800)$	x	$\Lambda_{5/2-}(1830)$
70, 8; 1/2	$\Sigma_{1/2-}(1620)$	$\Sigma_{3/2-}(1670)$	
70, 8; 3/2	$\Sigma_{1/2-}(1750)$	x	$\Sigma_{5/2-}(1775)$
70, 10; 1/2	x	x	

and $\Lambda_c^+(2625)$ benefit of the attractive spin–spin splitting for the light quark pair.

2. The second excitation band

In the HO model, the second excitation band contains states with either two units of angular momentum or one unit of radial excitation, with proper antisymmetrization in the case of identical quarks:

$$(D, L_N^P) = \underline{(56, 2_2^+)}, \ \underline{(70, 2_2^+)}, \qquad (23a)$$
$$(D, L_N^P) = \qquad\quad (20, 1_2^+), \qquad (23b)$$
$$(D, L_N^P) = \underline{(56, 0_2^+)}, \ \underline{(70, 0_2^+)}. \qquad (23c)$$

with either $(l_\rho, l_\lambda) = (0, 2)$ and $(2, 0)$ yielding the $(56, 2_2^+)$ multiplet, or with $l_\rho, l_\lambda = 1, 1$ coupling to $L = 0, 1, 2$ yielding $(70, 2_2^+)$, $(20, 1_2^+)$, and $(70, 0_2^+)$. The $(56, 0_2^+)$ supermultiplet comprises the first radial excitations with $(n_\rho, n_\lambda) = (0, 1)$ or $(1, 0)$. Both multiplets with $L^P = 0$ contain nucleons with spin-parity $1/2^+$, while for decuplet states, $J^P = 3/2^+$ for 56-plet members and $J^P = 1/2^+$ for 70-plet members.

We begin with $(D, L_N^P) = (56, 0_2^+)$. The most controversial state is the Roper resonance $N_{1/2+}(1440)$. In the HO model, it is degenerate with other $N = 2$ states, but in the experimental spectrum of the nucleon and Δ, it is almost degenerate, and even slightly below the $N = 1$ states with negative parity. Anharmonic corrections pushes this state down, and this perturbative result is confirmed in the hypercentral approximation (Hogaasen and Richard, 1983), which is a better approximation to confinement that is not quadratic. Even in exact treatments of the three-body problem, but with local, flavor independent potentials of confining type, the Roper resonance comes always *above* the first negative-parity states.

The "wrong" mass of the Roper resonance has initiated a longstanding debate if it is dynamically generated *or* if it is the nucleon first radial excitation and a quark-model state. We think it is both. An enlightening discussion of the (in-)possibility to distinguish meson-meson molecules from four-quark states can be found in (Jaffe, 2007). In Table XVII, the lowest-lying resonances having the same quantum numbers as their respective ground states and the mass square distance to them are listed. In colloquia, Nefkens calls them Roper, Loper, Soper, Xoper, and Doper (Nefkens, 2001), to underline that they play similar roles. If the Roper resonance should be generated by $\Delta\pi$ dynamics without any relation to the quark-model $(D, L_N^P) = (56, 0_2^+)$ state, $\Sigma_{1/2+}(1660)$ and $\Xi_{1/2+}(1690)$ could be generated by the same mechanism (making use of $\Sigma_{3/2+}(1385)\pi$ and $\Xi_{3/2+}(1530)\pi$). But there is no analogue mechanism which would lead to $\Lambda_{1/2+}(1600)$ and $\Delta_{3/2+}(1600)$. Understanding $N_{1/2+}(1440)$ from the interaction of mesons and baryons is an important step in understanding baryons and their interactions; S-wave thresholds may have an important impact on the precise

TABLE XVII Members of the $(D, L_N^P) = (56, 0_2^+)$ and $(D, L_N^P) = (70, 0_2^+)$ multiplets in the second excitation band and mass square difference (in GeV²) to the respective ground state. The expected values for the mass square differences are 1.08 and 2.16 GeV², respectively (see eq. (19) and Table XV).

56, 8; 1/2	$N_{1/2+}(1440)$	$\Lambda_{1/2+}(1600)$	$\Sigma_{1/2+}(1660)$	$\Xi_{1/2+}(1690)$
δM^2	1.19±0.11	1.31± 0.11	1.34±0.11	1.13±0.03
56, 10; 3/2		$\Delta_{3/2+}(1600)$	x	x
δM^2		1.04 ± 0.15		
70, 8; 1/2	$N_{1/2+}(1710)$	$\Lambda_{1/2+}(1810)$	$\Sigma_{1/2+}(1770)$	
δM^2	2.04±0.15	2.03± 0.15	1.72 ± 0.16	
70, 10; 1/2		$\Delta_{1/2+}(1750)$	$\Sigma_{1/2+}(1880)$	x
δM^2		1.54 ± 0.16	2.12±0.11	

TABLE XVIII $(D, L_N^P) = (56, 2_2^+)$, $(D, L_N^P) = (70, 2_2^+)$, and $(D, L_N^P) = (20, 1_2^+)$ resonances in the second excitation band.

D; s	J = 1/2	J = 3/2	J = 5/2	J = 7/2
56, 8; 1/2		$N_{3/2+}(1720)$	$N_{5/2+}(1680)$	
56, 8; 1/2		$\Lambda_{3/2+}(1890)$	$\Lambda_{5/2+}(1820)$	
56, 8; 1/2		$\Sigma_{3/2+}(1840)$	$\Sigma_{5/2+}(1915)$	
56,10; 3/2	$\Delta_{1/2+}(1910)$	$\Delta_{3/2+}(1920)$	$\Delta_{5/2+}(1905)$	$\Delta_{7/2+}(1950)$
56,10; 3/2	x	$\Sigma_{3/2+}(2080)$	$\Sigma_{5/2+}(2070)$	$\Sigma_{7/2+}(2030)$
70, 8; 3/2	$N_{1/2+}(1880)$	$N_{3/2+}(1900)$	$N_{5/2+}(1890)$	$N_{7/2+}(1990)$
70, 8; 3/2	x	x	$\Lambda_{5/2+}(2110)$	$\Lambda_{7/2+}(2020)$
70, 8; 3/2	x	x	x	x (Σ)
70, 8; 1/2		x	x	(N, Λ, Σ)
70,10; 1/2		x	x	(Δ, Σ)
20, 8; 1/2	x	x		(N, Λ, Σ)

location of poles and on the observed branching ratios. The pattern of states and their approximate mass values are, however, not or hardly affected.

Commonly, $N_{1/2+}(1710)$ and $\Delta_{1/2+}(1750)$ are candidates assigned to $(D, L_N^P) = (70, 0_2^+)$, and $\Sigma_{1/2+}(1880)$ belong to it as well. These baryons represent a new class: the two angular momenta l_ρ and l_λ are both one and couple to zero. $N_{1/2+}(1710)$ could also be assigned to the forth excitation band, with 2 units of radial excitation, but this interpretation is forbidden for $\Delta_{1/2+}(1750)$ and $\Sigma_{1/2+}(1880)$. The former is a 1-star resonance, the latter one has two stars; the PDG entry represents all claims above $\Sigma_{1/2+}(1770)$. Supposing their existence, we interpret the three states as members of the $(D, L^P) = (70, 0^+)$ multiplet.

We now turn to $(D, L_N^P) = (56, 2_2^+)$. In the nucleon spectrum, there should be (at 1.62 GeV) a spin doublet, in the Δ spectrum a spin quartet (at 1.92 GeV). These are all readily identified in the spectrum (see Table XVIII). For the Λ and Σ excitations, the corresponding states should be at 1.84 GeV and 2.03 GeV. All but one states are observed.

The situation is more difficult for $(D, L_N^P) = (70, 2_2^+)$. We expect a spin doublet (1.78 GeV; 1.90 GeV) and a spin quartet (1.92 GeV; 2.03 GeV) of octet states (mass estimates are for non-strange and strange baryons). The anchor for $L = 2, S = 3/2$ states are those having $J^P = 7/2^+$. These are the 2-star $N_{7/2+}(1990)$ and the 1-star $\Lambda_{7/2+}(2020)$. The nucleon quartet can be completed, the Λ quartet misses two states, and there is no evidence for a second Σ quartet. Most of the states have 1 or 2 stars, except the 3-star $\Lambda_{5/2+}(2110)$.

The interpretation of $\Sigma_{3/2+}(2080)$, $\Sigma_{5/2+}(2070)$, and $\Sigma_{7/2+}(2030)$ is ambiguous; in Table XVIII these states are assigned to the decuplet but they may as well be octet states. As 56-plet, they are strange partners of the quartet of Δ resonances mentioned above which are observed clearly in πN scattering. As 70-plet, they would be

partners of the more elusive $N_{1/2+}(1880)$, $N_{3/2+}(1900)$, $N_{5/2+}(1890)$, and $N_{7/2+}(1990)$.

In the second excitation band, the 56-plet is nearly complete and most states are well established. Spatial wave functions can be constructed which require excitation of one oscillator only. The 70-plet spatial wave functions have components in which a single oscillator is excited and components with both oscillators being excited. For the 70-plet, several candidates exist, mostly however with 1- or 2-star status.

In the non-strange sector, four supermultiplets, underlined in Table 23, are nearly full while the $(D, L_N^P) = (20, 1_2^+)$ multiplet is empty. It has an antisymmetric spatial wave function which is $\rho \times \lambda \psi_0$ in the HO model. Clearly, the wave function has no component with only one oscillator excited. Assuming (somewhat deliberately) that in πN scattering and in production experiments, only one of the oscillators is excited, we can "understand" the absence of this state in the observed spectrum.

3. The third excitation band

In the third band, the number of expected states increases significantly. In the harmonic oscillator basis, the following multiplets are predicted:

$$(D, L_N^P) = \underline{(56, 1_3^-)}, \; 2 \times (70, 1_3^-), (20, 1_3^-), \quad (24a)$$
$$(D, L_N^P) = (70, 2_3^-), \quad (24b)$$
$$(D, L_N^P) = (56, 3_3^-), \; \underline{(70, 3_3^-)}, \; (20, 3_3^-), \quad (24c)$$

Thus, 45 N^* and Δ^* resonances are expected while only 12 resonances are found in the 1800 to 2300 MeV mass range. Most of them are decorated with 1 or 2 stars, and some of them will be assigned to the fifth band. All

candidates belong just to the two underlined multiplets. The breakdown into states of defined spin and parity is given in Table XIX.

We first look for nucleon resonances with mass below $2.3\,\mathrm{GeV}$ and large angular momenta. These are $N_{7/2^-}(2190)$ and $N_{9/2^-}(2250)$. Based on the Regge trajectory of Fig. **??**, we assign $L = 3$ to both of them. We propose the assignments of Table XX as $(D, L_N^P) = (70, 3_3^-)$ states: $N_{7/2^-}(2190)$ is a 4-star "stretched" state with $L = 3, S = 3/2$; these often leave a more significant trace in the data then states which would fall onto a daughter Regge trajectory. Likewise, we propose $N_{7/2^-}(2190)$ to have $L = 3, S = 1/2$ with spin and orbital angular momenta aligned. The two states $N_{5/2^-}(2200)$ and $N_{7/2^-}(2190)$ could also be members of the spin quartet. The $N_{5/2^-}(2200)$ is observed, jointly with $N_{1/2^-}(1535)$ and $N_{3/2^+}(1720)$, to have strong coupling to $N\eta$. The pattern is used in (Bartholomy *et al.*, 2007) to argue that the state has $S = 1/2$. The two resonances $N_{1/2^-}(2090)$ and $N_{3/2^-}(2080)$ are tentatively interpreted as second radial excitations and are assigned to $(D, L_N^P) = (70, 1_5^-)$.

There is a striking sequence of negative-parity Δ states in the 1900-2000 MeV region, the $\Delta_{1/2^-}(1900)$, $\Delta_{3/2^-}(1940)$, and $\Delta_{5/2^-}(1930)$ resonances. The they could belong to two different doublets with $L = 1$ and $L = 3$; the partner of $\Delta_{5/2^-}(1930)$ would then be $\Delta_{7/2^-}(2200)$. In view of the absence of a large $\boldsymbol{LS}$ splitting in other cases, the mass separation seems rather large, and we do not follow this path. The discovery of a $7/2^-$ state below $2\,\mathrm{GeV}$ - as predicted by Glozman (pr. comm.) - would lead to a different interpretation.

We assign the three states to a triplet in the $(D, L_N^P) = (56, 1_3^-)$ multiplet. The triplet is separated in mass square from the doublet $(\Delta(1620)S_{31}, \Delta_{3/2^-}(1700))$ by $0.94\,\mathrm{GeV}^2$ (which is similar to the $N(1440)$–$N(940)$ mass square difference). If this is true, there must be a spin doublet nucleon pair of resonances with $J = 1/2^-$ and $J = 3/2^-$ below $1.9\,\mathrm{GeV}$ (to allow for a mass shift by a finite good-diquark fraction). This pair indeed exists, even though with debateable confidence. The states are listed in Table XIX. The 56-multiplet is full.

$\Delta_{9/2^-}(2400)$ has a mass which makes it unlikely to have (dominantly) $L = 5$ intrinsic orbital angular momentum. With $L = 3$, it needs a quark spin $S = 3/2$. Using quark model arguments only, $\Delta_{7/2^-}(2200)$ and $\Delta_{9/2^-}(2400)$ could both be $(D, L_N^P) = (56, 3_3^-)$ multiplet members. However, there is a 200 MeV mass difference between the two states and, in view of Fig. 37, we assign $\Delta_{7/2^-}(2200)$ to the $(D, L_N^P) = (70, 3_3^-)$ and $\Delta_{9/2^-}(2400)$ to $(D, L_N^P) = (56, 3_5^-)$.

We thus propose that odd-angular-momentum states are in a 56-plet if and only if there is a simultaneous excitation of the radial quantum number. The $\Delta_{5/2^-}(2350)$ resonance could be a spin partner of both these resonances, or the entry may comprise two resonances. The $\Delta_{1/2^-}(2150)$ is the third state with these quantum numbers. As discussed in section **??**, it might be a second

TABLE XIX Number of expected states in the third excitation band and observed states in the 1.8 to 2.4 GeV mass range (N and Δ).

	$N_{1/2^-}$	$N_{3/2^-}$	$N_{5/2^-}$	$N_{7/2^-}$	$N_{9/2^-}$
exptd	7	9	8	5	1
obsvd	2	2	1	1	1

	$\Delta_{1/2^-}$	$\Delta_{3/2^-}$	$\Delta_{5/2^-}$	$\Delta_{7/2^-}$	$\Delta_{9/2^-}$
exptd	3	5	4	2	1
obsvd	2	1	2	1	1

TABLE XX The negative parity states of the third excitation band $(D, L_N^P) = (56, 1_3^-)$ and $(D, L_N^P) = (70, 3_3^-)$.

D; s		$J = 1/2$	$J = 3/2$	$J = 5/2$
$\mathbf{56}, \mathbf{8}; 1/2$		$N_{1/2^-}(1905)$	$N_{3/2^-}(1860)$	
$\mathbf{56}, \mathbf{10}; 3/2$		$\Delta_{1/2^-}(1900)$	$\Delta_{3/2^-}(1940)$	$\Delta_{5/2^-}(1930)$

D; s	$J = 3/2$	$J = 5/2$	$J = 7/2$	$J = 9/2$
$\mathbf{70}, \mathbf{8}; 1/2$		$N_{5/2^-}(2070)$	$N_{7/2^-}(2190)$	
$\mathbf{70}, \mathbf{8}; 3/2$	x	$N_{5/2^-}(2200)$	x	$N_{9/2^-}(2250)$
$\mathbf{70}, \mathbf{10}; 1/2$		x	$\Delta_{7/2^-}(2200)$	

radial excitation and belong to $(D, L_N^P) = (70, 1_5^-)$.

4. Further excitation bands

In the forth band, the number of states is exploding while data are scarce. Expected is a large number of multiplets (25):

$$(D, L_N^P) = 2 \times (56, 0_4^+),\ 2 \times (70, 0_4^+), \tag{25a}$$
$$(D, L_N^P) = (20, 1_4^+),\ (70, 1_4^+), \tag{25b}$$
$$(D, L_N^P) = 2 \times (56, 2_4^+),\ 3 \times (70, 2_4^+),\ (20, 2_4^+), \tag{25c}$$
$$(D, L_N^P) = 2 \times (70, 3_4^+), \tag{25d}$$
$$(D, L_N^P) = \underline{(56, 4_4^+)},\ 2 \times (70, 4_4^+). \tag{25e}$$

The large number of expected states is one of the unsolved issues in baryon spectroscopy. It is known as problem of the *missing resonances*. Eq. 25 gives the breakdown of expected states into multiplets. While 93 N and Δ resonances are expected, 4 are found. All four observed states, $N_{9/2^+}(2220)$, $\Delta_{7/2^+}(2390)$, $\Delta_{9/2^+}(2300)$, and $\Delta_{11/2^+}(2420)$ interpreted as $L = 4$ $S = 1/2$ nucleon and $S = 3/2$ Δ resonances, belong to the $(D, L_N^P) = (56, 4_4^+)$ supermultiplet, in which a $N_{7/2^+}$ and a $\Delta_{5/2^+}$ are missing.

The spectrum continues with $\Delta_{5/2^-}(2350)$ and $\Delta_{9/2^-}(2400)$ ($L = 3, N = 1$), $N_{11/2^-}(2600)$ ($L = 5, N = 0$) in the 5th, with $N_{13/2^+}(2700)$ and $\Delta_{15/2^+}(2950)$ ($L = 6, N = 0$) in the 6th, and $\Delta_{13/2^-}(2750)$ ($L = 5, N = 1$) in the 7th band. The number of expected states increases

TABLE XXI Number of expected states in the forth excitation band and observed states in the 2.1 to 2.5 GeV mass range (N and Δ).

	$N_{1/2^+}$	$N_{3/2^+}$	$N_{5/2^+}$	$N_{7/2^+}$	$N_{9/2^+}$	$N_{11/2^+}$
exptd	10	14	16	12	7	2
obsvd	0	0	0	0	1	0

	$\Delta_{1/2^+}$	$\Delta_{3/2^+}$	$\Delta_{5/2^+}$	$\Delta_{7/2^+}$	$\Delta_{9/2^+}$	$\Delta_{11/2^+}$
exptd	5	8	8	7	3	1
obsvd	0	0	1	1	1	

dramatically. We conjecture that high masses, beyond 2.3 GeV, all observed baryons fall into a SU(3)$_f$ 56-plet; hence all nucleons $\boldsymbol{J} = \boldsymbol{L} + \boldsymbol{S}$ with spin 1/2 and all Δ resonances, spin 3/2.

5. Dynamical conclusions

In the low-mass region, in the first excitation shell, the quark model gives a perfect match of the number of expected and observed states. Starting from N = 2, only states are realized in which the ρ and the λ oscillator are excited coherently (e.g. with a wave function $\propto \rho^2 + \lambda^2$) while states with both oscillators excited simultaneously (e.g. with a wave function $\propto \rho \times \lambda$) have not been observed.

Positive-parity nucleon resonances with $L = 2, S = 3/2$ will have $J^P = 7/2^+$; indeed, a two-star $N_{7/2^+}(1990)$ exists. Above, there is a $N_{9/2^+}(2220)$ but no $11/2^+$ partner which should exist if $N_{9/2^+}(2220)$ had $L = 4, S = 3/2$. Instead it likely has $L = 4, S = 1/2$. Likewise, $N_{13/2^+}(2700)$ exists but no $15/2^+$ nucleon, and we assign $L = 6, S = 1/2$. The four states $N(940)$, $N_{5/2^+}(1680)$, $N_{9/2^+}(2220)$, and $N_{13/2^+}(2700)$ belong to the leading nucleon Regge trajectory.

Negative-parity nucleon resonances with the largest total angular momenta (in a given mass interval) are $N_{5/2^-}(1675)$, $N_{9/2^-}(2250)$, $N_{11/2^-}(2600)$, where the former two resonances obviously have $L = 1$ and $L = 3$ and $S = 3/2$, and the latter one $L = 5, S = 1/2$. We conclude that for up to $L = 3$, nucleon resonances can be in a 56 or in a 70-plet while for high masses, the observed nucleon resonances have spin $S = 1/2$.

High-spin positive parity Δ resonances are readily identified as $\Delta_{3/2^+}(1232)$, $\Delta_{7/2^+}(1950)$, $\Delta_{11/2^+}(2420)$, $\Delta_{15/2^+}(2950)$ with $L = 0, 2, 4, 6$ and $S = 3/2$ as leading contributions (and possibly some small higher-L components). The observed positive-parity Δ resonances all have spin $S = 3/2$. The $\Delta_{1/2^+}(1750)$ resonance is the only positive-parity $I = 3/2$ resonances which belongs to a 70-plet.

The negative-parity sector is a bit more complicated. Δ resonances with $L = 1$, $S = 3/2$ are forbidden for $n_\lambda = 0$, and resonances have either $S = 1/2$, $n_\lambda = 0$ (and belong to a 70-plet) or $S = 3/2$, $n_\lambda = 1$ (and belong to a 56-plet). For $L = 3$, Δ resonances still have either $S =$

TABLE XXII Observed multiplets at large angular momenta

N^* with $P = +$:	spin $S = 1/2$	$l_\lambda = L$; $n_\rho = 0$
N^* with $P = -$:		

Δ^* with $P = +$:	spin $S = 3/2$;	$l_\lambda = L$; $n_\rho = 0$
Δ^* with $P = -$:		$l_\lambda = L$; $n_\rho = 1$

$1/2$, $n_\lambda = 0$ and belong to $70, 3_3^-$, or they have $S = 3/2$, $n_\lambda = 1$ $(56, 1_3^-)$ even though HO wave functions do not forbid neither $S = 3/2$, $n_\lambda = 0$ $(56, 3_3^-)$ nor $S = 1/2$, $n_\lambda = 1$ $(70, 1_3^-)$. For $L = 5$, only $S = 3/2$ and $n_\lambda = 1$ is observed.

In summary, most observed resonances fall into 56-plets. Resonances in 70-plets are seen up to the third shell, not above. There are no states which would need to be assigned to a 20-plet. In other words, the experimentally known resonances above the third shell can be described by a diquark in S-wave (with the ρ-oscillator in the ground state) and the λ oscillator carrying the full excitation.

This rule leads to a selection of allowed multiplets which are summarized in Table XXII.

G. Exotic baryons

The search for exotic mesons, spin-parity exotics, and krypto-exotic states has been a continuous stimulation of the field. Examples are the $\pi_1(1400)$ and $\pi_1(1600)$ mesons with $J^{PC} = 1^{-+}$ (quantum numbers which cannot come from $q\bar{q}$), the flavor exotic states $Z^\pm(4050)$, $Z^\pm(4248)$, and $Z^\pm(4430)$ (Abe *et al.*, 2008; Mizuk *et al.*, 2008) (decaying into a pion and a $c\bar{c}$ resonance), or mesons like $f_0(980)$, $a_0(980)$, $f_0(1500)$, $X(3872)$ (Abe *et al.*, 2008) which have attracted a large number of theoretical papers trying to understand their nature either as quarkonium states or as Krypto-exotic states, as glueballs, as weakly or tightly bound tetraquarks or as molecular states (among other more exotic interpretations). The existence of exotic mesons as additional states in meson spectroscopy is not beyond doubt: see, e.g. (Klempt and Zaitsev, 2007) for a critical and (Crede and Meyer, 2008) for a more optimistic view.

Intruders into the world of baryons would be identified unambiguously when they have quantum numbers which differ from those of qqq baryons. There are no spin-parity exotic quantum numbers in baryon spectroscopy, but flavor exotic states (containing an antiquark in the flavor wave function) might exist. Most discussion is directed to the question if krypto-exotic baryons exist.

The Roper resonance $N_{1/2^+}(1440)$ is the lowest-mass nucleon resonance and has the quantum numbers of the nucleon. Its most natural explanation as first radial excitation is incompatible with quark models in which the radial excitation requires two harmonic-oscillator quanta

while the negative parity states like $N_{1/2^-}(1535)$ require one quantum only. Even including anharmonicity, the mass of the first radial excitation should always be above the first orbital-angular-momentum excitation. Within the constituent quark model with one-gluon-exchange (Capstick and Isgur, 1986) or instanton induced forces (Löring *et al.*, 2001b), the Roper $N_{1/2^+}(1440)$ should have a mass 80 MeV above the $N_{1/2^-}(1535)$ mass, and not ≈ 100 MeV below it. Models using Goldstone-boson exchange interactions (Glozman and Riska, 1996) improve on the Roper mass but this success is counterbalanced by two shortcomings: (1) the interaction is inappropriate to calculate the full hadronic spectrum; (2) restricted to light baryons, only the lowest-mass excitations were calculated with a comparatively large number of adjustable parameters. The Roper resonance has a surprisingly large width, and the transition photo-coupling amplitude has even the wrong sign (Capstick and Keister, 1995). Calculations on a lattice support the idea that the Roper is not the radial excitation of the nucleon (Borasoy *et al.*, 2006; Burch *et al.*, 2006) but, so far, final conclusions have not yet been reached. Hence $N_{1/2^+}(1440)$ is often interpreted as an intruder into the world of qqq baryons. There has been the claim that the Roper resonance region might house two resonances (Morsch and Zupranski, 2000), one at 1390 MeV with a small elastic width and large coupling to $N\pi\pi$, and a second one at higher mass – around 1460 MeV – with a large elastic width and small $N\pi\pi$ coupling. This idea was tested in (Sarantsev *et al.*, 2008) analyzing the overconstrained set of reactions $\pi^- p \to N\pi$, $\pi^- p \to n\pi^0\pi^0$, $\gamma p \to N\pi$, $\gamma p \to p\pi^0\pi^0$. A second pole was rejected unless its width was sufficiently narrow to allow the resonance to have its full phase motion in between the masses at which data are available.

The Roper resonance is accompanied by a series of "friends" with the same J^P but different flavor. These were nicknamed Doper $\Delta_{3/2^+}(1600)$, Loper $\Lambda_{1/2^+}(1600)$, Soper $\Sigma_{1/2^+}(1660)$ and Xoper $\Xi_{1/2^+}(1690)$ by Nefkens. Any interpretation of the Roper as intruder ought to explain all these states on the same footing.

Further examples of baryons which may deserve an interpretation beyond the quark model are $N_{1/2^-}(1535)$, a resonance which is observed at the expected mass but with an unusual large decay branching ratio to $N\eta$, and the $\Lambda_{1/2^-}(1405)$ and $\Lambda_{3/2^-}(1520)$ with their low mass and unusual splitting. A consistent (Liu and Zou, 2006; Zou, 2008) – even though controversial – (Liu and Zou, 2007; Sibirtsev *et al.*, 2007) picture for these possibly kryptoexotic baryons ascribes the mass pattern to a large $qqqq\bar{q}$ fraction in the baryonic wave functions.

1. Pentaquarks

The question of the existence of multiquark hadrons has been raised at the beginning of the quark model, and is regularly revisited, either due to fleeting experimental evidence or to theoretical speculations. In the late 60's some analyses suggested a possible resonance with baryon number $B = 1$ and strangeness $S = -1$, opposite to that of the Λ or Σ hyperons.

In 1976, a stable dihyperon H was proposed (Jaffe, 1977), whose tentative binding was due to coherences in the chromomagnetic interaction. In 1987, Gignoux et al., and, independently, Lipkin (Gignoux *et al.*, 1987; Lipkin, 1987) showed that the same mechanism leads to a stable $(Q\bar{q}^4)$ below the threshold for spontaneous dissociation into $(Q\bar{q}) + (\bar{q}^3)$. This calculation, and Jaffe's for his $H = (u^2 d^2 s^2)$ gave 300 MeV of binding if the light quark are treated in the SU(3) limit (and Q infinitely heavy for the pentaquark) and if the short-range correlation $\langle \delta^{(3)}(r_{ij}) \rangle$ is borrowed from ordinary baryons. However, relaxing these strong assumptions always go in the direction of less and less binding, and even instability. The H was searched for in dozens of experiments (Ashery, 1996). The 1987-vintage pentaquark was searched for by the experiment E791 at Fermilab, (Aitala *et al.*, 1998), but the results are not conclusive.

Some years ago, a lighter pentaquark was found in photoproduction, called $\Theta^+(1540)$ (Nakano *et al.*, 2003), inspired by the beautiful theoretical speculation in a chiral soliton model predicting a narrow (anti-) decuplet of narrow baryons by (Diakonov *et al.*, 1997), following, in turn, a number of earlier paper. The $\Theta^+(1540)$ was confirmed in a series of low-statistics experiments. The decuplet was enriched by the doubly charged $\Phi(1860)$ (Alt *et al.*, 2004); the missing members were identified with $N_{1/2^+}(1710)$ and $\Sigma_{1/2^+}(1890)$. A narrow peak in the pD^{*-} and $\bar{p}D^{*+}$ distributions signalled a baryon with an intrinsic $\bar{c}$-quark, $\Theta_c^0(3100)$ (Aktas *et al.*, 2004).

These observations initiated a large number of further experimental and theoretical studies which were reviewed by (Dzierba *et al.*, 2005) and (Hicks, 2005). Recent experiments had partly a very significant increase in statistics but no narrow pentaquark state was confirmed. The list of experiments and upper limits for pentaquark production can be found in PDG (Wohl, 2008b) from where we quote the final conclusion: *The whole story - the discoveries themselves, the tidal wave of papers by theorists and phenomenologists that followed, and the eventual "undiscovery" - is a curious episode in the history of science.* The evidence for a pentaquark interpretation (Kuznetsov *et al.*, 2008) of a narrow peak in the $n\eta$ invariant mass spectrum at 1680 MeV is weak; the peak is observed in photoproduction of η-mesons off neutrons in a deuteron (Fantini *et al.*, 2008; Jaegle *et al.*, 2008; Kuznetsov *et al.*, 2007) but can be understood quantitatively with standard properties of $N_{1/2^-}(1535)$ and $N_{1/2^-}(1650)$ and interference between them (Anisovich *et al.*, 2008).
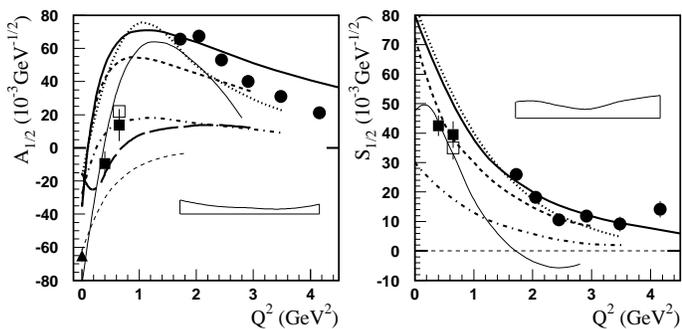
FIG. 39 Transverse (left) and longitudinal (right) helicity amplitudes for the $\gamma^* p \to N_{1/2^+}(1440)$ transition. The data points are from CLAS (Aznauryan *et al.*, 2008). The full triangle gives the value at the photon point (Amsler *et al.*, 2008). The lines represent various quark model calculations: dotted (Capstick and Keister, 1995) dashed (Weber, 1990), dash-dotted (Cardarelli *et al.*, 1997), long-dashed (Julia-Diaz *et al.*, 2004), solid (Aznauryan, 2007), and thin solid curves are from (Cano and Gonzalez, 1998; Cano *et al.*, 1996), respectively. The thin dashed curves are obtained assuming that N(1440)P$_{11}$ is a q^{3}G hybrid state (Li *et al.*, 1992).

2. Baryonic hybrids

Baryons with properties incompatible with quark model predictions can be suspected to be baryonic hybrids. This fate is shared by a number of states, the Roper resonance $N_{1/2^+}(1440)$ being one example. Likewise, $\Lambda_{1/2^+}(1600)$ (Kisslinger, 2004), $\Sigma_{1/2^+}(1600)$ and $\Xi_{1/2^+}(1660)$ have low masses and could be hybrids as well. The mass gap between $\Lambda_{1/2^-}(1405)$ and $\Lambda_{3/2^-}(1520)$ is larger than expected in quark models but can be reproduced assuming them to be of hybrid nature (Kittel and Farrar, 2005) where a possible hybrid nature is also suggested for $\Lambda_c(2593)$ and $\Lambda_c(2676)$.

First bag-model predictions of hybrid-baryon masses suggested that some hybrids could have masses (Barnes and Close, 1983; Golowich *et al.*, 1983) below 2 GeV making a hybrid interpretation of $N_{1/2^+}(1440)$ unlikely. Also in a non-relativistic flux-tube model, the lowest hybrid-baryon mass was estimated to 1870 ± 100 MeV (Barnes *et al.*, 1995; Capstick and Page, 2002). Within a relativistic quark model (Gerasyuta and Kochkin, 2002) arrived at hybrid masses suggesting that $N_{1/2^+}(1710)$ and $\Delta_{3/2^+}(1600)$ could be be hybrid baryons. QCD sum rules predict, however, a hybrid mass of 1500 MeV and $N_{1/2^+}(1440)$ remains a hybrid candidate (Kisslinger and Li, 1995).

The most convincing experimental evidence providing an interpretation of the Roper resonance is derived from recent measurements of nucleon resonance transition form factors. Fig. 39 shows the transverse and longitudinal electro-coupling amplitudes $A_{1/2}$ and $S_{1/2}$ of the transition to the $N_{1/2^+}(1440)$ resonance. At the photon point $A_{1/2}$ is negative. The amplitude rises steeply with Q^2 and a sign change occurs near $Q^2 = 0.5$ GeV^2. At $Q^2 = 2$ GeV^2 the amplitude has about the same magnitude but opposite sign as at $Q^2 = 0$. Then it falls off slowly. The longitudinal amplitude $S_{1/2}$ is large at low Q^2 and drops off smoothly with increasing Q^2. The bold curves represent various quark model calculations, the thin dashed line is for a gluonic excitation (Li *et al.*, 1992). The hybrid hypothesis misses the sign change in $A_{1/2}$; $S_{1/2}$ is predicted to vanish identically. In contrast, most quark models qualitatively reproduce the experimental findings: the Roper $N_{1/2^+}(1440)$ resonance is the first radial excitation of the nucleon.

3. Dynamically generated resonances

The study of the dynamics of meson-baryon interactions is a challenging issue both in theoretical and experimental hadron-nuclear physics. The first historical example is $\Lambda(1405)$ which was suggested to be a $\bar{K}N$ quasi-bound state (Dalitz and Tuan, 1959, 1960). Modern theories of low-energy meson-baryon interactions are based on an effective chiral Lagrangian with an expansion in increasing powers of derivatives of the meson fields and quark masses (Gasser and Leutwyler, 1984, 1985). The theories are popular and very successful in understanding many properties of the meson-baryon system at low energies.

A number of further states has been suggested to be of dynamical origin but, before entering a discussion of individual cases, we specify different views of the meaning of dynamically generated resonances. The $\Delta^{++}(1232)$ resonance, e.g., can be considered as $\pi^+ p$ bound state or as state of three *up* quarks with spins aligned. In the quark model, it is a (qqq) resonance but its Fock decomposition certainly contains a $\pi^+ p$ component. When a resonance is close to the threshold for an important decay mode, in particular for decays into two hadrons in S-wave, the molecular component can become large and the properties of the resonance can be derived from its decays, the resonance can be generated dynamically. Nevertheless, the core of the resonance, tested at high Q^2, retains the (qqq) structure.

These quark-model baryon resonances can be interpreted using a different language. In low-energy QCD, hadrons are rather the effective degrees of freedom rather and not quarks and gluons. A possible direction to systematize the baryon spectrum is the construction of an effective field theory in terms of hadrons and to constrain that theory by as many properties of QCD as possible. In this approach, all baryon resonances should be viewed at as originating from the interaction of ground-state (pseudoscalar and vector) mesons with ground-state baryons (in the octet and decuplet representation). In this sense, dynamically generation of resonances is an alternative view of the spectrum and each individual resonance should find its interpretation as quark-model state and as dynamically generated resonance. Naively, one should expect from $(8 \otimes 8) \oplus (8 \otimes 10)$ an even larger num-

ber of resonances than from $3 \otimes 3 \otimes 3$ but the number of states in the molecular view could be reduced by further symmetries. So far, the molecular view suffers from the lack of any attempt to predict the full spectrum of resonances. Hence in this review, experimental results are compared with quark-model expectations.

However, dynamically generated resonances are often considered to be additional states. In this case, the origin of the resonance is of different nature and both species, quark-model states and dynamically generated resonances, exist on their own right. Then, they can mix and a doubling of states is expected.

Dynamically generated states can possibly be identified by a study of their behavior as a function of the number of colors (Lutz and Kolomeitsev, 2002). (Hanhart, 2008) points out that the analytic structure of the meson-baryon scattering matrix at important thresholds is different for (tightly-bound) qqq states and (weakly-bound) molecular states, and this provides a means to identify the nature of a resonance.

We now turn to a discussion of some specific cases.

The Roper resonance: The difficulties with the mass of the Roper resonance encouraged attempts to explain the data dynamically, without introducing a resonance. In a coupled-channel meson exchange model based on an effective chiral-symmetric Lagrangian (Krehl *et al.*, 2000), no genuine qqq-resonance was needed to fit πN phase shifts and inelasticity, in agreement with (Schneider *et al.*, 2006). Again, the sign change in the helicity amplitude as a function of Q^2 (Aznauryan *et al.*, 2008) does not support this interpretation; it rather suggest a node in the wave function and thus a radially excited state. The result does of course not rule out a $qqqq\bar{q}$ ($N\pi$) component in the wave function as suggested by (Julia-Diaz and Riska, 2006; Li and Riska, 2006).

We mention here a few further $N_{1/2^+}$ states: a narrow $N(1680)$ which might have been observed in $n\eta$ photoproduction was already discussed as $N_{1/2^+}(1680)$ in the section on pentaquarks. A $N_{1/2^+}(1880)$ was recently reported by (Castelijns *et al.*, 2007) from photoproduction and has been observed by (Manley *et al.*, 1984) in the reaction $\pi^- p \to p\pi^+\pi^-$. The latter observation is listed in the PDG under $N_{1/2^+}(2100)$. The $N_{1/2^+}(1710)$ resonance, questioned in the most recent analysis of πN elastic scattering (Arndt *et al.*, 2006), was required in fits to $\pi N \to N\eta$ and $\pi N \to \Lambda K$ (Ceci *et al.*, 2006a,b).

$N_{1/2^-}(1535)$: 3-quark resonance or $N\eta$-ΣK coupled channel effect? This resonance is observed at a mass expected in quark models but its large decay branching ratio to $N\eta$ invited speculations that it might be created dynamically. Effective chiral Lagrangian rely on an expansion in increasing powers of derivatives of the meson fields and quark masses, has been successful in understanding many properties of the meson-baryon system at low energies(Kaiser *et al.*, 1995). More recent studies – with more data but similar conclusions – are presented in (Doring *et al.*, 2008; Geng *et al.*, 2008; Hyodo *et al.*,
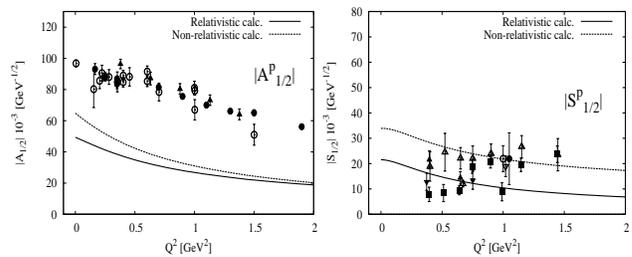
FIG. 40 Transverse (left) and longitudinal (right) helicity amplitudes for the $\gamma^* p \to N_{1/2^-}(1535)$ transition. The data points are from CLAS (Denizli *et al.*, 2007). The value at the photon point is from (Amsler *et al.*, 2008). The lines represent calculations by (Jido *et al.*, 2008).

2008).

Experimentally, response functions, photo-couplings, and ηN coupling strengths as functions of the invariant squared momentum transfer (measured for Q^2=0.13–3.3 GeV^2) was deduced from a measurement of cross sections for the reaction $ep \to e'\eta p$ for total center of mass energies W=1.5–2.3 GeV (Denizli *et al.*, 2007).

The helicity amplitudes were calculated within a coupled channel chiral unitary approach assuming that $N_{1/2^-}(1535)$ is dynamically generated from the strong interaction of mesons and baryons (Jido *et al.*, 2008). The Q^2 dependence is reproduced, the absolute height not (even though this is difficult to determine reliably from the data). The ratios obtained between the $S_{1/2}$ and $A_{1/2}$ for the two charge states of the $N_{1/2^-}(1535)$ agree qualitatively with experiment. The are not inconsistent this resonance being dynamically generated. However, there are indications – e.g. the harder Q^2 dependence in the data compared to the prediction – that a genuine quark-state component could improve the agreement between experiment and prediction.

$\Lambda_{1/2^-}(1405)$: The $\Lambda_{1/2^-}(1405)$ is one of the resonances having a mass which is difficult to reproduce in quark models. It falls just below the $N\bar{K}$ threshold; hence the attractive interaction between N and $\bar{K}$ and the coupling to the $\Sigma\pi$ channel could lead to a threshold enhancement or attract the pole of a not-too-far qqq resonance (Dalitz *et al.*, 1967). In models exploiting chiral symmetry and imposing unitarity, $\Lambda_{1/2^-}(1405)$ can be generated dynamically from the interaction of mesons and baryons in coupled channels.

A detailed study within a chiral unitary model revealed that the $N\bar{K}$–$\Sigma\pi$ coupled channel effects is considerably more complex. (Jido *et al.*, 2003) suggest that $\Lambda_{1/2^-}(1405)$ may contain two resonances; one at lower energies - mainly SU(3)$_f$ singlet - with a larger width and a stronger coupling to $\pi\Sigma$, the other one at higher energies, which is mostly SU(3)$_f$ octet and couples mostly to the $N\bar{K}$. The lower mass state is mostly observed in the $\pi^- p \to K^0\pi\Sigma$ reaction while the reaction $K^- p \to \pi^0\pi^0\Sigma^0$ produces a relatively narrow ($\Gamma = 38$ MeV) peak at 1420 MeV (Magas *et al.*, 2005).

This is a unique (or rare) example where the predictions of chiral dynamics and the quark model are at variance. Quark models predict one $1/2^-$ resonance at 1400 MeV, $\Lambda(1405)$. The model of (Jido *et al.*, 2003) predicts two resonances, a singlet at 1360 MeV decaying into $\pi\Sigma$ and an octet at 1426 MeV decaying into $\bar{K}N$.

We propose to test these ideas by a measurement of

$$J/\psi \to \ (\Lambda_{1/2^-} \to \pi\Sigma) \ (\Lambda_{1/2^-} \to \pi\Sigma) \qquad (26\text{a})$$

$$J/\psi \to \ (\Lambda_{1/2^-} \to \bar{K}N) \ (\Lambda_{1/2^-} \to \pi\Sigma) \qquad (26\text{b})$$

$$J/\psi \to \ (\Lambda_{1/2^-} \to \bar{K}N) \ (\Lambda_{1/2^-} \to \bar{K}N). \qquad (26\text{c})$$

In J/ψ decays $SU(3)_f$ singlet and octet states can be produced pairwise, but simultaneous production of one octet and one singlet state is suppressed. Hence reaction (26b) should occur with a much reduced rate compared to reactions (26a,c). In case, there is one $\Lambda(1405)$ only, reaction (26b) is not suppressed. If reactions (26a,c) occur with frequencies A and C, then reaction (26b) should occur with frequency $B = 2\sqrt{AC}$. We anticipate that the latter prediction is correct. We note in passing that (Wohl, 2008a) in PDG compares light and heavy baryons and concludes that $\Lambda_{1/2^-}(1405)$ is a 3-quark resonance.

4. Parity doublets, chiral multiplets

The existence of parity doublets in the baryon spectrum has been noticed as early as 1968 in (Minami, 1968). Parity doublets are expected in a world of chiral symmetry. The large mass difference between the nucleon and its chiral partner with $J = 1/2$ but negative parity, $N_{1/2^-}(1535)$, evidences that chiral symmetry is broken spontaneously. Glozman deserves the credit to have consistently pointed out (in at least 20 papers on arXiv, we quote here (Cohen and Glozman, 2002a,b; Glozman, 2000) that at high masses, mesons and baryons often occur in nearly mass-degenerate pairs of states with given spin but opposite parity: parity doublets are observed and possibly even chiral multiplets in which all (four) nucleon and Δ states with identical J^P should be degenerate in mass. Table XXIII summarizes the multiplets for $J^P = 1/2^\pm, \cdots 9/2^\pm$. In spite of an intense discussion in the literature, reviewed e.g. by (Jaffe *et al.*, 2006) and (Glozman, 2007) there is no consensus whether parity doubling emerges from the spin-orbital dynamics of the 3-quark system or if it reflects a deep symmetries in QCD. With the present status of the data, this question will likely remain unsettled.

In the harmonic oscillator approximation, a three-quark system is characterized by successive shells of positive and negative parity. Formally, this corresponds to masses being proportional to L + 2N. Parity doubling is not expected. In AdS/QCD parity doubling arises naturally due to the L + N dependence of the nucleonic mass levels. Within their collective model of baryons by (Bijker *et al.*, 1994, 1997) parity doubling is explained by the "geometric structure" of excitations (Iachello, 1989).

TABLE XXIII Parity doublets and chiral multiplets of N^* and Δ^* resonances of high mass. List and star rating are taken from (Amsler *et al.*, 2008). States not found in the recent analysis of the GWU group (Arndt *et al.*, 2006) are marked by [a].

$J=\frac{1}{2}$	$N_{1/2^+}(2100)^a$ *	$N_{1/2^-}(2090)^a$ *	$\Delta_{1/2^+}(1910)$ ****	$\Delta_{1/2^-}(1900)^a$ **
$J=\frac{3}{2}$	$N_{3/2^+}(1900)^a$ **	$N_{3/2^-}(2080)^a$ **	$\Delta_{3/2^+}(1920)^a$ ***	$\Delta_{3/2^-}(1940)^a$ *
$J=\frac{5}{2}$	$N_{5/2^+}(2000)^a$ **	$N_{5/2^-}(2200)^a$ **	$\Delta_{5/2^+}(1905)$ ****	$\Delta_{5/2^-}(1930)^a$ ***
$J=\frac{7}{2}$	$N_{7/2^+}(1990)^a$ **	$N_{7/2^-}(2190)$ ****	$\Delta_{7/2^+}(1950)$ ****	$\Delta_{7/2^-}(2200)^a$ *
$J=\frac{9}{2}$	$N_{9/2^+}(2220)$ ****	$N_{9/2^-}(2250)$ ****	$\Delta_{9/2^+}(2300)$ **	$\Delta_{9/2^-}(2400)^a$ **

In Regge phenomenology, the separation of states scales with $\delta M^2 = \text{const}$, or $M_1 - M_2 = \text{const}/(M_1 + M_2)$. Experimentally, the masses of states with positive and negative parity often show mass-degeneracy, but not in all cases. Clearly, a definition is needed when two masses are called mass degenerate (within experimental errors) or not. Based on quantitative tests, (Klempt, 2003) and (Shifman and Vainshtein, 2008) remain sceptical if the observed mass pattern are related to a symmetry of QCD and is not due a dynamical symmetry like absence of spin-orbit forces.

V. SUMMARY AND PROSPECTS

The recent years have seen a remarkable boost in our knowledge of baryons with heavy flavors, with the number of known baryons with b-quarks increasing from 1 to 7 in the last 4 years, and that of charmed states from 16 to 34. However, many points remain to be clarified: in most cases, the quantum numbers of heavy-flavor baryons are deduced from quark-model expectation, and a direct measurement would be desirable. One exception is the $\Lambda_c(2880)$, determined experimentally to be $J^P = 5/2^+$ exploiting the decay angular distribution in the sequential $\Lambda_c(2880)^+ \to (\Sigma_c(2455)\pi)^+$ decay (Fig. 3), but the mass spectrum suggests rather spin $1/2$ or $3/2$ and negative parity. The heaviest baryon known so far, Ω_b, has a mass of 6.165 GeV which seems almost 100 MeV too high by comparison with the strangeness-excitation energy in the sector of charmed baryons.

The double-charmed baryon, Ξ_{cc}^+ has been seen in only one experiment, and the measured mass seems a little too low as compared to model prediction. It is surprising that the mechanism of double $c\bar{c}$ production, which is responsible, e.g., for the observation of $J/\psi + \eta_c$ in e^+e^- collisions does not produce more often $cc + \bar{c}\bar{c}$, whose hadronization would lead to double-charm baryons. Triple-charm (or (ccb), (cbb) or (bbb))

spectroscopy will be to baryons what heavy quarkonium is for mesons: a laboratory for high-precision QCD studies. It is expected, for instance, that the analog of the Roper resonance for these baryons would be stable, and lie below the negative-parity excitations.

The experimental prospects for heavy baryon spectroscopy are bright provided the chance are used. Remember that discussions and even workshops are regularly held to use the production potential of heavy-ion collisions for the spectroscopy of exotic and heavy-flavored hadrons, but the corresponding upgrade of detectors, triggers and analysis programs has not yet started.

Doubled charmed baryons will be produced abundantly at LHC and even (ccc) states are not beyond the possibility. The upgrade of BELLE will improve the statistics in B decays and of background e^+e^- annihilation events very substantially; most information we have at present stems from the predecessors BaBaR, the present BELLE and from CLEO. PANDA offers a further unique possibility to study the physics of heavy flavors.

Light baryon spectroscopy has become again into the focus of a large community. Intense efforts are undertaken to carry out photoproduction experiments with linearly and circularly polarized photons and protons polarized along the direction of the incoming photon beam, or transversely. The reaction $\gamma p \to \Lambda K^+$ offers the best chance to perform a complete experiment, in which the full photoproduction amplitude can be reconstructed in an energy-independent partial-wave analysis. Important steps have been marked by experiments like CBELSA, CLAS, GRAAL, and different experiments at MAMI; several groups are attacking the difficult task of extracting from the data resonant and non-resonant contributions in energy-dependent partial-wave analyses. The confirmation of a few states ($N_{3/2^+}(1900)$, $\Delta 3/2^+(1920)$, $\Delta 3/2^-(1940)$) which had been observed in the old analyses of Höhler and of Cutkovsky and which were missing in the recent analysis of the GWU group substantiates the hope that photoproduction of multi-particle final states is a well-suited method for uncovering new baryon resonances.

The known baryon resonances show a few very surprising results. First, the apparent absence (or smallness) of spin-orbit forces leads to clear spin multiplets and thus allows one to assign intrinsic orbital and spin angular momenta to a given baryon resonance. The four nearly mass-degenerate states $\Delta_{1/2^+}(1910)$, $\Delta_{3/2^+}(1920)$, $\Delta_{5/2^+}(1905)$, and $\Delta_{7/2^+}(1950)$ form a quartet of resonance. It is counting the number of states and not relying on a model which determines the total quark spin to $S = 3/2$ and the orbital angular momentum to $L = 2$. Mixing with other states is not excluded, but giving mixing angles is (so far) a model-dependent statement. On this basis, all nucleon and Δ resonances can be assigned to a few SU(6) multiplets while other multiplets remain completely empty. At large masses, all known resonances are compatible with nucleon exci-

tations having a total quark spin $S = 1/2$ and Δ excitations having $S = 3/2$. At low energies, including the second excitation shell, the full richness offered by the 3-particle problem seems to be realized, except for one multiplet with an antisymmetric orbital wave function in which the angular momenta of the two oscillators with $l_\rho = 1$ and $l_\lambda = 1$ couple to a total angular momentum $L = 1$. Based on the systematics of baryon masses, we expect a spin doublet $N_{1/2^+}$ and $N_{3/2^+}$ at a mass of about $1.75 - 1.85\,\mathrm{GeV}$. Since both oscillators are excited, direct production of these states may be suppressed. But the two states have to mix with the two known states $N_{1/2^+}(1710)$ and $N_{3/2^+}(1720)$, and we expect a pattern which is difficult to resolve. Indeed, inconsistencies in the properties of the two resonances as produced in photoproduction and in πN elastic scattering may be a first hint for these elusive resonances. In the intermediate region, in the third shell, some multiplets are rather completely filled while others remain empty. There is no obvious systematic behavior which mass levels QCD has decided to populate and which one not.

The masses of nucleon and Δ resonances exhibit intriguing spin-parity doublets, pairs of states with $J^P = J^\pm$, and even evidence for chiral multiplets, of four mass-degenerate nucleon and two Δ resonances, all having the same J. The absence of strong spin-orbit forces leads to a degeneracy of states with given L and S but coupling to different J. Thus, the spectrum reveals a high level of symmetries. Different interpretations have been offered to explain the symmetries, restoration of chiral symmetry in the high-mass region (Table XXIII), and AdS/QCD (Table XV). The two interpretations predict different mass values for the lowest-mass $N_{7/2^-}$ state. In AdS/QCD this state should have intrinsic $L = 3, S = 1/2$ and $2.12\,\mathrm{GeV}$ mass. When chiral symmetry is restored, it should be found at $1.95\,\mathrm{GeV}$. A search for $N_{7/2^-}$ resonances is thus urgently requested.

Photo-induced reactions seems to favor production of low-angular-momentum states while pion-induced reactions (at least πN elastic scattering) is rich in high-angular-momentum states. To get a complete picture, hadron-induced reactions will be needed for a full understanding of the baryon resonance spectrum. (Bugg, 2007) has underlined that relatively simple experiments with no charged-particle tracking and with no magnetic field but a good electromagnetic calorimeter and a polarized target would give decisive new information on the hadronic mass spectrum, for both mesons and baryons, provided a good pion beam – which in the sixties of last century used to be the most natural thing in the world – would be available.

The chances for breakthroughs in the spectroscopy of light and heavy baryons are there and need to be pursued. The additional degrees of freedom in baryons – compared to the much simpler mesons – offer the possibility to test how strong QCD responds in such a complex environment: which of the multitude of configurations are realized and what are the effective agents and forces

leading to the highly degenerate pattern of energy levels. A related question is whether iterating the binding mechanisms seen at work for baryons lead to exotic hadrons, in particular multiquark states.

Acknowledgments

References

Aaltonen, T., *et al.*, 2007a, Phys. Rev. Lett. **99**, 202001.
Aaltonen, T., *et al.*, 2007b, Phys. Rev. Lett. **99**, 052002.
Abazov, V. M., *et al.*, 2006, Nucl. Instrum. Meth. **A565**, 463.
Abazov, V. M., *et al.*, 2007, Phys. Rev. Lett. **99**, 052001.
Abazov, V. M., *et al.*, 2008, eprint 0808.4142.
Abe, K., *et al.*, 2007, Phys. Rev. Lett. **98**, 262001.
Abe, K., *et al.* (Belle), 2008, Phys. Rev. Lett. **100**, 142001.
Abrams, G. S., *et al.*, 1974, Phys. Rev. Lett. **33**, 1453.
Acosta, D. E., *et al.*, 2005, Phys. Rev. **D71**, 032001.
Ahrens, J., *et al.*, 2000, Phys. Rev. Lett. **84**, 5950.
Ahrens, J., *et al.*, 2001, Phys. Rev. Lett. **87**, 022003.
Ahrens, J., *et al.*, 2003, Phys. Rev. Lett. **97**.
Ahrens, J., *et al.*, 2005, Phys. Lett. **B624**, 173.
Ahrens, J., *et al.*, 2006, Phys. Rev. **C74**, 045204.
Ahrens, J., *et al.*, 2007, Eur. Phys. J. **A34**, 11.
Aitala, E. M., *et al.*, 1998, Phys. Rev. Lett. **81**, 44.
Ajaka, J., *et al.*, 2006, Phys. Rev. Lett. **96**, 132003.
Ajaka, J., *et al.*, 2008, Phys. Rev. Lett. **100**, 052003.
Aker, E., *et al.*, 1992, Nucl. Instrum. Meth. **A321**, 69.
Aktas, A., *et al.*, 2004, Phys. Lett. **B588**, 17.
Albrecht, H., *et al.*, 1989, Nucl. Instrum. Meth. **A275**, 1.
Albrecht, H., *et al.*, 1993, Phys. Lett. **B317**, 227.
Albrecht, H., *et al.*, 1997, Phys. Lett. **B402**, 207.
Albrow, M. G., *et al.*, 1970, Nucl. Phys. **B25**, 9.
Albrow, M. G., *et al.*, 1972, Nucl. Phys. **B37**, 594.
Alekseev, I. G., *et al.*, 1991, Nucl. Phys. **B348**, 257.
Alekseev, I. G., *et al.*, 1995, Phys. Lett. **B351**, 585.
Alekseev, I. G., *et al.*, 1997, Phys. Rev. **C55**, 2049.
Alekseev, I. G., *et al.*, 2000, Phys. Lett. **B485**, 32.
Alekseev, I. G., *et al.*, 2006, Eur. Phys. J. **C45**, 383.
Alexander, J. P., *et al.*, 1999, Phys. Rev. Lett. **83**, 3390.
Alt, C., *et al.*, 2004, Phys. Rev. Lett. **92**, 042003.
Ambrozewicz, P., *et al.*, 2007, Phys. Rev. **C75**, 045203.
Ammar, R., *et al.*, 2001, Phys. Rev. Lett. **86**, 1167.
Amsler, C., *et al.*, 2008, Phys. Lett. **B667**, 1.
Anderson, R. L., *et al.*, 1969, Phys. Rev. Lett. **23**, 721.
Anderson, R. L., *et al.*, 1976, Phys. Rev. **D14**, 679.
Anisovich, A., V. Anisovich, M. Matveev, V. Nikonov, J. Nyiri, and A. Sarantsev, 2008, World Scientific, Singapore , 580.

Anisovich, A., E. Klempt, V. Nikonov, A. Sarantsev, and U. Thoma, 2009, Eur. Phys. J., in preparation.
Anisovich, A., E. Klempt, A. Sarantsev, and U. Thoma, 2005, Eur. Phys. J. **A24**, 111.
Anisovich, A. V., V. V. Anisovich, E. Klempt, V. A. Nikonov, and A. V. Sarantsev, 2007a, Eur. Phys. J. **A34**, 129.
Anisovich, A. V., V. V. Anisovich, E. Klempt, V. A. Nikonov, and A. V. Sarantsev, 2007b, Eur. Phys. J. **A34**, 129.
Anisovich, A. V., *et al.*, 2005, Eur. Phys. J. **A25**, 427.
Anisovich, A. V., *et al.*, 2007, Eur. Phys. J. **A34**, 243.
Anisovich, A. V., *et al.*, 2008, eprint 0809.3340.
Arndt, R. A., W. J. Briscoe, I. I. Strakovsky, and R. L. Workman, 2006, Phys. Rev. **C74**, 045205.
Artru, X., M. Elchikh, J.-M. Richard, J. Soffer, and O. V. Teryaev, 2008, eprint 0802.0164.
Artuso, M., *et al.*, 2001, Phys. Rev. Lett. **86**, 4479.
Ashery, D., 1996, Hyperfine Interact. **103**, 253.
Assafiri, Y., *et al.*, 2003, Phys. Rev. Lett. **90**, 222001.
Aston, D., *et al.*, 1988, Phys. Lett. **B215**, 799.
Aston, D., *et al.*, 1990, invited talk given at 15th APS Div. of Particles and Fields General Mtg., Houston, TX, Jan 3-6, 1990.
Athar, S. B., *et al.*, 2005, Phys. Rev. **D71**, 051101.
Aubert, B., *et al.*, 2002, Nucl. Instrum. Meth. **A479**, 1.
Aubert, B., *et al.*, 2005, Phys. Rev. **D72**, 052006.
Aubert, B., *et al.*, 2006a, 33rd International Conference on High Energy Physics (ICHEP 06), Moscow, Russia, 26 Jul - 2 Aug 2006, hep-ex/0607042., eprint hep-ex/0607042.
Aubert, B., *et al.*, 2006b, Phys. Rev. Lett. **97**, 232001.
Aubert, B., *et al.*, 2006c, Phys. Rev. **D74**, 011103.
Aubert, B., *et al.*, 2006d, 33rd International Conference on High Energy Physics (ICHEP 06), Moscow, Russia, 26 Jul - 2 Aug 2006, hep-ex/0607086., eprint hep-ex/0607086.
Aubert, B., *et al.*, 2007, Phys. Rev. Lett. **98**, 012001.
Aubert, B., *et al.*, 2008, Phys. Rev. **D77**, 012002.
Aubert, J. J., *et al.*, 1974, Phys. Rev. Lett. **33**, 1404.
Augustin, J. E., *et al.*, 1974, Phys. Rev. Lett. **33**, 1406.
Avakian, H., *et al.*, 2004, Phys. Rev. **D69**, 112004.
Avery, P., *et al.*, 1989, Phys. Rev. Lett. **62**, 863.
Aznauryan, I. G., 2007, Phys. Rev. **C76**, 025212.
Aznauryan, I. G., V. D. Burkert, and T. S. H. Lee, 2008, eprint 0810.0997.
Aznauryan, I. G., *et al.*, 2008, eprint 0804.0447.
Bagan, E., M. Chabab, H. G. Dosch, and S. Narison, 1993, Phys. Lett. **B301**, 243.
Bagan, E., H. G. Dosch, P. Gosdzinsky, S. Narison, and J. M. Richard, 1994, Z. Phys. **C64**, 57.
Ballam, J., *et al.*, 1972, Phys. Rev. **D5**, 545.
Ballam, J., *et al.*, 1973, Phys. Rev. **D7**, 3150.
Barber, D. P., *et al.*, 1982, Zeit. Phys. **C12**, 1.
Barber, D. P., *et al.* (LAMP2 GROUP), 1984, Z. Phys. **C26**, 343.
Bari, G., *et al.*, 1991a, Nuovo Cim. **A104**, 1787.
Bari, G., *et al.*, 1991b, Nuovo Cim. **A104**, 571.
Barker, I. S., A. Donnachie, and J. K. Storrow, 1975, Nucl. Phys. **B95**, 347.
Barmin, V. V., *et al.*, 2003, Phys. Atom. Nucl. **66**, 1715.
Barnes, T., and F. E. Close, 1983, Phys. Lett. **B123**, 89.
Barnes, T., F. E. Close, and E. S. Swanson, 1995, Phys. Rev. **D52**, 5242.
Barnes, V. E., *et al.*, 1964, Phys. Rev. Lett. **12**, 204.
Barrow, S. P., *et al.*, 2001, Phys. Rev. **C64**, 044601.
Bartalini, O., *et al.*, 2002, Phys. Lett. **B544**, 113.
Bartalini, O., *et al.*, 2005, Eur. Phys. J. **A26**, 399.

Bartalini, O., *et al.*, 2007, eprint arXiv:0707.1385 [nucl-ex].

Barth, J., *et al.*, 2003a, Eur. Phys. J. **A18**, 117.

Barth, J., *et al.*, 2003b, Eur. Phys. J. **A17**, 269.

Barth, J., *et al.*, 2003c, Phys. Lett. **B572**, 127.

Bartholomy, O., *et al.*, 2005, Phys. Rev. Lett. **94**, 012003.

Bartholomy, O., *et al.*, 2007, Eur. Phys. J. **A33**, 133.

Basdevant, J. L., and S. Boukraa, 1986, Z. Phys. **C30**, 103.

Battaglieri, M., *et al.*, 2003, Phys. Rev. Lett. **90**, 022002.

Beck, R., 2006, Eur. Phys. J. **A28, s01**, 173.

Berezhnoi, A. V., V. V. Kiselev, A. K. Likhoded, and A. I. Onishchenko, 1998, Phys. Rev. **D57**, 4385.

Bernard, V., N. Kaiser, and U.-G. Meissner, 1995, Int. J. Mod. Phys. **E4**, 193.

Bernotas, A., and V. Simonis, 2008, eprint 0808.1220.

Biagi, S. F., *et al.*, 1983, Phys. Lett. **B122**, 455.

Biagi, S. F., *et al.*, 1985, Z. Phys. **C28**, 175.

Bienlein, J. K., and E. D. Bloom, 1981, pRC 81/09.

Bijker, R., F. Iachello, and A. Leviatan, 1994, Ann. Phys. **236**, 69.

Bijker, R., F. Iachello, and A. Leviatan, 1997, Phys. Rev. **D55**, 2862.

Biselli, A. S., *et al.*, 2008, eprint 0804.3079.

Borasoy, B., P. C. Bruns, U. G. Meissner, and R. Lewis, 2006, Phys. Lett. **B641**, 294.

Bradford, R., *et al.*, 2006, Phys. Rev. **C73**, 035202.

Bradford, R., *et al.*, 2007, Phys. Rev. **C75**, 035205.

Brambilla, N., *et al.*, 2004, eprint hep-ph/0412158.

Briscoe, W., R. Arndt, I. Strakovsky, and R. Workman, 2005, international Workshop on the Physics of Excited Baryons (NSTAR 05), Tallahassee, Florida, 10-15 Oct 2005.

Brodsky, S. J., 2007, Eur. Phys. J. **A31**, 638.

Brodsky, S. J., and G. F. de Teramond, 2008, eprint arXiv:0802.0514 [hep-ph].

Brown, G. E., and M. Rho, 1979, Phys. Lett. **B82**, 177.

Brown, R. M., *et al.*, 1978, Nucl. Phys. **B144**, 287.

Bugg, D. V., 2007, eprint 0709.1256.

Burch, T., *et al.*, 2006, Phys. Rev. **D74**, 014504.

Butterworth, J. M., and M. Wing, 2005, Rept. Prog. Phys. **68**, 2773.

Cano, F., and P. Gonzalez, 1998, Phys. Lett. **B431**, 270.

Cano, F., P. Gonzalez, S. Noguera, and B. Desplanques, 1996, Nucl. Phys. **A603**, 257.

Capstick, S., and N. Isgur, 1986, Phys. Rev. **D34**, 2809.

Capstick, S., and B. D. Keister, 1995, Phys. Rev. **D51**, 3598.

Capstick, S., and P. R. Page, 2002, Phys. Rev. **C66**, 065204.

Capstick, S., and W. Roberts, 2000, Prog. Part. Nucl. Phys. **45**, S241.

Cardarelli, F., E. Pace, G. Salme, and S. Simula, 1997, Phys. Lett. **B397**, 13.

Castelijns, R., *et al.*, 2007, eprint nucl-ex/0702033.

Cazzoli, E. G., *et al.*, 1975, Phys. Rev. Lett. **34**, 1125.

Ceci, S., A. Svarc, and B. Zauner, 2006a, Phys. Rev. Lett. **97**, 062002.

Ceci, S., A. Svarc, and B. Zauner, 2006b, Few Body Sys. **39**, 27.

Ceci, S., A. Svarc, B. Zauner, M. Manley, and S. Capstick, 2008, Phys. Lett. **B659**, 228.

Chan, H.-M., *et al.*, 1978, Phys. Lett. **B76**, 634.

Chekanov, S., *et al.*, 2004, Phys. Lett. **B591**, 7.

Cheng, H.-Y., and C.-K. Chua, 2007, Phys. Rev. **D75**, 014006.

Chew, G. F., and S. C. Frautschi, 1961, Phys. Rev. Lett. **7**, 394.

Chew, G. F., and S. C. Frautschi, 1962, Phys. Rev. Lett. **8**, 41.

Chew, Goldberger, Low, Nambu, 1957, Phys. Rev. **106**, 1345.

Chiang, W.-T., and F. Tabakin, 1997, Phys. Rev. **C55**, 2054.

Chiang, W.-T., S. N. Yang, L. Tiator, M. Vanderhaeghen, and D. Drechsel, 2003, Phys. Rev. **C68**, 045202.

Chistov, R., *et al.*, 2006, Phys. Rev. Lett. **97**, 162001.

Choe, S., 1998, Eur. Phys. J. **A3**, 65.

Chung, Y., H. G. Dosch, M. Kremer, and D. Schall, 1982, Nucl. Phys. **B197**, 55.

Cohen, T. D., and L. Y. Glozman, 2002a, Phys. Rev. **D65**, 016006.

Cohen, T. D., and L. Y. Glozman, 2002b, Int. J. Mod. Phys. **A17**, 1327.

Corthals, T., D. G. Ireland, T. Van Cauteren, and J. Ryckebusch, 2007a, Phys. Rev. **C75**, 045204.

Corthals, T., J. Ryckebusch, and T. Van Cauteren, 2006, Phys. Rev. **C73**, 045207.

Corthals, T., T. Van Cauteren, P. Van Craeyveld, J. Ryckebusch, and D. G. Ireland, 2007b, Phys. Lett. **B656**, 186.

Cottingham, W. N., 1963, Ann. Phys. (N.Y.) **25**, 424.

Cox, C. R., *et al.*, 1969, Phys. Rev. **184**, 1453.

Craig, K., *et al.*, 2003, Phys. Rev. Lett. **91**, 102301.

Crede, V., and C. A. Meyer, 2008, eprint 0812.0600.

Crede, V., *et al.*, 2005, Phys. Rev. Lett. **94**, 012004.

Csorna, S. E., *et al.*, 2001, Phys. Rev. Lett. **86**, 4243.

Cutkosky, R. E., C. P. Forsyth, J. B. Babcock, R. L. Kelly, and R. E. Hendrick, 1980, presented at 4th Int. Conf. on Baryon Resonances, Toronto, Canada, Jul 14-16, 1980.

Cutkosky, R. E., C. P. Forsyth, R. E. Hendrick, and R. L. Kelly, 1979, Phys. Rev. **D20**, 2804, 2839.

Dalitz, R. H., and S. F. Tuan, 1959, Phys. Rev. Lett. **2**, 425.

Dalitz, R. H., and S. F. Tuan, 1960, Annals Phys. **10**, 307.

Dalitz, R. H., T. C. Wong, and G. Rajasekaran, 1967, Phys. Rev. **153**, 1617.

Dalton, M., *et al.*, 2008, eprint 0804.3509.

Danilov, M. V., and R. V. Mizuk, 2008, Phys. Atom. Nucl. **71**, 605.

De Masi, R., *et al.*, 2008, Phys. Rev. **C77**, 042201.

De Rujula, A., H. Georgi, and S. L. Glashow, 1975, Phys. Rev. **D12**, 147.

DeGrand, T. A., R. L. Jaffe, K. Johnson, and J. E. Kiskis, 1975, Phys. Rev. **D12**, 2060.

Denizli, H., *et al.*, 2007, Phys. Rev. **C76**, 015204.

Diakonov, D., V. Petrov, and M. V. Polyakov, 1997, Z. Phys. **A359**, 305.

Donoghue, J. F., C. Ramirez, and G. Valencia, 1989, Phys. Rev. **D39**, 1947.

Doring, M., E. Oset, and B. S. Zou, 2008, Phys. Rev. **C78**, 025207.

Dosch, H. G., M. Jamin, and S. Narison, 1989, Phys. Lett. **B220**, 251.

Drechsel, D., S. S. Kamalov, and L. Tiator, 2007, Eur. Phys. J. **A34**, 69.

Drechsel, D., and T. Walcher, 2008, Rev. Mod. Phys. **80**, 731.

Drell, S. D., and A. C. Hearn, 1966, Phys. Rev. Lett. **16**, 908.

Dugger, M., *et al.*, 2002, Phys. Rev. Lett. **89**, 222002.

Dugger, M., *et al.*, 2006, Phys. Rev. Lett. **96**, 062001.

Dugger, M., *et al.*, 2007, Phys. Rev. **C76**, 025211.

Durand, J., B. Julia-Diaz, T. S. H. Lee, B. Saghai, and T. Sato, 2008, eprint 0804.3476.

Dutz, H., *et al.*, 2003, Phys. Rev. Lett. **91**, 192001.

Dziembowski, Z., M. Fabre de la Ripelle, and G. A. Miller, 1996, Phys. Rev. **C53**, 2038.

Dzierba, A. R., C. A. Meyer, and A. P. Szczepaniak, 2005, J.

Phys. Conf. Ser. **9**, 192.

Ebert, D., R. N. Faustov, and V. O. Galkin, 2008, Phys. Lett. **B659**, 612.

Ecker, G., J. Gasser, A. Pich, and E. de Rafael, 1989, Nucl. Phys. **B321**, 311.

Edwards, K. W., *et al.*, 1995, Phys. Rev. Lett. **74**, 3331.

Egiyan, H., *et al.*, 2006, Phys. Rev. **C73**, 025204.

Elsner, D., *et al.*, 2006, Eur. Phys. J. **A27**, 91.

Elsner, D., *et al.*, 2007, Eur. Phys. J. **A33**, 147.

Engelfried, J., *et al.*, 1998, Nucl. Instrum. Meth. **A409**, 439.

Erbe, R., *et al.* (Aachen-Berlin-Bonn-Hamburg-Hedielberg-Munich), 1968, Phys. Rev. **175**, 1669.

Fantini, A., *et al.*, 2008, Phys. Rev. **C78**, 015203.

Fedotov, G., *et al.*, 2008, eprint 0809.1562 [nucl-ex].

Fleck, S., and J. M. Richard, 1989, Prog. Theor. Phys. **82**, 760.

Fleck, S., and J. M. Richard, 1990, Part. World **1**, 67.

Flynn, J. M., F. Mescia, and A. S. B. Tariq (UKQCD), 2003, JHEP **07**, 066.

Forkel, H., M. Beyer, and T. Frederico, 2007a, Int. J. Mod. Phys. **E16**, 2794.

Forkel, H., M. Beyer, and T. Frederico, 2007b, JHEP **07**, 077.

Forkel, H., and E. Klempt, 2008, eprint 0810.2959.

Frabetti, P. L., *et al.*, 1994, Phys. Rev. Lett. **72**, 961.

Frabetti, P. L., *et al.*, 1996, Phys. Lett. **B365**, 461.

Franklin, J., 1999, Phys. Rev. **D59**, 117502.

Franklin, J., 2008, eprint 0811.2143.

Frolov, V. V., *et al.*, 1999, Phys. Rev. Lett. **82**, 45.

Gaiser, J., *et al.*, 1986, Phys. Rev. **D34**, 711.

Garcia-Recio, C., J. Nieves, E. Ruiz Arriola, and M. J. Vicente Vacas, 2003, Phys. Rev. **D67**, 076009.

Garcilazo, H., J. Vijande, and A. Valcarce, 2007, J. Phys. **G34**, 961.

Gasser, J., and H. Leutwyler, 1984, Ann. Phys. **158**, 142.

Gasser, J., and H. Leutwyler, 1985, Nucl. Phys. **B250**, 465.

Gell-Mann, M., 1962, Phys. Rev. **125**, 1067.

Gell-Mann, M., and Y. Ne'eman, 1964, *The eightfold way*, Frontiers in Physics (Benjamin, New York, NY).

Geng, L. S., E. Oset, B. S. Zou, and M. Doring, 2008, eprint 0807.2913.

Gerasimov, S. B., 1966, Sov. J. Nucl. Phys. **2**, 430, [Yad. Fiz. **2** (1966) 598].

Gerasyuta, S. M., and V. I. Kochkin, 2002, Phys. Rev. **D66**, 116001.

Gignoux, C., B. Silvestre-Brac, and J. M. Richard, 1987, Phys. Lett. **B193**, 323.

Glander, K. H., *et al.*, 2004, Eur. Phys. J. **A19**, 251.

Glozman, L. Y., 2000, Phys. Lett. **B475**, 329.

Glozman, L. Y., 2007, Phys. Rept. **444**, 1.

Glozman, L. Y., and D. O. Riska, 1996, Phys. Rept. **268**, 263.

Goloskokov, S. V., 2007, eprint 0712.0490.

Golowich, E., E. Haqq, and G. Karl, 1983, Phys. Rev. **D28**, 160.

Gopal, G. P., 1980, invited talk given at 4th Int. Conf. on Baryon Resonances, Toronto, Canada, Jul 14-16, 1980.

Greenberg, O. W., 1964, Phys. Rev. Lett. **13**, 598.

Greenberg, O. W., and H. J. Lipkin, 1981, Nucl. Phys. **A370**, 349.

Guberina, B., B. Melic, and H. Stefancic, 2000, Phys. Lett. **B484**, 43.

Guberina, B., R. Ruckl, and J. Trampetic, 1986, Z. Phys. **C33**, 297.

Guo, F.-K., C. Hanhart, and U.-G. Meissner, 2008, JHEP **09**, 136.

Guo, L., *et al.*, 2007, Phys. Rev. **C76**, 025208.

Gutz, E., *et al.*, 2008, Eur. Phys. J. **A35**, 291.

Hadjidakis, C., *et al.*, 2005, Phys. Lett. **B605**, 256.

Hanhart, C., 2008, Eur. Phys. J. **A35**, 271.

Hasenfratz, P., R. R. Horgan, J. Kuti, and J. M. Richard, 1980, Phys. Lett. **B94**, 401.

Hasenfratz, P., and J. Kuti, 1978, Phys. Rept. **40**, 75.

He, X.-G., X.-Q. Li, X. Liu, and X.-Q. Zeng, 2007, Eur. Phys. J. **C51**, 883.

Helbing, K., 2006, Prog. Part. Nucl. Phys. **57**, 405.

Hey, A. J. G., and R. L. Kelly, 1983, Phys. Rept. **96**, 71.

Hicks, K. H., 2005, Prog. Part. Nucl. Phys. **55**, 647.

Hleiqawi, I., *et al.*, 2007, Phys. Rev. **C75**, 042201.

Hogaasen, H., and J. M. Richard, 1983, Phys. Lett. **B124**, 520.

Höhler, G., 2004, Determination of pole parameters in πN scattering, report, unpublished.

Höhler, G., F. Kaiser, R. Koch, and E. Pietarinen, 1979, Physics Data **12-1**.

Höhler, G., and R. L. Workman, 2008, N and Delta Resonances, in (Yao *et al.*, 2006).

't Hooft, G., 1976, Phys. Rev. **D14**, 3432.

Horn, I., *et al.*, 2007, eprint 0711.1138.

Horn, I., *et al.*, 2008, eprint 0806.4251.

Hyodo, T., D. Jido, and A. Hosaka, 2008, Phys. Rev. **C78**, 025203.

Hyslop, J. S., R. A. Arndt, L. D. Roper, and R. L. Workman, 1992, Phys. Rev. **D46**, 961.

Iachello, F., 1989, Phys. Rev. Lett. **62**, 2440.

Iijima, T., and E. Prebys, 2000, Nucl. Instrum. Meth. **A446**, 75.

Inopin, A., and G. S. Sharov, 2001, Phys. Rev. **D63**, 054023.

Ioffe, B. L., 1981, Nucl. Phys. **B188**, 317, erratum, B191 (1981) 591.

Iori, M., *et al.*, 2007, eprint hep-ex/0701021.

Isgur, N., 1980, Phys. Rev. **D21**, 779, erratum: D23 (1981) 817.

Isgur, N., 2000, why N*'s are important. N*2000 Summary. Published in: Newport News 2000, Excited nucleons and hadronic structure, p403-422., eprint nucl-th/0007008.

Jaegle, I., *et al.*, 2008, Phys. Rev. Lett. **100**, 252002.

Jaffe, R. L., 1977, Phys. Rev. Lett. **38**, 195, erratum, ibid.38, 617 (1977).

Jaffe, R. L., 2005, Phys. Rept. **409**, 1.

Jaffe, R. L., 2007, AIP Conf. Proc. **964**, 1.

Jaffe, R. L., D. Pirjol, and A. Scardicchio, 2006, Phys. Rept. **435**, 157.

Jaffe, R. L., and F. Wilczek, 2003, Phys. Rev. Lett. **91**, 232003.

Jessop, C. P., *et al.*, 1999, Phys. Rev. Lett. **82**, 492.

Jido, D., M. Doering, and E. Oset, 2008, Phys. Rev. **C77**, 065207.

Jido, D., J. A. Oller, E. Oset, A. Ramos, and U. G. Meissner, 2003, Nucl. Phys. **A725**, 181.

Joo, K., *et al.*, 2005, Phys. Rev. **C72**, 058202.

Julia-Diaz, B., T. S. H. Lee, A. Matsuyama, and T. Sato, 2007, Phys. Rev. **C76**, 065201.

Julia-Diaz, B., T. S. H. Lee, A. Matsuyama, T. Sato, and L. C. Smith, 2008, Phys. Rev. **C77**, 045205.

Julia-Diaz, B., and D. O. Riska, 2006, Nucl. Phys. **A780**, 175.

Julia-Diaz, B., D. O. Riska, and F. Coester, 2004, Phys. Rev. **C69**, 035212.

Junkersfeld, J., *et al.*, 2007, Eur. Phys. J. **A31**, 365.

Kaiser, N., P. B. Siegel, and W. Weise, 1995, Nucl. Phys.

A594, 325.

Kamano, H., B. Julia-Diaz, T. S. H. Lee, A. Matsuyama, and T. Sato, 2008, eprint 0807.2273.

Kernel, G., *et al.*, 1989a, Phys. Lett. **B216**, 244.

Kernel, G., *et al.*, 1989b, Phys. Lett. **B225**, 198.

Kernel, G., *et al.*, 1990, Z. Phys. **C48**, 201.

Kisslinger, L. S., 2004, Phys. Rev. **D69**, 054015.

Kisslinger, L. S., and Z. P. Li, 1995, Phys. Rev. **D51**, 5986.

Kittel, O., and G. R. Farrar, 2005, eprint hep-ph/0508150.

Klein, F., *et al.*, 2008, eprint 0807.0594.

Klempt, E., 2003, Phys. Lett. **B559**, 144.

Klempt, E., 2008, Eur. Phys. J. **A38**, 187.

Klempt, E., A. V. Anisovich, V. A. Nikonov, A. V. Sarantsev, and U. Thoma, 2006, Eur. Phys. J. **A29**, 307.

Klempt, E., B. C. Metsch, C. R. Munz, and H. R. Petry, 1995, Phys. Lett. **B361**, 160.

Klempt, E., and A. Zaitsev, 2007, Phys. Rept. **454**, 1.

Knapp, B., *et al.*, 1976, Phys. Rev. Lett. **37**, 882.

Knöchlein, G., D. Drechsel, and L. Tiator, 1995, Z. Phys. **A352**, 327.

Kokkedee, J. J. J., 1969, *The quark model*, Frontiers in Physics (Benjamin, New York, NY), based on a series of lectures given at CERN in Autumn 1967.

Koniuk, R., and N. Isgur, 1980, Phys. Rev. **D21**, 1868.

Kopp, S. E., 1996, Nucl. Instrum. Meth. **A384**, 61.

Körner, J. G., M. Kramer, and D. Pirjol, 1994, Prog. Part. Nucl. Phys. **33**, 787.

Kozlenko, N. G., *et al.*, 2003, Phys. Atom. Nucl. **66**, 110.

Krehl, O., C. Hanhart, S. Krewald, and J. Speth, 2000, Phys. Rev. **C62**, 025207.

Krusche, B., and S. Schadmand, 2003, Prog. Part. Nucl. Phys. **51**, 399.

Kuznetsov, V., *et al.*, 2007, Phys. Lett. **B647**, 23.

Kuznetsov, V., *et al.*, 2008, Acta Physica Polonica **8**, 1949.

Lawall, R., *et al.*, 2005, Eur. Phys. J. **A24**, 275.

Lee, T. S. H., 2007, eprint 0711.2193.

Lewis, R., N. Mathur, and R. M. Woloshyn, 2001, Phys. Rev. **D64**, 094509.

Li, Q. B., and D. O. Riska, 2006, Phys. Rev. **C74**, 015202.

Li, Z.-p., V. Burkert, and Z.-j. Li, 1992, Phys. Rev. **D46**, 70.

Lichtenberg, D. B., 1977, Phys. Rev. **D16**, 231.

Lichtenberg, D. B., R. Roncaglia, and E. Predazzi, 1996, Phys. Rev. **D53**, 6678.

Lipkin, H. J., 1987, Phys. Lett. **B195**, 484.

Liu, B. C., and B. S. Zou, 2006, Phys. Rev. Lett. **96**, 042002.

Liu, B. C., and B. S. Zou, 2007, Phys. Rev. Lett. **98**, 039102.

Liu, X., H.-W. Ke, Q.-P. Qiao, Z.-T. Wei, and X.-Q. Li, 2008, Phys. Rev. **D77**, 035014.

Lleres, A., *et al.*, 2007, Eur. Phys. J. **A31**, 79.

Lleres, A., *et al.*, 2008, eprint 0807.3839.

Lowe, J., *et al.*, 1991, Phys. Rev. **C44**, 956.

Lutz, M. F. M., and E. E. Kolomeitsev, 2002, Nucl. Phys. **A700**, 193.

MacCormick, M., *et al.*, 1996, Phys. Rev. **C53**, 41.

Magas, V. K., E. Oset, and A. Ramos, 2005, Phys. Rev. Lett. **95**, 052301.

Manley, D. M., R. A. Arndt, Y. Goradia, and V. L. Teplitz, 1984, Phys. Rev. **D30**, 904.

Manley, D. M., and E. M. Saleski, 1992, Phys. Rev. **D45**, 4002.

Manley, D. M., *et al.*, 2002, Phys. Rev. Lett. **88**, 012002.

Manweiler, R., *et al.*, 2008, Phys. Rev. **C77**, 015205.

Mart, T., and A. Sulaksono, 2006, Phys. Rev. **C74**, 055203.

Martin, A., 1986, Z. Phys. **C32**, 359.

Martin, J. F., *et al.*, 1975, Nucl. Phys. **B89**, 253.

Mathur, N., *et al.*, 2005, Phys. Lett. **B605**, 137.

Matsuyama, A., T. Sato, and T. S. H. Lee, 2007, Phys. Rept. **439**, 193.

Mattson, M., *et al.*, 2002, Phys. Rev. Lett. **89**, 112001.

Meadows, B. T., 1980, in Proceedings Baryon 1980, Toronto (1980), p. 283-300.

Mecking, B. A., *et al.*, 2003, Nucl. Instrum. Meth. **A503**, 513.

Melde, T., W. Plessas, and B. Sengl, 2008, Phys. Rev. **D77**, 114002.

Melde, T., W. Plessas, and R. F. Wagenbrunn, 2005, Phys. Rev. **C72**, 015207.

Melnitchouk, W., *et al.*, 2003, Phys. Rev. **D67**, 114506.

Merkel, H., *et al.*, 2007, Phys. Rev. Lett. **99**, 132301.

Metsch, B., U. Loring, D. Merten, and H. Petry, 2003, Eur. Phys. J. **A18**, 189.

Mibe, T., *et al.*, 2005, Phys. Rev. Lett. **95**, 182001.

Michael, C., 2006, PoS **LAT2005**, 008.

Migura, S., D. Merten, B. Metsch, and H.-R. Petry, 2006, Eur. Phys. J. **A28**, 41.

Minami, S., 1968, Prog. Theor. Phys. **40**, 1068.

Mizuk, R., *et al.*, 2005, Phys. Rev. Lett. **94**, 122002.

Mizuk, R., *et al.* (Belle), 2008, eprint 0806.4098.

Mokeev, V. I., *et al.*, 2008, eprint 0809.4158.

Mokhtari, A., *et al.*, 1985, Phys. Rev. Lett. **55**, 359.

Mokhtari, A., *et al.*, 1987, Phys. Rev. **D35**, 810.

Morand, L., *et al.*, 2005, Eur. Phys. J. **A24**, 445.

Morrow, S. A., *et al.*, 2008, eprint 0807.3834.

Morsch, H. P., and P. Zupranski, 2000, Phys. Rev. **C61**, 024002.

Nadkarni, S., and H. B. Nielsen, 1986, Nucl. Phys. **B263**, 1.

Nakabayashi, T., *et al.*, 2006, Phys. Rev. **C74**, 035202.

Nakano, T., *et al.*, 2003, Phys. Rev. Lett. **91**, 012002.

Nakayama, K., Y. Oh, and H. Haberzettl, 2008, eprint 0803.3169.

Nanova, M., *et al.*, 2008, Eur. Phys. J. **A35**, 333.

Narison, S., 2004, *QCD as a theory of hadrons: from partons to confinement; electronic version* (Cambridge Univ. Press, Cambridge).

Nasseripour, R., *et al.*, 2008, Phys. Rev. **C77**, 065208.

Nefkens, B., 2001, 18th Students Workshop on Electromagnetic Interactions in Bosen/Saar, Sept. 2-7.

Niiyama, M., *et al.*, 2008, eprint 0805.4051.

Nikonov, V. A., A. V. Anisovich, E. Klempt, A. V. Sarantsev, and U. Thoma, 2008, Phys. Lett. **B662**, 245.

Nussinov, S., and M. A. Lampert, 2002, Phys. Rept. **362**, 193.

Ocherashvili, A., *et al.*, 2005, Phys. Lett. **B628**, 18.

Oller, J. A., E. Oset, and A. Ramos, 2000, Prog. Part. Nucl. Phys. **45**, 157.

Olmsted, J., *et al.*, 2004, Phys. Lett. **B588**, 29.

Oset, E., and A. Ramos, 1998, Nucl. Phys. **A635**, 99.

van Pee, H., *et al.*, 2007, Eur. Phys. J. **A31**, 61.

Penner, G., and U. Mosel, 2002a, Phys. Rev. **C66**, 055211.

Penner, G., and U. Mosel, 2002b, Phys. Rev. **C66**, 055212.

Petersen, B. A., 2006, eprint hep-ex/0610049.

Pocanic, D., *et al.*, 1994, Phys. Rev. Lett. **72**, 1156.

Polchinski, J., and M. J. Strassler, 2002, Phys. Rev. Lett. **88**, 031601.

Prakhov, S., *et al.*, 2004a, Phys. Rev. **C70**, 034605.

Prakhov, S., *et al.*, 2004b, Phys. Rev. **C69**, 045202.

Prakhov, S., *et al.*, 2004c, Phys. Rev. **C69**, 042202.

Prakhov, S., *et al.*, 2005, Phys. Rev. **C72**, 015203.

Löring, U., K. Kretzschmar, B. C. Metsch, and H. R. Petry,

2001a, Eur. Phys. J. **A10**, 309.

Löring, U., B. C. Metsch, and H. R. Petry, 2001b, Eur. Phys. J. **A10**, 395.

Löring, U., B. C. Metsch, and H. R. Petry, 2001c, Eur. Phys. J. **A10**, 447.

Ratti, S. P., 2003, Nucl. Phys. Proc. Suppl. **115**, 33.

Regge, T., 1959, Nuovo Cim. **14**, 951.

Regge, T., 1960, Nuovo Cim. **18**, 947.

Reinders, L. J., H. Rubinstein, and S. Yazaki, 1985, Phys. Rept. **127**, 1.

Rho, M., D. O. Riska, and N. N. Scoccola, 1992, Z. Phys. **A341**, 343.

Richard, J. M., 1981, Phys. Lett. **B100**, 515.

Richard, J. M., 1992, Phys. Rept. **212**, 1.

Richard, J. M., and P. Taxil, 1983, Ann. Phys. **150**, 267.

Ripani, M., *et al.*, 2003, Phys. Rev. Lett. **91**, 022002.

Rosner, J. L., 2007, J. Phys. **G34**, S127.

Sadler, M. E., *et al.*, 2004, Phys. Rev. **C69**, 055206.

Santoro, J. P., *et al.*, 2008, eprint 0803.3537.

Sarantsev, A. V., V. A. Nikonov, A. V. Anisovich, E. Klempt, and U. Thoma, 2005, Eur. Phys. J. **A25**, 441.

Sarantsev, A. V., *et al.*, 2008, Phys. Lett. **B659**, 94.

Sasaki, K., and S. Sasaki, 2005, Phys. Rev. **D72**, 034502.

Schneider, S., S. Krewald, and U.-G. Meissner, 2006, Eur. Phys. J. **A28**, 107.

Schumacher, R., 2006, eprint nucl-ex/0611035.

Schwille, W. J., *et al.*, 1994, Nucl. Instrum. Meth. **A344**, 470.

Seftor, C. J., *et al.*, 1989, Phys. Rev. **D39**, 2457.

Semay, C., F. Brau, and B. Silvestre-Brac, 2001, Phys. Rev. **C64**, 055202.

Sengl, B., T. Melde, and W. Plessas, 2007, Phys. Rev. **D76**, 054008.

Sevior, M. E., *et al.*, 1991, Phys. Rev. Lett. **66**, 2569.

Shifman, M., and A. Vainshtein, 2008, Phys. Rev. **D77**, 034002.

Shifman, M. A., A. I. Vainshtein, and V. I. Zakharov, 1979, Nucl. Phys. **B147**, 385.

Shklyar, V., H. Lenske, and U. Mosel, 2005a, Phys. Rev. **C72**, 015210.

Shklyar, V., H. Lenske, and U. Mosel, 2007, Phys. Lett. **B650**, 172.

Shklyar, V., H. Lenske, U. Mosel, and G. Penner, 2005b, Phys. Rev. **C71**, 055206.

Shuryak, E. V., and J. L. Rosner, 1989, Phys. Lett. **B218**, 72.

Sibirtsev, A., J. Haidenbauer, and U. G. Meissner, 2007, Phys. Rev. Lett. **98**, 039101.

Sibirtsev, A., *et al.*, 2007, Eur. Phys. J. **A34**, 49.

Stanley, D. P., and D. Robson, 1980, Phys. Rev. Lett. **45**, 235.

Starostin, A., *et al.*, 2005, Phys. Rev. **C72**, 015205.

Stepanyan, S., *et al.*, 2003, Phys. Rev. Lett. **91**, 252001.

Strauch, S., *et al.*, 2005, Phys. Rev. Lett. **95**, 162003.

Sumihama, M., *et al.*, 2006, Phys. Rev. **C73**, 035214.

Suzuki, N., T. Sato, and T. S. H. Lee, 2008, eprint 0806.2043.

Tang, A., and J. W. Norbury, 2000, Phys. Rev. **D62**, 016006.

Tariq, A. S. B., 2007, PoS **LAT2007**, 136.

de Teramond, G. F., and S. J. Brodsky, 2005, Phys. Rev. Lett. **94**, 201601.

Thoma, U., *et al.*, 2008, Phys. Lett. **B659**, 87.

Thomas, A. W., S. Theberge, and G. A. Miller, 1981, Phys. Rev. **D24**, 216.

Trilling, G., 2008, Pentaquark update, in (Yao *et al.*, 2006).

Ungaro, M., *et al.*, 2006, Phys. Rev. Lett. **97**, 112003.

Valcarce, A., F. Fernandez, P. Gonzalez, and V. Vento, 1996, Phys. Lett. **B367**, 35.

Varga, K., M. Genovese, J.-M. Richard, and B. Silvestre-Brac, 1999, Phys. Rev. **D59**, 014012.

Viehhauser, G., 2000, Nucl. Instrum. Meth. **A446**, 97.

Vijande, J., A. Valcarce, and J. M. Richard, 2007, Phys. Rev. **D76**, 114013.

Vrana, T. P., S. A. Dytman, and T. S. H. Lee, 2000, Phys. Rept. **328**, 181.

Walcher, T., 1988, Ann. Rev. Nucl. Part. Sci. **38**, 67.

Weber, H. J., 1990, Phys. Rev. **C41**, 2783.

Weis, M., *et al.*, 2007, eprint 0705.3816.

Wilczek, F., 2004, eprint hep-ph/0409168.

Wohl, C. G., 2008a, Charmed Baryons, in (Amsler *et al.*, 2008) .

Wohl, C. G., 2008b, Pentaquarks, in (Amsler *et al.*, 2008) .

Workman, R., 1999, Few Body Syst. Suppl. **11**, 94.

Workman, R. L., and R. A. Arndt, 2008, eprint 0808.2176.

Wright, A. M., *et al.*, 1995, prepared for 7th International Conference on the Structure of Baryons, Santa Fe, New Mexico, 3-7 Oct 1995.

Wu, C., *et al.*, 2005, Eur. Phys. J. **A23**, 317.

Yao, W. M., *et al.* (Particle Data Group), 2006, J. Phys. **G33**, 1.

Ynduráin, F. J., 1999, *The theory of quark and gluon interactions; 3rd ed.*, Texts and monographs in physics (Springer, Berlin).

Zegers, R. G. T., *et al.*, 2003, Phys. Rev. Lett. **91**, 092001.

Zhu, L. Y., *et al.*, 2003, Phys. Rev. Lett. **91**, 022003.

Zhu, L. Y., *et al.*, 2005, Phys. Rev. **C71**, 044603.

Zou, B. S., 2008, Eur. Phys. J. **A35**, 325.